The design, development and application of novel, screen-printed amperometric glutamate biosensors

Gareth Hughes BSc (Hons)

A thesis submitted in part fulfilment of the requirements of the University of the West of England, for the degree of Doctor of Philosophy

Faculty of Health and Applied Sciences

University of the West of England, Bristol

September 2015

Abstract

The aim of the studies presented in this thesis was to develop a screen-printed electrochemical biosensor for the measurement of glutamate and to apply this device to the determination of the analyte in food, serum and toxicity studies.

Chapter 1 serves as an introduction to both the physiological significance of glutamate and the fundamental principles underpinning the electrochemical techniques used throughout this thesis.

Chapter 2 is a review chapter, separated into two main sections. The first section details glutamate biosensors fabricated with glutamate oxidase (GluOx), the second section details biosensors fabricated with glutamate dehydrogenase (GLDH). The immobilization techniques, ease of fabrication and sample preparation techniques employed are compared. Biosensor characteristics such as sensitivity, limit of detection and linear range are summarised within a table.

The studies described in Chapter 3 focus on the development of a non-reagentless glutamate biosensor. A Meldola's Blue screen-printed carbon electrode (MB-SPCE) was employed as the base transducer. The biosensor was constructed by drop coating the biopolymer chitosan (CHIT) and GLDH onto the surface of the MB-SPCE. For this study, NAD^+ was present in free solution. Meldola's Blue served as the electrocatalyst, whereby NADH produced by the GLDH/NAD^+ reaction, was electrocatalytically oxidised at a low operating potential (+0.1V (vs. Ag/AgCl)). The applied potential, temperature, pH and concentration of the co-factors required for the biosensor operation were optimised in this study. The assay exhibited a linear range of 12.5 μM to 150 μM, limit of detection of 1.5 μM, response time of 2s and a sensitivity of 0.44 nA/ μM. The optimised biosensor was subsequently applied to the determination of endogenous and fortified concentrations of glutamate in both serum and food samples (OXO cubes). The serum was fortified with and the resulting mean recovery

was 96% with a CV of 3.3% (n = 6). For the food sample, an unfiltered beef OXO cube was analysed for monosodium glutamate (MSG) content. The endogenous content of MSG was 125.43 mg/g, with a CV of 8.98% (n = 6). The solution was fortified with 100mM of glutamate and a resulting mean recovery of 91% with a CV of 6.39% (n = 6) was determined.

In Chapter 4, the glutamate biosensor was further developed in order to produce a reagentless device whereby the cofactor NAD^+ and GLDH were immobilized on to the surface of the electrode utilising CHIT. The reagentless device was developed in order to monitor glutamate release from human liver carcinoma cells (HepG2) as a result of cell toxicity from exposure to paracetamol. The biosensor was miniaturised in the form of a microband biosensor, whereby one dimension of the electrode is of micrometre size and the other millimetre size. Micro bands exhibit unique diffusion properties in comparison to conventional sized electrodes. Calibration studies were carried out with an applied potential of +0.1V (vs. Ag/AgCl) using both phosphate buffer and cell media. In phosphate buffer the following microband biosensor characteristics were determined: linear range; 25 - 125µM, sensitivity; 0.0636 nA/µM and a theoretical limit of detection of 1.20µM. In cell media; linear range; 25 – 150 µM, sensitivity; 0.128 nA/µM and a theoretical limit of detection of 4.2µM. As the HepG2 cells were grown in an incubator at a fixed temperature and pH, studies were carried out at pH 7, 37ºC, in a 5% CO_2 atmosphere. The miniaturised biosensor was applied to the determination of glutamate and the quantification was done by standard addition in cell media after 24 hours exposure to various concentrations of paracetamol. The average endogenous concentrations for glutamate released from the HepG2 cells was 52.07µM (CoV: 13.74%, n = 3), 93.30µM (CoV: 18.41%, n = 3) and 177.14µM (CoV: 14.54% n = 3) for 1mM, 5mM, 10mM doses of paracetamol respectively. The microband biosensor was also applied to the real time monitoring of glutamate over 8 hours. The standard deviations for the final current generated after eight hours are as follows; 1mM (coefficient of variation (CoV): 3.3%), 5mM (CoV: 9.056%) and 10mM (CoV: 13.18%).

The study showed that the magnitudes of the steady state currents increased in proportion to the concentration of added paracetamol. The study also demonstrated the possibility of applying microband biosensors, over extended time periods, for toxicity studies; there is no significant removal of analyte owning to the small biosensor dimensions.

Chapter 5 describes the development of a reagentless conventional sized glutamate biosensor whereby the cofactor NAD^+ and GLDH were immobilized using a combination of multi-walled carbon nanotubes (MWCNT), CHIT and additional water based MB in a layer-by-layer fashion. The MWCNT/CHIT/MB combination facilitates electron transfer to the surface of working electrode. The MWCNT/CHIT also entraps GLDH and the NAD^+ on the surface of the electrode. The pH, temperature, optimum applied potential, concentrations of NAD^+, CHIT and the addition of water-based MB were optimised. The electrocatalyst MB allowed a operating potential of +0.1V (vs. Ag/AgCl) to be utilised. The biosensor was examined with standard glutamate solutions and the following biosensor characteristics were determined; linear range; 7 - 105μM, LOD; 3 μM, sensitivity; 0.39 nA/μM, response time 20-30s. A food sample was analysed for MSG and found to contain 90.56 mg/g with a CV of 7.52% (n = 5). The reagentless biosensor was also applied to the determination of glutamate in serum. The endogenous concentration was found to be 1.44mM (n = 5), CV: 8.54%. The recovery of glutamate in fortified serum was 104% (n = 5), CV of 2.91%. The results indicate that the new biosensor holds promise for food and biomedical studies.

Acknowledgements

Firstly I would like to express my gratitude to Prof. John Hart, who provided endless enthusiasm and support throughout my studies. Our scientific and musical discussions over morning coffee (latte's) was a source of invaluable guidance.

I would also like to thank Dr. Roy Pemberton for his excellent support, advice and enthusiasm throughout the PhD.

My thanks also go to Prof. Peter Fielden, for his support. Gwent Electronic Materials must also be mentioned and thanked for their provision of the screen-printed carbon electrodes.

I'm extremely grateful to Dr. Adrian Crew and Dr. Kevin Honeychurch for putting up with me in the lab, providing answers to my questions and for all the laughs over the past three years.

Thanks to all the support from all my friends at UWE!

Friends beyond UWE, many thanks for the support and nodding politely when I've attempted to explain my work after a few ciders.

Huge thanks go my family: Robert, Llinos, Tadcu James, Tadcu Hughes, Mamgu Hughes and Scooby providing endless support.

Copyright Disclaimer

Abbreviations

Abbreviation	Meaning
BSA	Bovine Serum Albumin
CE	Counter electrode
CHIT	Chitosan
ES	Enzyme-substrate complex
E_{app}	Applied Potential
GLDH	Glutamate Dehydrogenase
H_2O_2	Hydrogen Peroxide
HDV	Hydrodynamic Voltammetry
MSG	Monosodium Glutamate
MWCNT	Multi-walled Carbon Nanotubes
MB_{ox}	Meldola's Blue (oxidised form)
MB_{red}	Meldola's Blue (reduced form)
NAD^+	Nicotinamide adenine dinucleotide (oxidised form)
NADH	Nicotinamide adenine dinucleotide (reduced form)
OHP	Outer Helmholtz plane
P	Product
PVC	Poly(vinyl) chloride
R	Reactant
RE	Reference Electrode
SPCE	Screen Printed Carbon Electrode

Oral Presentations

9th Post Graduate Research Topics Meeting in Electroanalysis and Sensing.
Studies towards the development of a disposable screen-printed amperometric biosensor and its possible applications. 4th December 2014, Birkbeck, University of London

CRIB Seminar

Studies towards the development of a disposable screen-printed amperometric biosensor and its possible applications. 5th December, 2014, University of the West of England, Bristol

Great Western Electrochemistry Meeting

Studies towards the development of a disposable screen-printed amperometric biosensor and its possible applications. 22nd of June 2015, University of Bath, Bath.

Publications

G. Hughes, R.M. Pemberton, P.R. Fielden, J.P. Hart, *Development of a Disposable Screen Printed Amperometric Biosensor Based on Glutamate Dehydrogenase, for the Determination of Glutamate in Clinical and Food Applications*, Anal. Bioanal. Electrochem. **6** (2014) 435–449. http://abechem.com/No. 4-2014/2014,6_4_,435-449.pdf.

G. Hughes, R.M. Pemberton, P.R. Fielden, J.P. Hart*, Development of a novel reagentless, screen–printed amperometric biosensor based on glutamate dehydrogenase and NAD+, integrated with multi–walled carbon nanotubes for the determination of glutamate in food and clinical applications*, Sensors Actuators B Chem. (2015). doi:10.1016/j.snb.2015.04.066.

P. Kanyong, G. Hughes, R. M. Pemberton, S. K. Jackson and J. P.Hart, (2015) *"Amperometric Screen-Printed Galactose Biosensor for Cell Toxicity Applications,"* Analytical Letters. 49, 2, 1–9.

G. Hughes, R. M. Pemberton, P. R. Fielden, and J. P. Hart. *"The design, development and application of electrochemical glutamate biosensors, (Review)"*. Trends in Analytical Chemistry, accepted for publication

G. Hughes, R. M. Pemberton, P. R. Fielden, and J. P. Hart. *"A reagentless, screen–printed amperometric biosensor for the determination of glutamate in food and clinical applications, (Book Chapter)". Methods in Molecular Biology (Springer),* submitted

Contents

CHAPTER ONE

An Introduction to Electrochemical Glutamate Biosensors

1. Contents

1.1 Introduction

1.1.1 Glutamate

Glutamate is considered to be the primary neurotransmitter in the mammalian brain and facilitates normal brain function [1]. It is a non-essential endogenous excitatory amino acid that is synthesised in neurons, from precursors such as glutamine and 2-oxoglutarate. Along with aspartate and homocysteine, glutamate contributes to excitatory neurotransmission in the central nervous system (CNS), whilst its immediate precursor gamma-aminobutyric acid (GABA) acts as an endogenous inhibitory neurotransmitter [2]. Neurotoxicity, which causes damage to brain tissue, can induced by glutamate at high concentrations. The accumulation of high concentrations of glutamate leads to the over activation of NMDA and AMPA receptors [3], which may link it to a number of neurodegenerative disorders such as Parkinson's disease, multiple sclerosis [4] and Alzheimer's disease [5].

In cellular metabolism, glutamate also contributes to the urea cycle and tricarboxylic acid cycle (TCA)/Krebs cycle. It plays a vital role in the assimilation of NH_4^+ [6]. Glutamate is synthesised from NH_4^+ and alpha-ketoglutarate by glutamate dehydrogenase (GLDH). The process is a reversible reaction, whereby glutamate can also be converted to alpha-ketoglutarate by oxidative deamination. The reaction can only occur in the presence of the coenzyme nicotine adenine dinucleotide (NAD^+). The direction of the reaction is primarily dependent on the relative concentrations of glutamate, alpha-ketoglutarate, ammonia and the ratio of oxidized to reduced coenzymes.

Intracellular glutamate levels outside of the brain are typically 2–5 mmol/L, whilst extracellular concentrations are ~0.05 mmol/L [7] and is present in high concentrations throughout the liver, brain, kidney and skeletal muscle [8]. Glutamate has a significant role in the disposal of ammonia, which is typically produced from the digestion of dietary amino acids, protein and the ammonia produced by intestinal tract bacteria. Glutamate can also dispose of ammonia by being converted to glutamine by glutamine synthase.

Due to glutamate's ubiquity throughout the human body and its central metabolic role, it is an excellent biomarker for toxicity. Many pharmaceutical compounds act upon disease causing cells by inducing cytoxicity via apoptosis and/or necrosis. This results in a loss of cell membrane integrity leading to the release of its cell contents, which includes glutamate [9].

1.1.2 Drug Development and Toxicology

Toxicology and cellular toxicity tests aim to study the potential effects on the human body that may be induced upon exposure to a substance, in an effort to monitor for any associated health risks that may occur. The process in determining the toxicity of a compound prior to clinical usage requires extensive testing. The average cost of developing a pharmaceutical drug, from its initial development to marketing, is around $2.5 billion and can take up to ten years [10]. As a result measures to improve efficiency and reduce the cost of testing prospective compounds are of great interest to the pharmaceutical industry.

Preclinical trials of a prospective drugs require *in vivo* testing. By utilising an animal model, the characterisation of the toxicity, pharmacokinetic action and the efficacy of a drug may be determined [11]. However, there are many arguments as to whether testing on animals is an effective or acceptable means of predicting potential human toxicology [12]. Much concern is also placed on the ethical impact of testing on animals.

In vitro testing concerns the analysis of the effects of toxic compounds upon cellular metabolism, without requirement of an animal model. Current toxicological analytical techniques include ELISA kits, neutral red uptake [13] and comet tests [14]; however these analytical techniques are time consuming, expensive and require specialist equipment. These techniques do not offer real time analysis or the ability to monitor the ongoing toxicological effect that a drug may have on the cells. Thus, the development of a high throughput system for *in vitro* cellular toxicity based on human cells for drug discovery purposes is of great clinical interest. Current high throughput systems for in vitro drug

toxicity screening include CellTiterGlow, ToxiLight, lactate dehydrogenase assay, CyQuant and Trypan Blue assays. These assays evaluate the effects of the anti-metabolic effects by utilising luminescent assays, fluorescent assays, the ability for the cell to uptake a reagent or by monitoring the release of an enzyme [15].

The development of electrochemical biosensors in order to monitor the effects of toxicological challenge upon cells offers promising advantages over existing toxicological techniques. Biosensors offer specificity for biologically relevant analytes due to their utilisation of an enzyme as part of their sensing system [16].

1.1.3 HepG2

The *in vitro* toxicity tests described later in the thesis utilise HepG2 as the cell culture model. HepG2 cells are immortalized human liver carcinoma cells. This cell line has been previously used to determine the cytotoxicity of compounds [17]–[20]. Indicators of HepG2 cytotoxicity include glucose secretion, LDH leakage and elevated levels of gamma-glutamyl transferase [18]. The HepG2 cell line expresses many of the enzymes associated with cytochrome (CYP), in particular, phase I and phase II metabolic enzymes [21], [22].

HepG2 cells may also be cultured into 3D aggregates known as spheroids, which behave like “mini-livers”. However, the drug toxicity interactions for 3D HepG2 cells are less established than monolayer interactions. In addition, other difficulties such as increased culturing complexity, significantly slower maturation of the cell line and inability to accurately count the number of cells due to aggregation may arise [23]. Thus, based on current *in vitro* toxicological methods currently utilised by pharmaceutical compounds, 3D-cells lines are currently unsuited.

1.2 Biosensor Principles and Applications

The first biosensor concept was proposed by Clark and Lyons from the Children Hospital in Cincinnati in 1962 [24]. The biosensor measured the depletion of oxygen generated by the oxidation of glucose in a thin layer of glucose oxidase over the gas permeable membrane of the sensor. The glucose oxidase biosensor has been developed enormously since its initial conception [25]. The analysis of glucose is considered vital to the management of blood glucose levels in diabetic patients [26] by the use of small glucose meters. The meters, both in the size and ease of use, have progressed vastly since the 1970's, with particular breakthroughs occurring in the 1990's, with the reduction in the volume of blood required to take a measurement and an increase in the accuracy in both high and low concentrations of glucose [27].

A biosensor is a chemical sensing device that relies on two basic components connected in series – a biochemical mechanism recognition system and a physio-chemical transducer. These provide a mean to convert chemical information such as the concentration of a sample into a useful signal which can be analysed [28]. The biological component of a biosensor can be split into two classifications; catalytic and non-catalytic. Catalytic components consist of micro-organisms, tissues and enzymes, whilst non-catalytic components comprise of antibodies, receptors and nucleic acids.

The transduction technique will be dependent on the biological component in use. Examples of transduction techniques include:

- Potentiometric – The measurement of the potential at zero current. The potential is proportional to the logarithm of the concentration of the substance being determined.
- Voltammetric – Increasing or decrease the potential that is applied to a cell until the oxidation or reduction of the analyte occurs. This generates a rise in current that is proportional to the concentration of the electroactive potential. Once the desired stable

oxidation/reduction potential is known, stepping the potential directly to that value and observing the current is known as amperometry.

- Conductiometric – Observing changes in electrical conductivity of the solution. [29]

The most commonly used type of biosensor both in commercial production and research are enzyme based systems, coupled with amperometric transduction. Biosensors such as those produced by Clark and Lyons are described as being "first generation" devices. The generation was originally denoted to describe the level at which the biosensor was integrated. "First generation" biosensors are devices where the signals generated from the detection of the analyte of interest are as a result of membrane entrapped or bound biocomponents. "Second generation" biosensors entrap the biocomponents onto the surface of the electrode, as a result direct electron transfer occurs between the enzyme active surface and transducer surface, shuttled by the mediator. "Third generation" biosensors differ from "second generation" biosensors by the lack of mediator required as direct electron transfer between the electrode surface and the active site of the enzyme occurs [30]. "Third generation" glucose biosensors have been developed [31], [32].

1.2.1 Biosensor Fabrication

Biosensors may be fabricated by the low cost method of screen printing. Other methods of fabrication such as ink-jet printing [33] and solid state technology [34] have been utilised to fabricate biosensors. Screen printing may be done by hand or by utilising an automated screen-printing machine.

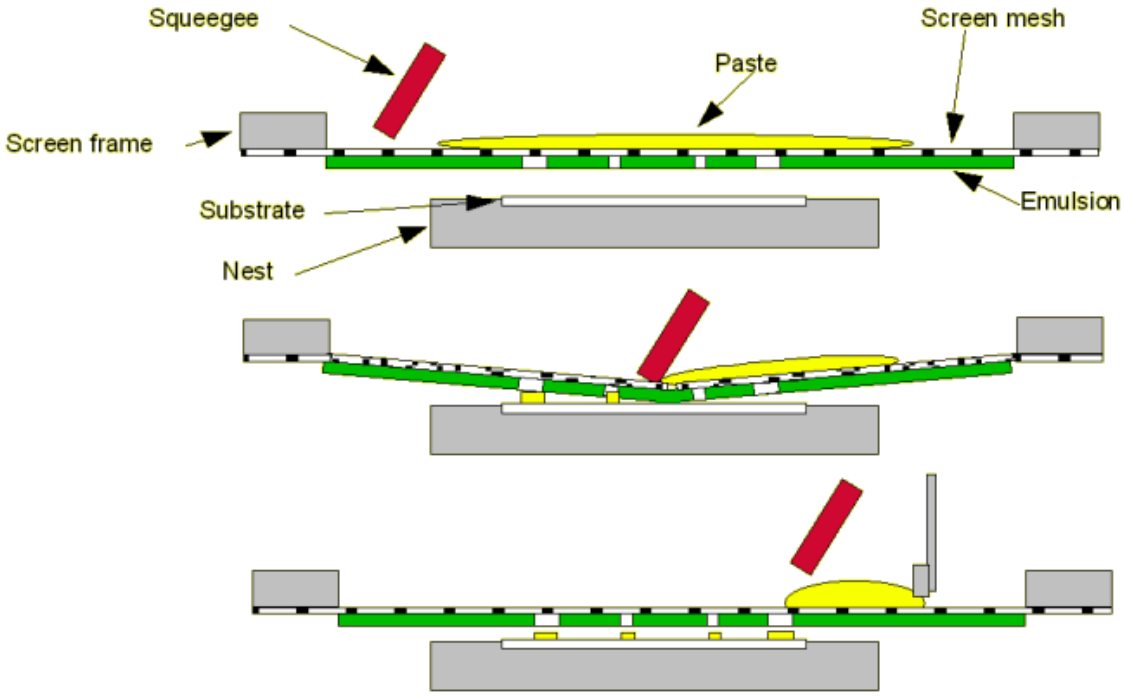

Figure 1-1. A diagram illustrating the screen-printing process. Used with permission from GEM.

The principle of screen printing is the graphic reproduction of an image by use of ink or other viscous compound which is deposited as a film of controlled pattern and thickness. To do so, the ink is squeezed using a squeegee through a mesh which is tightly stretched over a frame. The ink is then deposited onto a substrate to produce a screen-printed electrode, which can be utilised once dried. Typically, polyester, PVC or ceramic substrates are used. The screen printing process is illustrated in Figure 1-1.

Figure 1-2: Diagram of a Screen-Printed Carbon electrode with the working area defined by insulating tape.

The electrodes are then cut out from the card using scissors. An insulating dielectric layer, comprising a nonconductive ink, may then be applied to the electrode to define the working area if necessary, as demonstrated in Figure 1-2. Ag/AgCl reference electrodes may be also be produced by screen-printing methods.

1.3 Electrode Modification

1.3.1 Electrocatalysts

Commonly used working electrode materials include carbon, gold, mercury or platinum. The material should allow for the application of wide potential windows whilst exhibiting favourable redox behaviour and reproducible electron transfer, in order to effectively characterise the species of interest.

However, these materials require the use of large over-potentials to oxidize or reduce the electroactive species of interest. The over potential is the potential difference between the half-reaction reduction potential and the potential at which the redox reaction is observed. This presents some difficulties when analysing complex solutions and real samples as other compounds may also be electrocatalytically active at or around a similar potential as the analyte of interest. As a result, this may produce undesired interferences which reduce the signal-to-noise ratio, selectivity and sensitivity of the biosensor. By modifying the working

electrode by incorporating an electrocatalyst such as Meldola's Blue, the potential required to determine the electroactive species can be significantly lowered.

Meldola's Blue (8-dimethylamino-2,3-benzophenoxazine; designated MB) is an electron mediator that has been utilised as an electrocatalyst in numerous biosensors. MB increases the charge transfer between the analyte and the electrode. It also eliminates the interaction between the electrode and the analyte itself. This leads to a decrease in the formal potential required to be applied to the electrode to produce an analytical response and an increase in current density [35]. This also leads to a reduction in the likelihood of interferences directly interacting with the working electrode and being oxidised/reduced, leading to undesired amperometric signals. At high overpotentials, an increased likelihood of electrode fouling can occur. Use of MB can also increase sensitivity for the amperometric detection of NADH (Figure 1-3). Meldola's Blue was first utilised as a histochemical demonstrator of dehydrogenase activity [36], however, due to its excellent electron mediating abilities, it was soon patented and utilised as an electrocatalyst for the coenzyme regeneration and detection of NADH [37].

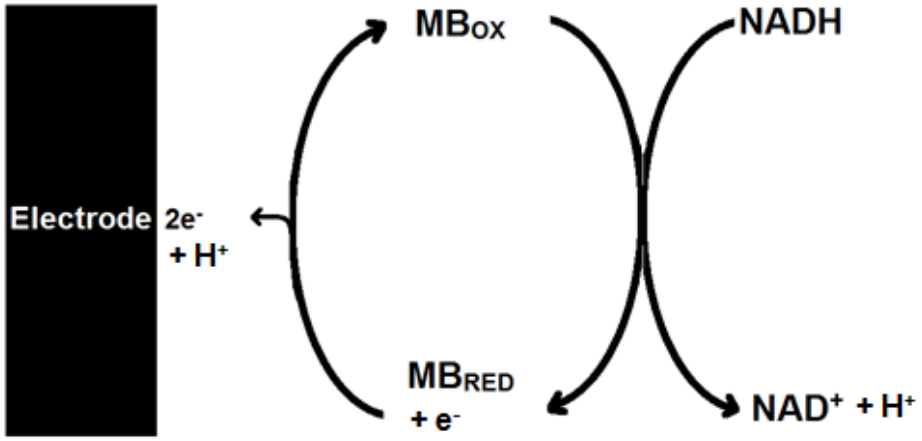

Figure 1-3 illustrates the charge transfer mechanism during the electrocatalytic reduction of MB. The active form of the electrode is then electrochemically regenerated.

The use of the mediator led to a 500mV reduction in potential required to electrocatalytically oxidise NADH, in comparison to an unmodified electrode [38]. At an unmodified screen-printed carbon electrode (SPCE), the anodic peak potential for NADH occurs at +0.500mV; with a modified MB-SPCE, the NADH oxidation occurs at -50mV [39].

In order to immobilise the Meldola's Blue to the surface of the electrode, various strategies have been used. Silica coated with niobium oxide was used to immobilize MB on a modified carbon paste electrode with well-defined electrochemical responses for NADH [40]. Functionalized carbon nanotubes, combined with MB, to form a nanocomposite film, have been used to non-covalently bind MB onto the surface of a glassy carbon electrode to detect NADH [41]. This method leads to excellent sensor characteristics such as low signal-to-noise, low detection limits and a wide linear range. Titanium phosphate was also used to immobilize Meldola's Blue onto a silica gel surface and subsequently incorporated into a carbon paste electrode [42]. Such immobilization techniques are often complex and time consuming. By incorporating Meldola's Blue into a screen-printed carbon electrode fabrication costs can be reduced due to the increased potential for mass production, thereby rendering it more suitable for commercial purposes. Incorporating the mediator within the ink allows for further modification of the electrode surface with biological components such as enzymes and/or cofactors.

In addition to the determination of NADH, biological compounds such as glucose [43], lactate [44][45], ammonia [46], glutamate [47], ethanol [48], fructose [49] and ascorbic acid [50] have also been determined utilising Meldola's Blue as a mediator in conjunction with a variety of different enzymes.

The biosensor described in this thesis will utilise the enzyme glutamate dehydrogenase (GLDH) and the coenzyme NAD^+ with a MB-SPCE to detect glutamate, by following the production and subsequent oxidation of the enzymatically generated NADH.

1.3.2 Biological Modification of Electrodes

Biosensors function by the coupling of a molecular recognition component with a physio-chemical detector in close proximity [51]. Enzymes are typically used due to their high specificity, robustness and ability to bind to the surface of the transducer. By reducing the distance between the active site of the enzyme and the transducer surface, an increase in the electron transfer efficiency occurs, and the target analyte analysis can facilitated [52]. This can be achieved by immobilizing enzymes on the surface of the transducer.

Enzymes can be immobilized using a variety of techniques, however it is important to select the appropriate method in order to retain as much of the enzyme activity as possible. Factors influencing the performance of an immobilized enzyme include the micro-environment of the carrier, diffusion constraints and the physical structure of the carrier [53]. Immobilisation may also result in the increased stability of the enzyme, resulting in potentially longer storage or operational times.

1.3.3 Immobilization Techniques

1.3.3.1 Covalent Bonding

Covalent bonding as an immobilization technique involves the formation of covalent bonds between the enzyme and the support matrix. Enzymes possess side chain amino acids such as aspartic acid, histidine and arginine and thus may bind to amino, thiol, carboxyl and phenolic groups present within the support matrix. Ideally, the groups associated with the binding must not be electrocatalytically active. Covalent bonds are extremely strong, but this approach suffers from the disadvantage of irreversibly altering the structure of the enzyme, thereby resulting in a loss of activity or its deactivation [54].

1.3.3.2 Entrapment

Entrapment is the caging of an enzyme within a gel or fibre by covalent or non-covalent interactions. Initial work in the entrapment of enzymes investigated the entrapment of glucose oxidase within conducting polypyrroles. The method involved the application of a potential to the working electrode immersed in a solution containing the enzyme and monomer. The enzymes near the working electrode were entrapped as the polymer grew [55]. However, due to the formation of a dense matrix upon the surface of the electrode, less substrate can diffuse deep into the matrix to reach the electrode surface. The enzyme may also leak into the surrounding solution.

1.3.3.3 Adsorption

Adsorption of an enzyme results from weak non-specific physical interactions such as Van Der Waals forces, ionic interactions and hydrogen bonding between the enzyme protein and the binding matrix utilised [56]. Adsorption results in little to no conformational change of the enzyme which thereby retains its original activity. The immobilization matrix employed is termed the "carrier". It is worth noting that not every enzyme will be successfully immobilized with every carrier, so it is important that the appropriate carrier, with the relevant functional groups, is selected.

Enzyme carriers can be divided into both organic and inorganic origin. Inorganic agents such as silica, silica gel, metal oxides and organic natural carriers such as chitin, chitosan, cellulose and alginate are often utilised as enzyme immobilization agents. In particular, chitosan has been utilised extensively throughout this thesis as the primary enzyme carrier.

1.3.3.3.1 Chitosan

Chitosan is a derivative of chitin, which is one of the world's most plentiful organic resources and is derived from the shells of crustaceans. It is a linear polyaminosaccharaide composed of randomly distributed β-(1,4)-linked D-glucosamine and N-acetyl-D-glucosamine groups. Due to its structure, chitosan possesses useful chemical and biological properties.

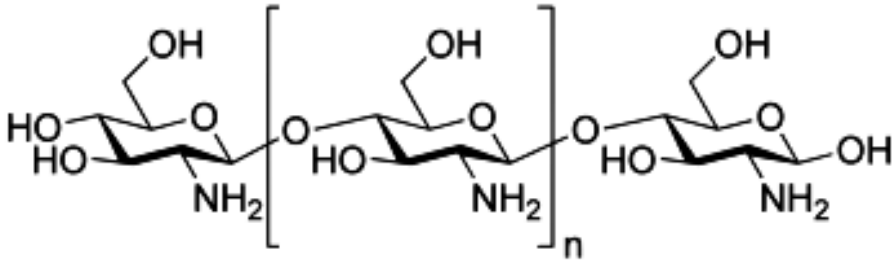

Figure 1-4 – Structure of Chitosan.

Chitosan is soluble in aqueous acidic media at pH < 6.5. When dissolved, it bears a high positive charge on its amino groups. Chitosan has gel-forming properties as a result of its ability to adhere to negatively charged surfaces and aggregate polyanionic compounds. It also possesses properties such as excellent biocompability, nontoxicity and protein affinity [57].

1.3.4 Enzymology

1.3.4.1 Enzyme Function

Enzymes are proteins which are highly selective catalysts. They function by lowering the activation energy required (which is often the rate limiting step) thereby increasing the rate of reaction, leading to an increase in both speed of formation, and quantity of the product. Enzymatic reactions are often much faster than that of un-catalysed reactions, however, due to their high specificity, the substrates of the reaction must conform to the catalytic requirements of the enzyme to function effectively. Some enzymes require non-protein

cofactors that allow them to increase their functionality or to function at all. Enzymes are not consumed during a chemical reaction nor do they alter the equilibrium of the reaction.

The specificity of an enzyme is dictated by its structure, charge and hydrophilic/hydrophobic characteristics. The specificity of an enzyme can be broken down into four types; absolute, group, linkage and stereochemical specificity. Absolute specificity restricts the enzyme to catalysing a single reaction, whilst group specificity only allows the enzyme to catalyse a specific functional group. Linkage specificity allows the enzyme to catalyse a reaction dependent on the presence of a specific type of chemical bond, whilst stereochemical specificity requires the enzyme to act on a specific stereoisomer which is dictated by the chirality of the enzyme active site [58].

The theories upon which the interactions of enzymes and substrates are based are known as the lock-and-key or induced fit hypothesis. The lock-and-key hypothesis, pictured in Figure 1-5a), states that only a specific substrate can correctly fit the active site of the enzyme. The induced fit hypothesis, proposed by Koshland and pictured in Figure 1-5b), suggests that a specific substrate can cause a three dimensional change in the enzyme, aligning the enzyme and substrate leading to the formation of a substrate-enzyme complex and consequently generating a product [59].

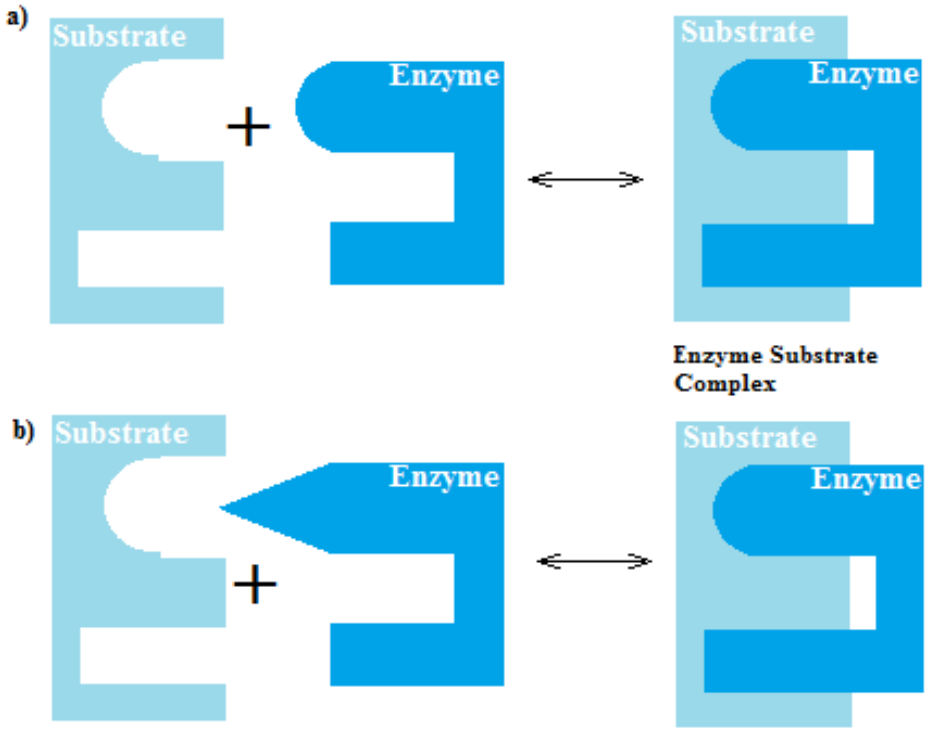

Figure 1-5: Schematic diagram of the a) lock and key model and (b) induced fit hypothesis. This illustrates substrate-active site interaction.

In the context of biosensors, the specificity of an enzyme can be a useful tool in fabricating biosensors that are selective for particular molecules.

1.3.4.2 Enzyme Kinetics

Enzyme kinetics is the study of reactions that are catalysed by enzymes. Specifically it investigates the rate of the reaction and how this is affected by varying the conditions of the reaction. The kinetics of an enzyme can reveal its mode of action and potential methods of inhibition.

Single substrate reactions are the simplest enzymatic conversions possible. As illustrated in Figure 1-5. The formation of an enzyme-substrate complex leads to an increase in the rate of reaction due to the lowering of the activation energy required for the reaction. Enzymatic reactions based on a single substrate obey the Michaelis-Menten model of enzyme kinetics. The rate of an enzyme-catalysed reaction is dependent on the

concentration of the substrate (S). Low concentrations of the substrate result in an initial rate that is proportional to the enzyme velocity (V_0) resulting in the linear part of the Michaelis-Menten plot illustrated in Figure 1-6, therefore first-order kinetics apply. Once the substrate has occupied all available enzyme sites and is forming enzyme-substrate complexes in equilibrium, the V_{max} has been reached, and zero-order kinetics apply [60].

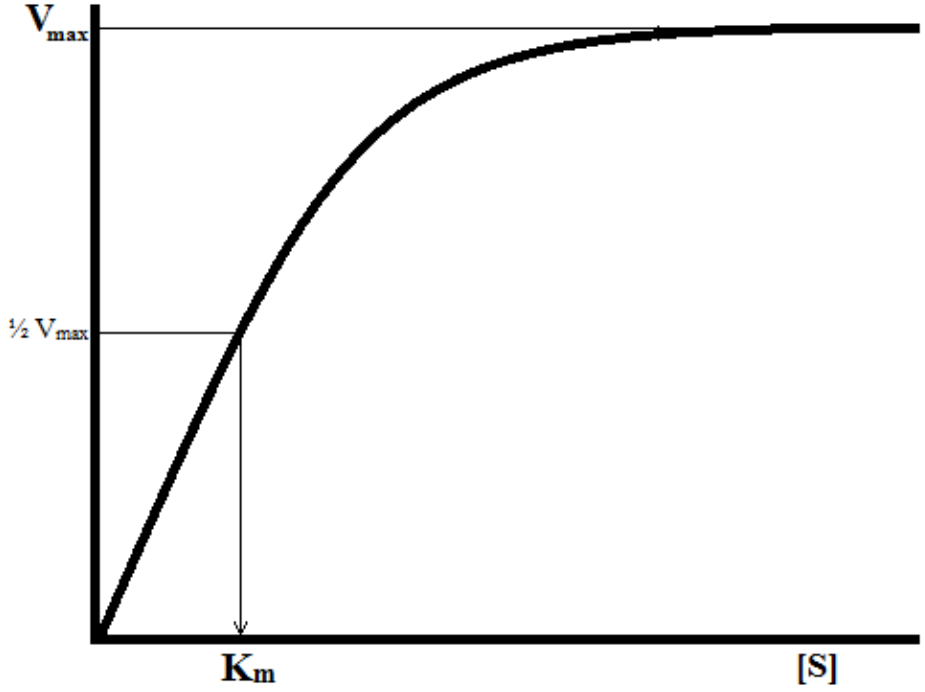

Figure 1-6: How the reaction rate is altered by the substrate concentration in the presence of constant enzyme concentration.

Figure 1-7: Enzyme substrate catalysis pathway.

Figure 1-7 describes the kinetic properties of many enzymes, whereby the enzyme (E), combines with S to form a ES complex, at a rate of dictated by the rate constant k_1. The complex can then either 1) dissociate to E + S by k_{-1} or 2) form the product (P) by k_2 [61].

The rate of formation and breakdown of ES is expressed as the following.

Formation $ES = K_1[E][S]$ Equation 1

Breakdown $ES = (K_{-1} + K_2)[ES]$ Equation 2

Assuming steady-state conditions, whereby the concentrations of [ES] remain constant due to the equal rate of formation and breakdown, regardless of if the concentrations of [S] and [P] are changing. This can be defined by the following equation:

$$\frac{[\mathrm{E}][\mathrm{S}]}{[ES]} = \frac{(K_{-1} + K_2)}{K_1} \quad \text{Equation 3}$$

This reaction can be simplified to the following, to give the Michaelis-Menten constant.

$$k_M = \frac{(K_{-1} + K_2)}{K_1} \quad \text{Equation 4}$$

The k_M substrate concentration at which half the enzyme active sites are filled. pH, temperature, the enzyme and the substrate may affect the k_M.

By deriving Equation 4 further, the Michaelis-Menten equation (Equation 5) describes the formation of a steady state enzyme-substrate complex. V_0 is the reaction rate, V_{max} is the maximum reaction rate, [S] is the substrate concentration and the K_M is the Michaelis-Menten constant. The enzymatic activity is measured as a function of substrate concentration. When [S] < K_{max}, the reaction proceeds under first-order kinetics, whilst when [S] > k_m, the reaction obeys zero-order kinetics. Therefore, the substrate concentration that produces half of the maximum reaction rate is termed the K_M which is equal to half the V_{MAX}.

$$V = \left(\frac{\mathrm{V_{max}}[\mathrm{S}]}{\mathrm{K_M} + [\mathrm{S}]}\right) \quad \text{Equation 5}$$

It is worth noting that some enzymes, such as dehydrogenases, require the presence of a cofactor, therefore in addition to the kinetics regarding the formation of an enzyme-substrate complex, the formation of an enzyme-cofactor complex (EC) must be also considered. Slow enzyme kinetics may arise if the cofactor concentration is not in excess of the enzyme concentration. By supplementing the mixture with an fixed excess concentration of the relevant cofactor, these issues can be overcome [62].

1.3.5 Dehydrogenase Enzymes

The enzyme utilised in this thesis to produce biosensors is glutamate dehydrogenase (GLDH). Dehydrogenases are a class of enzymes that oxidize a substrate by a reduction reaction. The reaction results in the transfer of one or more hydrides (H^-) to an electron acceptor, such as NAD^+. GLDH is a mitochondrial enzyme that is present in the liver, heart, muscle and kidneys. It is a hexameric enzyme composed of ~500 residues in the animal kingdom [63] and a molecular weight of 49.2kD [64]. The enzyme has a glutamate binding domain and two-coenzyme binding sites, one for NAD^+/$NAD(P)^+$ and one for ADP, NAD^+ and NADH. It catalyses the conversion of the amino group present on glutamate into a ammonium ion, by oxidative deamination. The reaction is a multi-step processes. The first step begins with the dehydrogenation of the carbon-nitrogen bond which leads to a Schiff-base intermediate; this is catalysed by glutamate dehydrogenase and the co-factor NAD+, which is reduced to NADH. The hydrolysis of the Schiff base leads to the formation of α-ketoglutarate [65].

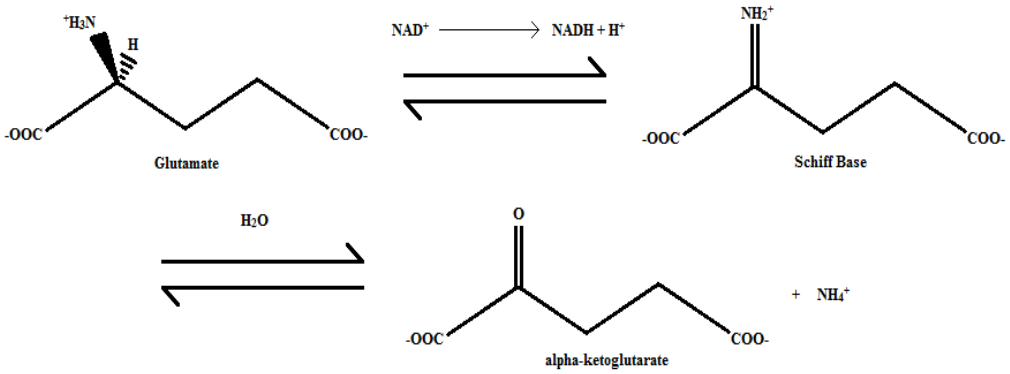

Figure 1-8 An example of a typical reversible dehydrogenase reaction. [66]

1.3.6 Cofactors

Cofactors can be either metals or coenzymes, whose primary function is to assist enzyme activity. Coenzymes are organic, non-protein molecules which assist in biological reactions but do not form a permanent bond to the enzyme structure.

Dehydrogenase enzymes require the presence of a cofactor such as NAD^+. During an oxidation sequence such as the one illustrated by the reverse reaction in Figure 1-8, NAD^+ is reduced to NADH by the transfer of H^+ from the substrate (eg: glutamate) to NAD^+ and the exchange of a proton into the media [67]. Coenzymes are continuously consumed and recycled.

NAD^+ is a dinucleotide consisting of an adenine base and nicotinamide joined by a phosphate bond between two phosphate groups. Its primary function is to facilitate redox reactions and is found in two forms; NAD^+ an oxidising agent and NADH a reducing agent.

1.4 Equipment utilised for electrochemical techniques

1.4.1 Electrochemical Cell

Typically electrochemical reactions take place in an electrochemical cell (Figure 1-9) which is made from quartz or glass, into which the sample solution is added. The sample solution must be of sufficient depth to cover the two or three electrodes utilised. Variables such as temperature can be controlled by utilising a water-jacket cell, which is connected to a thermostatically controlled water bath. Experiments such as amperometry require stirring, thus a magnetic stirrer bar can sit at the bottom of the solution, which is controlled by a magnetic stirrer that sits underneath the electrochemical cell. The stirrer geometry should allow for consistent stirring.

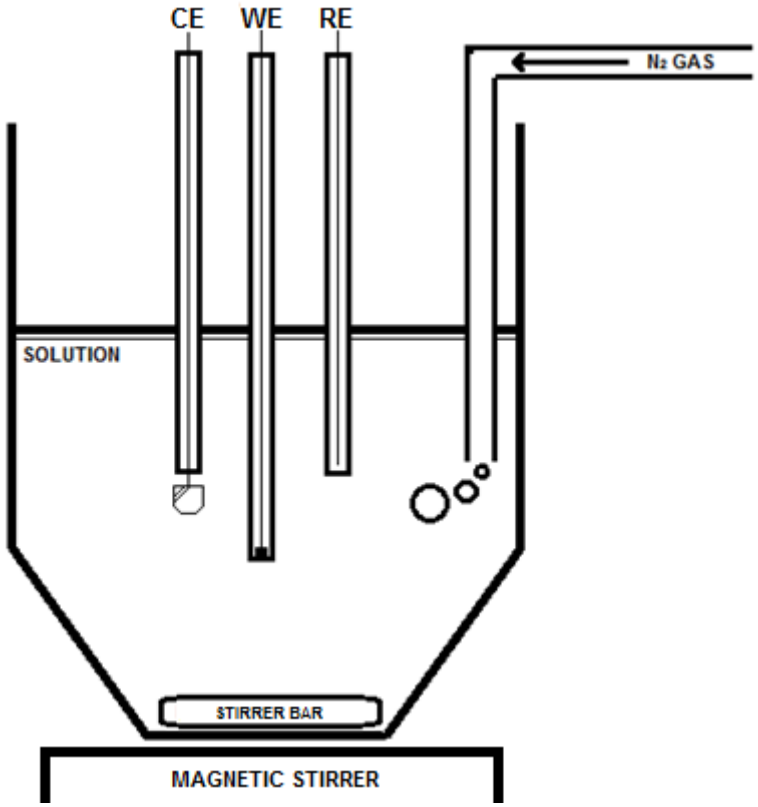

Figure 1-9 Schematic Diagram of a voltammetric cell based on a three electrode system. CE: counter electrode, WE: Working electrode, RE: Reference electrode. This is an example of a three electrode uncovered cell.

1.4.2 Working Electrode (WE)

The working electrode (WE) is the location at which the reaction of interest takes place. The working electrode must be made of a material that is stable in the electrolyte medium utilised during the experiment, eg: carbon. This is to ensure that the electrode does not corrode or become fouled, thereby altering the surface area, and to prevent other compounds reducing in the potential range of interest. Working electrodes should have high surface reproducibility with a uniform distribution of potential across the surface to prevent *IR* drop. The background current within the potential region of interest should be low. The cost, availability and toxicity of the material should also be considered.

1.4.3 Reference Electrode

A reference electrode acts as a half-cell which has a stable and accurately maintained potential which is used a reference for the measurement of voltage applied by the counter electrode (CE). It is potentiometric and thus has zero current flowing through it. The potentiostat compensates if a difference in voltage is detected between the AE and WE and adjusts the output accordingly until the difference is zero, this action is known as feedback [68]. An example of a commonly used reference electrode the silver-silver chloride (Ag/AgCl) which is frequently used with screen printed carbon electrodes [69]. For applications such as chromoamperometry where small currents are flowing for short time periods, two electrode systems may be used, where the counter electrode assumes the role of RE and WE. Since current flowing through the reference electrode may alter its stability over time [70], three electrode systems with a counter electrode are often utilised in experimental situations, and for amperometric applications over prolonged time periods.

1.4.4 Counter Electrode

The function of the counter electrode (CE) is to complete the circuit by applying a voltage difference respectively to the WE, thereby allowing charge to flow. The CE is composed of an inert material such as carbon or platinum.

1.4.5 Potentiostat

The instrument used to control the potential difference applied across the electrochemical cell is called a potentiostat (Figure 1-10). A potentiostat adjusts the voltage difference between the anode and the cathode in order to maintain a constant working electrode potential [71]. A potential is applied to the working electrode, resulting in a flow of charge towards the counter electrode. A potential drop (*iR*) is caused by the electrolyte conductivity, the distance between the electrodes, the magnitude of the current and resistance across the electrode material. If the *iR* drop is uncompensated, the reaction will no longer operate at the desired potential, and the reaction may cease. The reference electrode monitors the potential at the working electrode and feeds the value back to the op-amp. If a difference in potential is observed between the RE and WE, the potential applied to the CE is altered to compensate. A second op-amp is used as a current-voltage converter to measure the flow of current, with a resistor used to output the voltage per unit current.

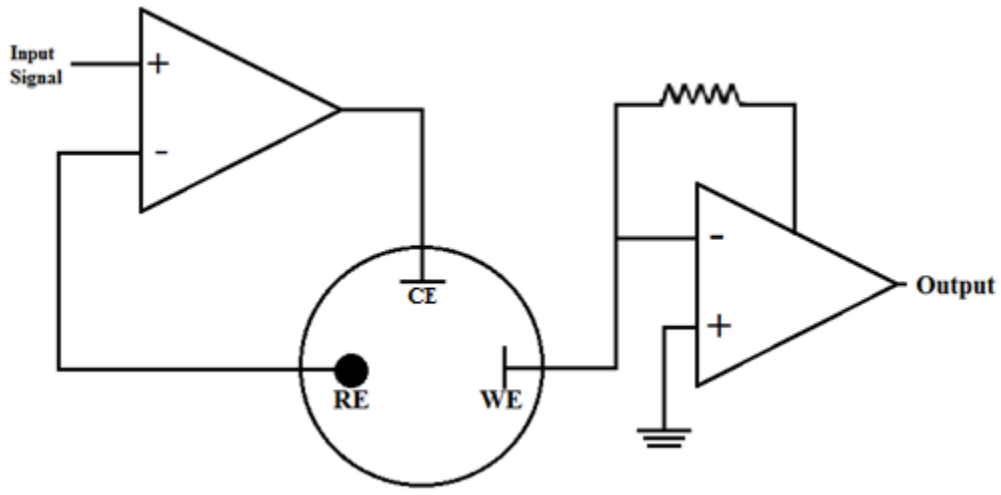

Figure 1-10 A simplified circuit diagram of a three-electrode potentiostat.

1.4.6 Fundamentals of Electrochemistry

1.4.6.1 Faradaic currents

The Faradaic current is the current that flows through an electrochemical cell that is generated by the change in oxidation state of the electroactive species occurring at the electrode surface, combined with the current contribution due to the charge transfer between the electrode and the background analyte present in solution. The faradaic current obeys Faraday's law.

1.4.6.2 Charging currents and the Electrical Double Layer

The application of a potential to the electrode surface causes ions near the electrode surface to migrate towards or away from the electrode depending on the respective charge of the electrode and the ions. This forms an electrical double layer, comprised of the electrical charge at the surface of the electrode and the charge of the ions in the solution near the electrode. This double layer leads to the generation of a non-faradaic charging current.

The electrical double layer is an array of charged particles and orientated dipoles. It is composed of two layers; the layer closest to the electrode is known as the inner Helmholtz plane (IHP) and the outer Helmholtz plane (OHP) (Figure 1-11). The planes were discovered by Hermann von Helmholtz in 1853. The IHP is composed of solvent molecules and specifically adsorbed ions, whilst the OHP represents the imagined outer layer closest to the electrode that passes through the centre of solvated ions, but is separated by the molecules at the IHP [35]. These layers are both held at the surface of the electrode. The behaviour of the interface between the electrode and the solution is similar to that of a capacitor.

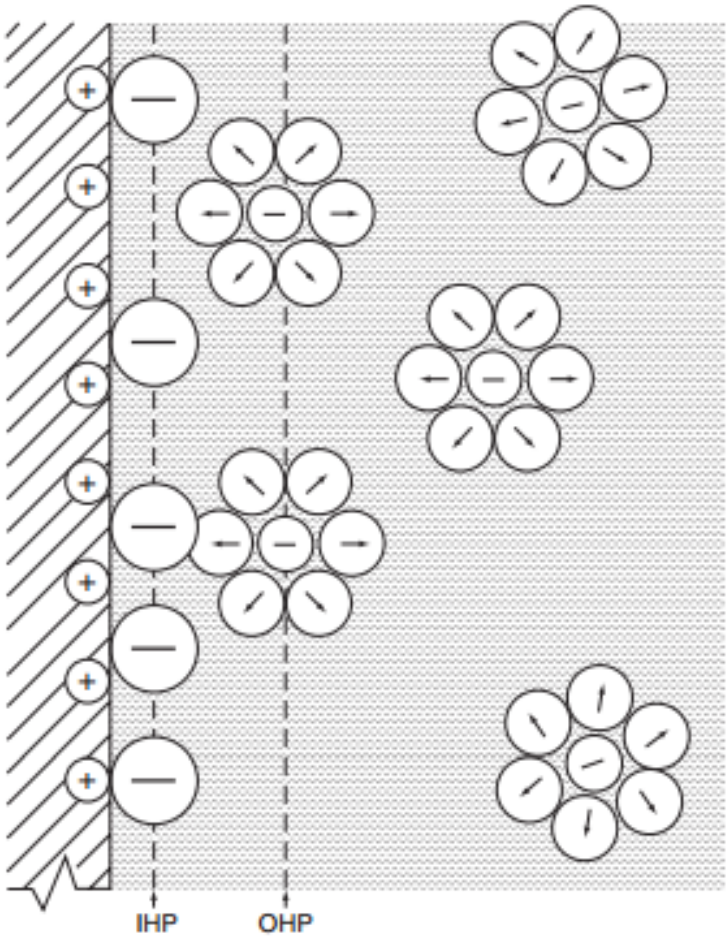

Figure 1-11: Schematic representation of the electrical double layer. Reproduced with permission from Wiley.

Beyond the double layer, is a diffuse layer of scattered ions that extents into the bulk solution. These ions are ordered relative to the coulombic forces acting upon them and the random motion of the solution by thermal motion.

The balance of the electrostatic forces on ions at the surface of the electrode, which are repelled or attracted dependent on their charge, is counterbalanced by the random motion of the diffuse layer. This causes a non-uniform distribution of ions near the electrode surface. As a result, the field strength of the potential applied to the electrode diminishes rapidly, thereby causing the double layer to be extremely thin at 10 – 20 nanometers in thickness [72], [73]. It is also essential to use a high electrolyte concentration, typically a 100 fold

greater than that of the analyte, as this concentrates the charge at the Helmholtz planes, therefore ensuring that diffusion is the dominant mechanism for mass transport [74].

1.4.6.3 Mass Transport

Mass transport occurs by three different modes:

- Diffusion: The spontaneous movement of particles as a result of a concentration gradient. Regions of high concentration move to regions of low concentration until equilibrium is established.
- Convection: The transport of particles to the electrode by an external mechanical energy such as stirring or flowing the solution, rotating or vibrating the electrode.
- Migration: The movement of charged particles along an electrical field.

1.5 Electro-analytical Techniques

The electrochemical techniques employed in this thesis study the current response of a biosensor by applying a potential (E) to a working electrode and measuring the resulting changes in current. The currents resulting from the interaction between the biosensor and the analyte can be used to quantify the analyte concentration. The technique employed will vary depending on what aspects of the cell are controlled and which are being measured. Common techniques include amperometry, chronoamperometry, cyclic voltammetry and hydrodynamic voltammetry. These techniques differ in the type of potential waveform utilised, the time that the potential is applied and wherever the measurements are conducted in a quiescent or stirred (forced convection) solution. The fundamental principles of these techniques will be discussed in this section.

1.5.1 Stirred Solution Techniques

Electrochemical techniques utilising forced convection obey Fick's first law of diffusion. Fick's first law describes the diffusional flux (*J*) in relation to the diffusion coefficient (D) and the concentration gradient (C(x)).

$$J_{(x,t)} = -D\frac{\partial C(x,t)}{\partial x} \qquad \text{Equation 6}$$

1.5.1.1 Nernst Diffusion Layer

At the surface of the electrode, a thin layer of stagnant solution known as the Nernst diffusion layer (δ) is formed. The equation for the Nernst diffusion layer is given below (Equation 7), whereby A is the electrode area, n represents the number of electrons, D is the diffusion layer constant and C_B is the concentration in bulk solution.

By deriving from Fick first law (Equation 6), an equation determining the relationship between the concentration gradient and diffusion flux within the δ. Therefore, any further increase in current is dependent on concentration in the bulk solution (C_B) [75]. The Nernst diffusion layer remains constant at a fixed stirring rate. The optimum applied potential is regarded as where the limiting current has been reached, resulting in no further increase in sensitivity. At this optimum potential, the current is limited by the diffusion of the electroactive species to the electrode surface through the δ, in accordance with Equation 7.

$$i_{LIM} = \frac{nFADC_B}{\boldsymbol{\delta}} \qquad \text{Equation 7}$$

1.5.1.2 Hydrodynamic Voltammetry

Hydrodynamic techniques are employed to determine the optimum applied potential (E_{app}) to achieve maximum sensitivity in fixed potential techniques. HDV is based on controlled convective mass transport which is achieved by stirring the solution or by rotating or vibrating of the electrode. Amperometry in stirred solution is the most commonly used HDV technique; however other techniques such as flow wall jet and rotating disc techniques are also used. The solution is stirred and the E_{app} is increased in sequential steps (Figure 1-12), until a current plateau is achieved (Figure 1-13). The steady state reached after each E_{app} increase is plotted to determine the limiting current (i_L) and therefore the optimum applied potential to be used for amperometric determinations.

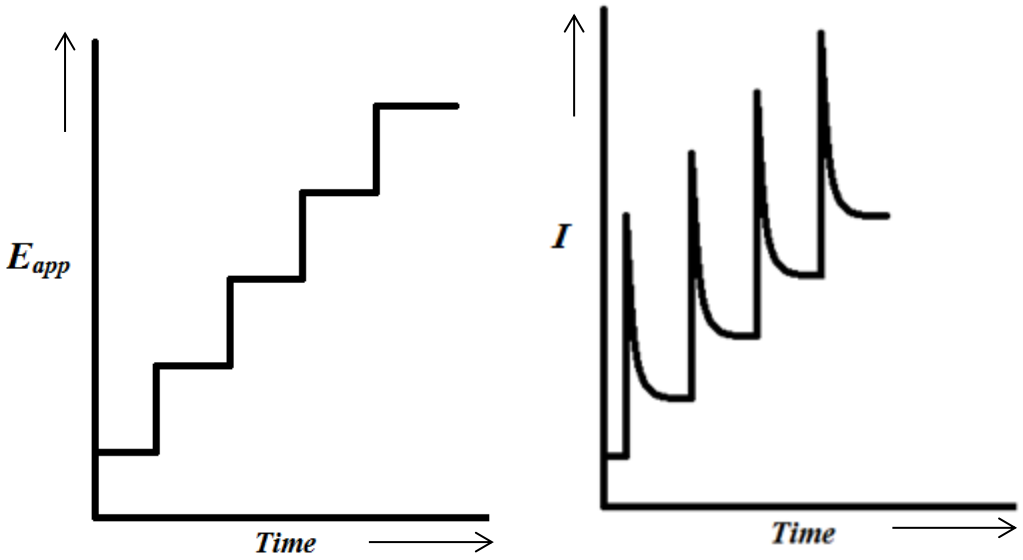

Figure 1-12 Typical electrode potential increases

Figure 1-13 Corresponding current output from potential increases

1.5.1.3 Amperometry

A fixed potential is applied to an electrode against a reference electrode (Figure 1-14) until a steady state current is generated. This is achieved more readily in a stirred solution due to the greater efficiency of mass transport. Stirring also ensures that the concentration gradient at the working electrode is constant. Once steady state is achieved, standard additions of the analyte of interest are added into the voltammetric cell. The additions result in increases in current, with each addition occurring after steady state has been achieved, the magnitude of the current is proportional to the concentration of the analyte, which in turn is proportional to the rate of the redox reaction at the working electrode surface. An example of a typical amperometric plot is shown in Figure 1-15.

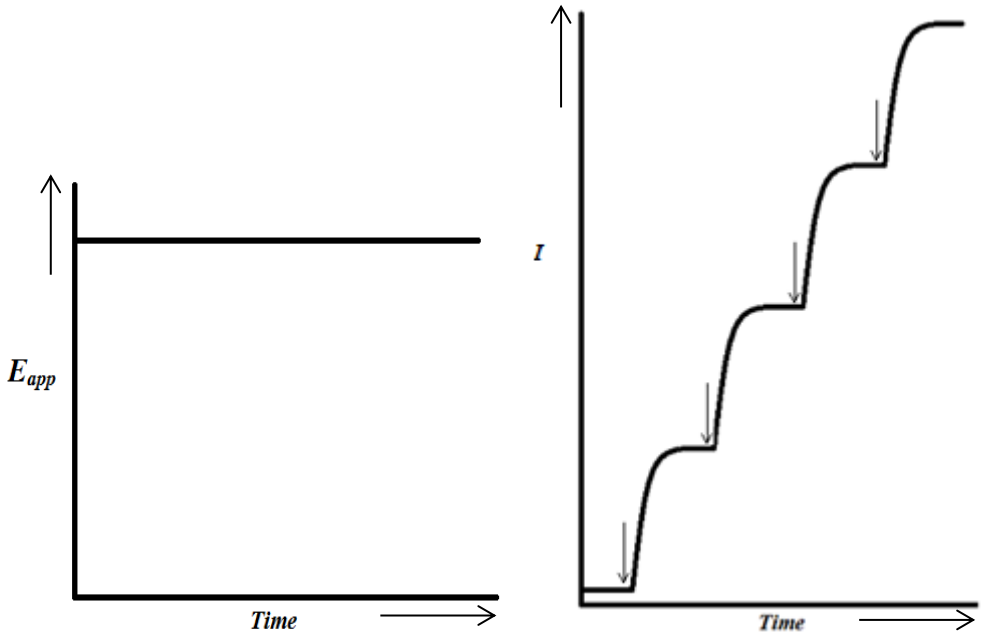

Figure 1-14: Current waveform for amperometric experiments.

Figure 1-15: A typical amperometric plot in stirred solution. Arrows indicate additions of the target analyte.

1.5.2 Quiescent Solution Techniques

In unstirred solutions, the diffusion layer (δ) is fixed. The magnitude of the current generated is derived from Ficks second law, which describes the rate of change of concentration with time, which is described in Equation 8 [76].

$$\frac{dC}{dt} = D(\frac{d^2C}{dx^2}) \qquad \text{Equation 8}$$

1.5.2.1 Cyclic Voltammetry

Cyclic voltammetry is a commonly used and versatile potentiodynamic electroanalytical technique used to study redox systems, the reversibility of the reaction, the stoichiometry of a system and the diffusion coefficient of an analyte. These can be used to determine the electrochemical characteristics and identity of an unknown compound.

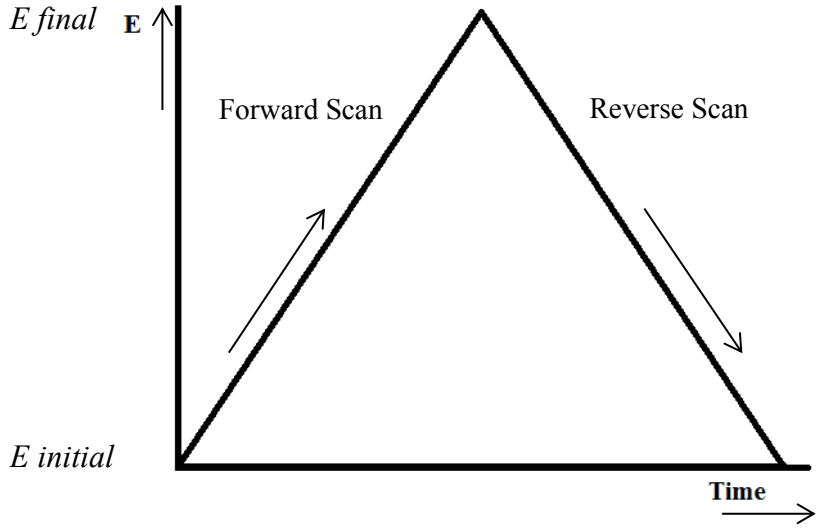

Figure 1-16. Cyclic voltammetry input waveform.

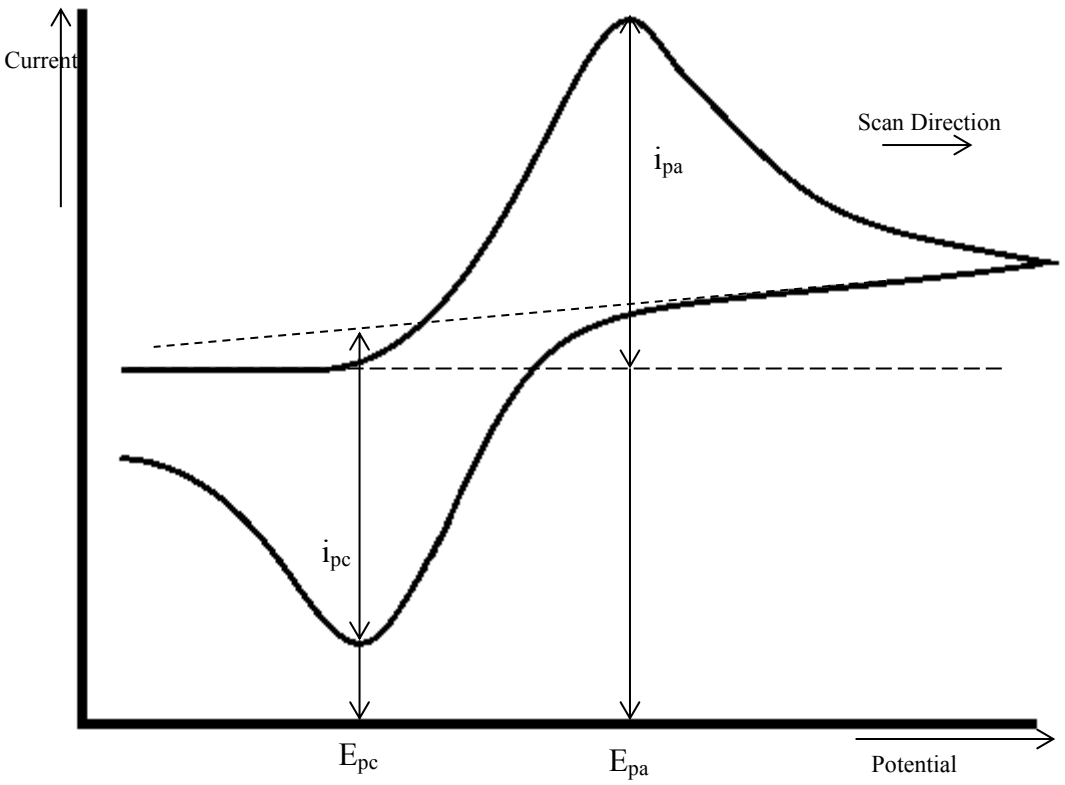

Figure 1-17 Typical Cyclic Voltammogram response for a reversible redox couple. [77]

Cyclic voltammograms are characterized by six important parameters.

- The cathodic (E_{pc}) and anodic (E_{pa}) peak potentials
- The cathodic (i_{pc}) and anodic (i_{pa}) peak currents
- The cathodic half-peak potential ($E_{p/2}$)
- The half wave potential ($E_{1/2}$)

Cyclic voltammetry linearly applies a triangular potential ramp to the working electrode at a defined scan rate (V/s)/(vt) until it has reached a set switching potential as shown in Figure 1-16. Once the switching potential on the triangular excitation potential ramp is reached, it begins a scan in the reverse direction. During the potential sweep, the current is measured resulting from the potential applied. The resulting plot of current vs. potential is known as a cyclic voltammogram, as illustrated in Figure 1-17.

The two peak currents (i_{pc}/i_{pa}) and two peak potentials (E_{pc}/E_{pa}) form the basis for the analysis of the cyclic voltammetric response to the analyte. The shape of the voltammogram is due to the concentration of the reactant (R) or product (P) at the electrode surface during the scan. Ideally, the scan begins at a potential of negligible current flow whereby the analyte is neither oxidized nor reduced. As the potential is ramped linearly, electron transfer between the electrode and the analyte in the solution begins to occur; this leads to an accumulation of product and a depletion of the reactant. The ramp increases in accordance to the Nernst Equation.

The Nernst equation relates the reduction potential of the half cell (E^o) with respect to the ratio of the concentrations of oxidized/reduced species at the surface of the electrode. This equation allows us to calculate to cell potential for any concentration. The Nernst equation is given in equation 9.

$$E = E^0 \mp \frac{RT}{nF} log_{10} \frac{[Ox]}{[Red]} \qquad \text{Equation 9}$$

Whereby, E represents the half-cell reduction potential, E^0 represents the standard half-cell reduction potential, R; the universal gas constant (8.314 J K^{-1} mol^{-1}), T; absolute temperature, n; number of electrons, F; Faraday constant, number of coulombs per mole of electrons (9.x 10^4 C mol^{-1}).

At the peak of the anodic wave the reaction becomes diffusion controlled, as the diffusion layer has grown sufficiently from the electrode that the flux of the product to the electrode is too slow to satisfy the Nernst equation. As a result, the concentration of the reactant at the surface reaches zero. Subsequently, the rate of diffusion then decreases, reducing the current flow, in accordance with the Cottrell equation. Once the potential ramp has reached the switching potential, the potential is ramped in the opposite direction resulting in a cathodic potential being applied.

The peak current for a reversible system is described by the Randles-Sevcik equation [72]. The current is directly proportional to the concentration and increases in respect to the square root of the scan rate. This dependence on scan rate implies the reaction at the electrode is controlled by mass transport. The equation applies at standard temperatures. (25°C, n = number of electrons involved, A = electrode area, D = diffusion co-efficient, C_B = bulk electrode concentration and v = scan rate).

$$ip = (2.69 * 10^5) n^{\frac{3}{2}} A D^{\frac{1}{2}} C_B v^{\frac{1}{2}} \qquad \text{Equation 10}$$

The reversibility of a electrochemically reversible couple can be identified by the measurement of the potential difference the two peak potentials. An electrochemically reversible system based on a one electron transfer process is denoted in equation A fast one electron transfer exhibits a ΔEp of 59mV.

$$\Delta Ep = Epa - Epc = \frac{59}{n} mV \qquad \text{Equation 11}$$

1.5.2.2 Chronoamperometry

Chronoamperometry differs from amperometry by being conducted in a quiescent, unstirred solution. A sufficient E_{app} is applied to drive a redox reaction at the surface (Figure 1-18a); this generates a large current which decays rapidly as the concentration of the analyte is depleted at the electrode surface due to the diffusion (Figure 1-18b).

The variation in the magnitude of current with time for a planar electrode is described by the Cottrell equation (Equation 12) [78], which is derived from Fick's second law. The equation is described as follows; N represents the number of electrons, F is the Faraday constant, A is the electrode area (cm^2), C^o is the bulk electrolyte concentration (mol/cm^3), t is time (seconds) and D is the diffusion coefficient (cm^2/s)

$$i_t = \frac{nFAC^0D^{\frac{1}{2}}}{\pi^{\frac{1}{2}}\,t^{\frac{1}{2}}} \qquad \text{Equation 12}$$

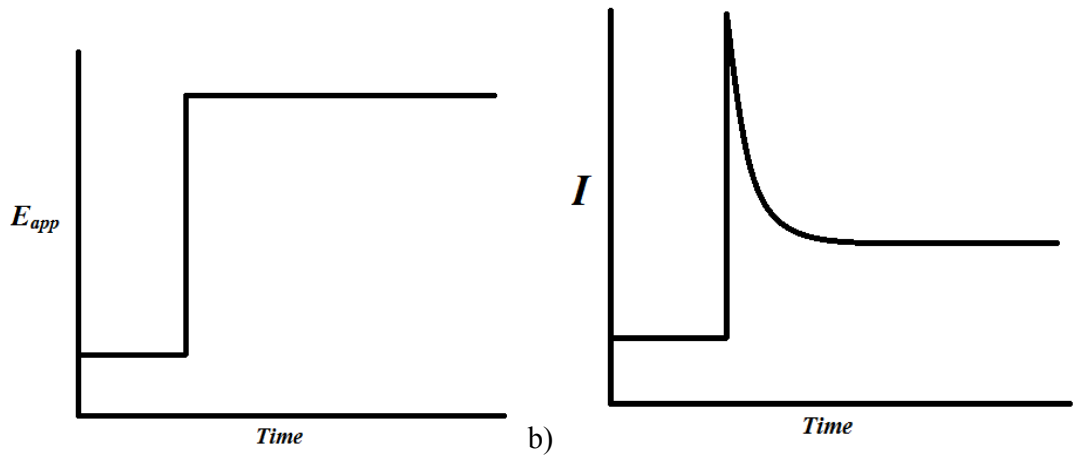

a) b)

Figure 1-18 - a) excitation waveform b) current response output generated from the excitation waveform.

1.5.3 Electrochemical Behaviour using Miniaturized Electrodes

In this section, a brief description of the types of voltammetric signals achieved at microelectrodes together with some important diagnostic equations to elucidate microelectrode behaviour will be discussed.

Microelectrodes differ from traditional conventional sized macroelectrodes by possessing one dimension that does not exceed 25 micrometers [79]. Microelectrodes possess the following properties: high current densities, the generation of small currents (typically on the picoamp / nanoamp scale), fast establishment of steady state signals, resistance to ohmic drop and short response times [80].

During short experimental timescales, for example, when conducting cyclic voltammetry with fast scan rates (>50 mV/s), planar diffusion occurs, thus the current will decay in accordance with the Cottrell equation (Equation 12). This only occurs in the short time in which the diffusion layer (δ), is smaller than the radius (*r*) of the electrode.

During long experimental timescales, when $\delta > r$, radial (nonplanar) diffusion dominates mass transport, thus under these conditions the current density becomes steady state as given by Equation 13, whereby r is the microelectrode radius, n is number of electrons in the reaction, D is the diffusion coefficient in cm^2/s, C is the bulk concentration of the electroactive species in mol/cm^3, and r is the radius of the microelectrode in cm.

$$i_d = \frac{nFDc^{\infty}}{r_s} \qquad \text{Equation 13}$$

The steady state limiting current is directly proportional to the concentration of the analyte and the diffusion coefficient. Therefore, if the diffusion coefficient is known, the concentration of the analyte can also be calculated.

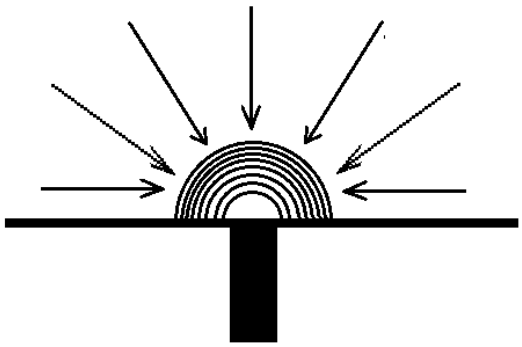

Figure 1-19: Radial diffusion at the surface of a microelectrode and the hemispherical shape of the diffusion layer extending out into the bulk solution. Arrows indicate the direction of diffusion to the electrode.

Due to this increased flux to the surface, a concentration gradient between the electrode and the bulk solution occurs, known as the diffusion layer. At longer experimental time scales this diffusion layer exceeds the radius of the microelectrode, becoming a spherical diffusion field as illustrated in Figure 1-19. This increased flux, results in more efficient mass transport, leading to steady state responses and increased current densities.

Subsequent studies discussed in the thesis are based on microband electrodes. These microelectrodes possess a different geometry to co-planar disc-shaped microelectrodes, thus Equation 14 will be applied to illustrate microband behaviour [81]. Microband electrodes possess an increased electrode area due to the 3mm length, whilst the width of the microelectrode is within the micrometre range, therefore radial diffusion is diffusion is dominant leading to microelectrode characteristics [82].

$$i_{LIM} = 2\pi FCDl \frac{1}{\ln(4Dt\pi/W^2)} \qquad \text{Equation 14}$$

Radial diffusion, as illustrated in Figure 1-19, leads to higher current densities under steady-state (time independent) conditions, as a result of the increased flux of electroactive species to the surface of the electrode. However, the diffusion that occurs at a microband electrode as shown in Figure 1-20, is not uniform, thus edge mass transport dominates [83].

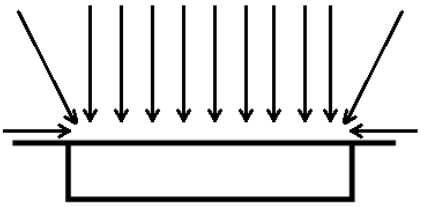

Figure 1-20: A schematic diagram of a microband electrode.

Figure 1-21 illustrates a typical microelectrode voltammogram in a under state-state conditions in an electrochemically reversible system at a slow scan rate. Microelectrodes present voltammograms possessing a sigmoidal shape with no peaks, smaller current magnitudes and steady-state/constant currents. If the scan rate is increased planar diffusion occurs and typical cyclic voltammetric behaviour is observed.

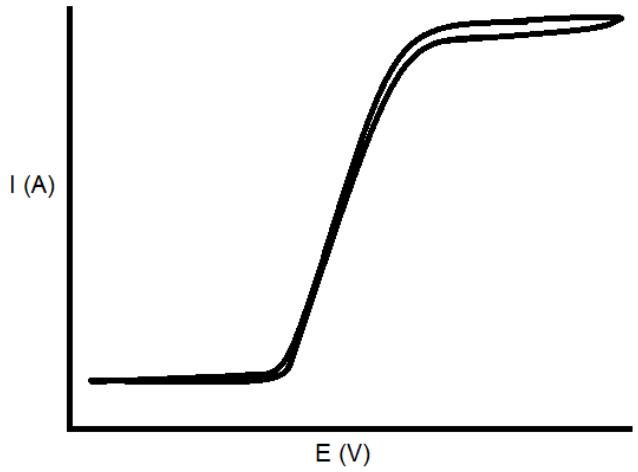

Figure 1-21: A typical cyclic voltammogram displaying microelectrode behaviour, at a slow scan rate.

1.6 Aims and Objectives

The aim of the work described in this thesis was to develop amperometric, screen printed glutamate biosensors and to apply these devices for the determination of glutamate in clinical and food studies, as well as to toxicity studies. For the latter the intention was to monitor, glutamate released by HepG2 cells in response to toxic challenge from paracetamol. The objectives were;

- Development of a glutamate biosensor utilising glutamate dehydrogenase, NAD^+ based on Meldola's Blue screen printed carbon electrodes.
- Immobilisation of the enzyme glutamate dehydrogenase to the surface of the working electrode the MB-SPCE to produce glutamate biosensors.
- Optimisation of the biosensor working conditions and the determination of the glutamate content of food and clinical samples utilising standard addition.
- Further development of the biosensor to immobilize the cofactor NAD^+ onto the surface of the screen-printed carbon electrode.
- The miniaturisation of the biosensor in order to develop microband biosensors for the determination of glutamate released by HepG2 cells in response to toxic challenge.
- Development of an electrode holder to simultaneously immerse the biosensor within the cell media solution for the interrogation of the cells, whilst reducing evaporation and allowing for gas exchange between the cell media and atmosphere.
- Development of a conventional sized reagentless glutamate biosensor.
- Optimisation of the biosensor components and working conditions, in order to apply the reagentless biosensor to the determination of glutamate in complex samples.

1.7 References

[1] D. Purves, G. J. Augustine, D. Fitzpatrick, L. C. Katz, A.-S. LaMantia, J. O. McNamara, and S. M. Williams, "Glutamate." Sinauer Associates, (2001).

[2] E. M. Tsapakis, (2002), "Glutamate and psychiatric disorders," *Adv. Psychiatr. Treat.*, **8**, 189–197.

[3] J. J. Vornov, R. C. Tasker, and J. Park, (1995), "Neurotoxicity of acute glutamate transport blockade depends on coactivation of both NMDA and AMPA/Kainate receptors in organotypic hippocampal cultures.," *Exp. Neurol.*, **133**, 7–17.

[4] A. Lau and M. Tymianski, (2010), "Glutamate receptors, neurotoxicity and neurodegeneration.," *Pflugers Arch.*, **460**, 525–42.

[5] D. A. Butterfield and C. B. Pocernich, (2003), "The glutamatergic system and Alzheimer's disease: therapeutic implications.," *CNS Drugs*, **17**, 641–52.

[6] J. M. Berg, J. L. Tymoczko, and L. Stryer, "The First Step in Amino Acid Degradation Is the Removal of Nitrogen." W H Freeman, (2002).

[7] J. T. Brosnan, (2000), "Glutamate, at the interface between amino acid and carbohydrate metabolism.," *J. Nutr.*, **130**, 988S–90S.

[8] J. T. Brosnan, K. C. Man, D. E. Hall, S. A. Colbourne, and M. E. Brosnan, (1983), "Interorgan metabolism of amino acids in streptozotocin-diabetic ketoacidotic rat.," *Am. J. Physiol.*, **244**, E151–8.

[9] S. L. Fink and B. T. Cookson, (2005), "Apoptosis, pyroptosis, and necrosis: mechanistic description of dead and dying eukaryotic cells.," *Infect. Immun.*, **73**, 1907–16.

[10] "Cost to Develop New Pharmaceutical Drug Now Exceeds $2.5B - Scientific American." [Online]. Available: http://www.scientificamerican.com/article/cost-to-develop-new-pharmaceutical-drug-now-exceeds-2-5b/. [Accessed: 08-Apr-2015].

[11] M. R. Fielden and K. L. Kolaja, (2008), "The role of early in vivo toxicity testing in drug discovery toxicology.," *Expert Opin. Drug Saf.*, **7**, 107–10.

[12] M. B. Bracken, (2009), "Why animal studies are often poor predictors of human reactions to exposure.," *J. R. Soc. Med.*, **102**, 120–2.

[13] G. Repetto, A. del Peso, and J. L. Zurita, (2008), "Neutral red uptake assay for the estimation of cell viability/cytotoxicity.," *Nat. Protoc.*, **3**, 1125–31.

[14] R. R. Tice, E. Agurell, D. Anderson, B. Burlinson, A. Hartmann, H. Kobayashi, Y. Miyamae, E. Rojas, J. C. Ryu, and Y. F. Sasaki, (2000), "Single cell gel/comet assay: guidelines for in vitro and in vivo genetic toxicology testing.," *Environ. Mol. Mutagen.*, **35**, 206–21.

[15] A. Astashkina, B. Mann, and D. W. Grainger, (2012), "A critical evaluation of in vitro cell culture models for high-throughput drug screening and toxicity.," *Pharmacol. Ther.*, **134**, 82–106.

[16] R. C. Alkire, D. M. Kolb, and J. Lipkowski, Eds., *Advances in Electrochemical Science and Engineering*. Weinheim, Germany: Wiley-VCH Verlag GmbH & Co. KGaA, (2011).

[17] W. G. E. J. Schoonen, J. A. D. M. de Roos, W. M. A. Westerink, and E. Débiton, (2005), "Cytotoxic effects of 110 reference compounds on HepG2 cells and for

60 compounds on HeLa, ECC-1 and CHO cells. II mechanistic assays on NAD(P)H, ATP and DNA contents.," *Toxicol. In Vitro*, **19**, 491–503.

[18] J. Xu, M. Ma, and W. M. Purcell, (2003), "Characterisation of some cytotoxic endpoints using rat liver and HepG2 spheroids as in vitro models and their application in hepatotoxicity studies. I. Glucose metabolism and enzyme release as cytotoxic markers," *Toxicol. Appl. Pharmacol.*, **189**, 100–111.

[19] R. M. Pemberton, F. J. Rawson, J. Xu, R. Pittson, G. A. Drago, J. Griffiths, S. K. Jackson, and J. P. Hart, (2010), "Application of screen-printed microband biosensors incorporated with cells to monitor metabolic effects of potential environmental toxins," *Microchim. Acta*, **170**, 321–330.

[20] S. Knasmüller, V. Mersch-Sundermann, S. Kevekordes, F. Darroudi, W. W. Huber, C. Hoelzl, J. Bichler, and B. J. Majer, (2004), "Use of human-derived liver cell lines for the detection of environmental and dietary genotoxicants; current state of knowledge.," *Toxicology*, **198**, 315–28.

[21] J. V. Castell and M. José Gómez-Lechón, *In Vitro Methods in Pharmaceutical Research*. Academic Press, (1996).

[22] S. Wilkening, F. Stahl, and A. Bader, (2003), "Comparison of primary human hepatocytes and hepatoma cell line Hepg2 with regard to their biotransformation properties.," *Drug Metab. Dispos.*, **31**, 1035–42.

[23] S. J. Fey and K. Wrzesinski, (2012), "Determination of drug toxicity using 3D spheroids constructed from an immortal human hepatocyte cell line.," *Toxicol. Sci.*, **127**, 403–11.

[24] L. C. CLARK and C. LYONS, (1962), "Electrode systems for continuous monitoring in cardiovascular surgery.," *Ann. N. Y. Acad. Sci.*, **102**, 29–45.

[25] J. Wang, (2001), "Glucose Biosensors: 40 Years of Advances and Challenges," *Electroanalysis*, **13**, 983–988.

[26] J. Wang, (2008), "Electrochemical glucose biosensors.," *Chem. Rev.*, **108**, 814–25.

[27] S. F. Clarke and J. R. Foster, (2012), "A history of blood glucose meters and their role in self-monitoring of diabetes mellitus.," *Br. J. Biomed. Sci.*, **69**, 83–93.

[28] D. Thévenot, K. Toth, R. Durst, and G. Wilson, (2001), "Electrochemical biosensors: recommended definitions and classification," *Biosens. Bioelectron.*, **16**, 121–131.

[29] B. R. Eggins, *Chemical Sensors and Biosensors (Google eBook)*. John Wiley & Sons, (2008).

[30] L. Gorton, *Biosensors and Modern Biospecific Analytical Techniques*. Elsevier, (2005).

[31] F. Tasca, M. N. Zafar, W. Harreither, G. Nöll, R. Ludwig, and L. Gorton, (2011), "A third generation glucose biosensor based on cellobiose dehydrogenase from Corynascus thermophilus and single-walled carbon nanotubes.," *Analyst*, **136**, 2033–6.

[32] M. N. Zafar, G. Safina, R. Ludwig, and L. Gorton, (2012), "Characteristics of third-generation glucose biosensors based on Corynascus thermophilus cellobiose

dehydrogenase immobilized on commercially available screen-printed electrodes working under physiological conditions.," *Anal. Biochem.*, **425**, 36–42.

[33] J. D. Newman, A. P. F. Turner, and G. Marrazza, (1992), "Ink-jet printing for the fabrication of amperometric glucose biosensors," *Anal. Chim. Acta*, **262**, 13–17.

[34] I. Takatsu and T. Moriizumi, (1987), "Solid state biosensors using thin-film electrodes," *Sensors and Actuators*, **11**, 309–317.

[35] J. Wang., *Analytical electrochemistry*. Wiley-VCH.

[36] P. Kugler and K. H. Wrobel, (1978), "Meldola blue: a new electron carrier for the histochemical demonstration of dehydrogenases (SDH, LDH, G-6-PDH).," *Histochemistry*, **59**, 97–109.

[37] "Electrode for the electrochemical regeneration of coenzyme, a method of making said electrode, and the use thereof." (25-Dec-1984).

[38] L. Gorton, A. Torstensson, H. Jaegfeldt, and G. Johansson, (1984), "Electrocatalytic oxidation of reduced nicotinamide coenzymes by graphite electrodes modified with an adsorbed phenoxazinium salt, meldola blue," *J. Electroanal. Chem. Interfacial Electrochem.*, **161**, 103–120.

[39] S. D. Sprules, J. P. Hart, S. A. Wring, and R. Pittson, (1994), "Development of a disposable amperometric sensor for reduced nicotinamide adenine dinucleotide based on a chemically modified screen-printed carbon electrode," *Analyst*, **119**, 253.

[40] A. S. Santos, R. S. Freire, and L. T. Kubota, (2003), "Highly stable amperometric biosensor for ethanol based on Meldola's blue adsorbed on silica gel modified with niobium oxide," *J. Electroanal. Chem.*, **547**, 135–142.

[41] L. Zhu, J. Zhai, R. Yang, C. Tian, and L. Guo, (2007), "Electrocatalytic oxidation of NADH with Meldola's blue functionalized carbon nanotubes electrodes."

[42] L. T. Kubota, F. Gouvea, A. N. Andrade, B. G. Milagres, and G. De Oliveira Neto, (1996), "Electrochemical sensor for NADH based on Meldola's blue immobilized on silica gel modified with titanium phosphate," *Electrochim. Acta*, **41**, 1465–1469.

[43] G. Marko-Varga, R. Appelqvist, and L. Gorton, (1986), "A glucose sensor based on glucose dehydrogenase adsorbed on a modified carbon electrode," *Anal. Chim. Acta*, **179**, 371–379.

[44] S. D. Sprules, J. P. Hart, S. A. Wring, and R. Pittson, (1995), "A reagentless, disposable biosensor for lactic acid based on a screen-printed carbon electrode containing Meldola's Blue and coated with lactate dehydrogenase, NAD+ and cellulose acetate," *Anal. Chim. Acta*, **304**, 17–24.

[45] M. Piano, S. Serban, R. Pittson, G. a Drago, and J. P. Hart, (2010), "Amperometric lactate biosensor for flow injection analysis based on a screen-printed carbon electrode containing Meldola's Blue-Reinecke salt, coated with lactate dehydrogenase and NAD+.," *Talanta*, **82**, 34–7.

[46] A. K. Abass, J. P. Hart, D. C. Cowell, and A. Chappell, (1998), "Development of an amperometric assay for NH+4 based on a chemically modified screen-printed NADH sensor," *Anal. Chim. Acta*, **373**, 1–8.

[47] R. Doaga, T. McCormac, and E. Dempsey, (2009), "Electrochemical Sensing of NADH and Glutamate Based on Meldola Blue in 1,2-Diaminobenzene and 3,4-Ethylenedioxythiophene Polymer Films," *Electroanalysis*, **21**, 2099–2108.

[48] S. D. Sprules, I. C. Hartley, R. Wedge, J. P. Hart, and R. Pittson, (1996), "A disposable reagentless screen-printed amperometric biosensor for the measurement of alcohol in beverages," *Anal. Chim. Acta*, **329**, 215–221.

[49] C. A. B. Garcia, G. de Oliveira Neto, L. T. Kubota, and L. A. Grandin, (1996), "A new amperometric biosensor for fructose using a carbon paste electrode modified with silica gel coated with Meldola's Blue and fructose 5-dehydrogenase," *J. Electroanal. Chem.*, **418**, 147–151.

[50] R. F. de Castilho, E. B. R. de Souza, R. V. da Silva Alfaya, and A. A. da Silva Alfaya, (2008), "Meldola's Blue Immobilized on a SiO2/SnO2/Phosphate Xerogel, a New Sensor for Determination of Ascorbic Acid in Medicine and Commercial Fruit Juice," *Electroanalysis*, **20**, 157–162.

[51] F. Scheller and F. Schubert, *Biosensors*, **21**. Elsevier, (1991).

[52] R. C. Alkire, D. M. Kolb, J. Lipkowski, and P. N. Ross, *Bioelectrochemistry: Fundamentals, Applications and Recent Developments*. John Wiley & Sons, (2013).

[53] S. Datta, L. R. Christena, and Y. R. S. Rajaram, (2012), "Enzyme immobilization: an overview on techniques and support materials," *3 Biotech*, **3**, 1–9.

[54] R. A. Sheldon, (2007), "Enzyme Immobilization: The Quest for Optimum Performance," *Adv. Synth. Catal.*, **349**, 1289–1307.

[55] N. C. Foulds and C. R. Lowe, (1986), "Enzyme entrapment in electrically conducting polymers. Immobilisation of glucose oxidase in polypyrrole and its application in amperometric glucose sensors," *J. Chem. Soc. Faraday Trans. 1 Phys. Chem. Condens. Phases*, **82**, 1259.

[56] T. Jesionowski, J. Zdarta, and B. Krajewska, (2014), "Enzyme immobilization by adsorption: a review," *Adsorption*, **20**, 801–821.

[57] B. Krajewska, (2004), "Application of chitin- and chitosan-based materials for enzyme immobilizations: a review," *Enzyme Microb. Technol.*, **35**, 126–139.

[58] H. S. Stoker, *Organic and Biological Chemistry*. Cengage Learning, (2012).

[59] D. E. Koshland, (1995), "The Key–Lock Theory and the Induced Fit Theory," *Angew. Chemie Int. Ed. English*, **33**, 2375–2378.

[60] R. B. Silverman, *The Organic Chemistry of Enzyme-catalyzed Reactions*. Academic Press, (2002).

[61] J. M. Berg, J. L. Tymoczko, and L. Stryer, "The Michaelis-Menten Model Accounts for the Kinetic Properties of Many Enzymes." W H Freeman, (2002).

[62] R. A. Copeland, *Enzymes: A Practical Introduction to Structure, Mechanism, and Data Analysis*. John Wiley & Sons, (2004).

[63] M. Li, C. Li, A. Allen, C. A. Stanley, and T. J. Smith, (2012), "The structure and allosteric regulation of mammalian glutamate dehydrogenase.," *Arch. Biochem. Biophys.*, **519**, 69–80.

[64] T. J. . B. P. J. . B. K. L. . R. D. W. Stillman, (1993), "Conformational flexibility in glutamate dehydrogenase. Role of water in substrate recognition and catalysis.," *J.Mol.Biol.*, **234**, 1131–1139.

[65] R. A. H. P. D., R. A. Harvey, and D. R. Ferrier, *Biochemistry*. Lippincott Williams & Wilkins, (2011).

[66] M. W. King, "Nitrogen Metabolism and the Urea Cycle," *The Medical Biochemistry Page*, (2013). [Online]. Available: http://themedicalbiochemistrypage.org/nitrogen-metabolism.php. [Accessed: 15-Nov-2013].

[67] M. J. Lobo, A. J. Miranda, and P. Tuñón, (1997), "Amperometric biosensors based on NAD(P)-dependent dehydrogenase enzymes," *Electroanalysis*, **9**, 191–202.

[68] V. S. Bagotsky, *Fundamentals of Electrochemistry*. John Wiley & Sons, (2005).

[69] J. Wang, B. Tian, V. B. Nascimento, and L. Angnes, (1998), "Performance of screen-printed carbon electrodes fabricated from different carbon inks," *Electrochim. Acta*, **43**, 3459–3465.

[70] *Electroanalytical Methods: Guide to Experiments and Applications*, **28**. Springer Science & Business Media, (2009).

[71] A. J. Fry, *Synthetic Organic Electrochemistry*. John Wiley & Sons, (1989).

[72] P. T. Kissinger and W. R. Heineman, (1983), "Cyclic voltammetry," *J. Chem. Educ.*, **60**, 702.

[73] P. T. Kissinger and W. R. Heineman, *Laboratory Techniques in Electroanalytical Chemistry, Second Edition, Revised and Expanded*. CRC Press, (1996).

[74] A. C. Fisher, *Electrode Dynamics*. Oxford University Press, (1996).

[75] T. Kuwana, *Physical Methods in Modern Chemical Analysis, Volume 3*. Elsevier, (1983).

[76] J. Cooper and T. Cass, *Biosensors*. Oxford University Press, USA, (2004).

[77] R. A. Marusak, K. Doan, and S. D. Cummings, *Integrated Approach to Coordination Chemistry*. Hoboken, NJ, USA: John Wiley & Sons, Inc., (2007).

[78] J. O. Bockris, A. K. N. Reddy, and M. Gamboa-Aldeco, *Modern Electrochemistry, Volume 2*. Springer, (2000).

[79] J. Wang, *Analytical Electrochemistry*. John Wiley & Sons, (2004).

[80] R. J. Forster, (1994), "Microelectrodes: new dimensions in electrochemistry," *Chem. Soc. Rev.*, **23**, 289.

[81] J. P. Metters, R. O. Kadara, and C. E. Banks, (2012), "Electroanalytical properties of screen printed graphite microband electrodes," *Sensors Actuators B Chem.*, **169**, 136–143.

[82] J. P. Metters, R. O. Kadara, and C. E. Banks, (2013), "Fabrication of co-planar screen printed microband electrodes.," *Analyst*, **138**, 2516–21.

[83] A. M. Bond, *Broadening Electrochemical Horizons: Principles and Illustration of Voltammetric and Related Techniques*. Oxford University Press, (2002).

CHAPTER TWO

Literature Review: The design, development and application of electrochemical glutamate biosensors

2. Contents

2.1 Introduction

This review discusses electrochemical biosensors fabricated based on glutamate oxidase or glutamate dehydrogenase. The method of enzyme immobilization and, where applicable, the application of glutamate biosensors to biological and food samples.

2.2 Biosensors based on glutamate oxidase

In this section, the fabrication methods are sub-divided according to the technique of enzyme immobilization. The electrochemical response can generally be described by the following equations:

$$\text{Glutamate} + O_2 \xrightarrow{\text{GluOx}} H_2O_2 + \alpha\text{-ketoglutarate} \quad (1)$$

$$H_2O_2 \longrightarrow 2H^+ + O_2 + 2e^- \quad (2)$$

Equation 1 represents the enzymatic oxidation of the glutamate to form α-ketoglutarate and H_2O_2. Equation 2 describes the electrochemical detection of hydrogen peroxide at the base transducer which generates the analytical response.

2.2.1 Entrapment

The entrapment of enzymes is defined as the integration of an enzyme within the lattice of a polymer matrix or a membrane, whilst retaining the protein structure of the enzyme [10]. In addition to the immobilization of enzymes, membranes can also eliminate potential interfering species that may be present in complex media such as serum and food.

A selective biosensor for the determination of glutamate in food seasoning was developed by incorporating glutamate oxidase into a poly(carbamoyl) sulfonate (PCS) hydrogel. The GluOx-PCS mixture was then drop-coated onto the surface of a thick-film platinum electrode [11]. Liquid samples (1, 10 and 100μL) were diluted to 10mL with phosphate buffer. The biosensor was then utilised to determine the glutamate recovery from different concentrations of the sample. The results generated correlated favourably with a L-glutamate colorimetric test kit.

A recent application of a micro glutamate biosensor for investigating artificial cerebrospinal fluid (CSF) under hypoxic conditions was described [12]. The fabrication method is a complex, multi-step process whereby glutamate oxidase is incorporated with chitosan and ceria-titania nanoparticles (Figure 1).

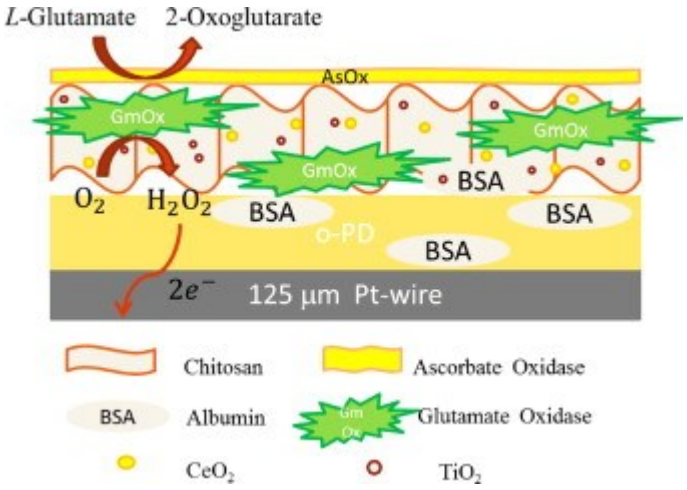

Figure 2-1: Schematic illustration of the biosensor design and the GluA detection principle. (Reprinted with permission from [12], Elsevier)

The nanoparticles are able to store and release oxygen in its crystalline structure; it can supply O_2 to GluOx to generate H_2O_2 in the absence of environmental oxygen. The biosensor was evaluated with artificial CSF which had been fortified with glutamate over the physiological range; the device was found to operate over the concentration of interest under anaerobic conditions.

A device for the measurement of glutamate in brain extracellular fluid utilising a relatively simple fabrication procedure has been reported [13]. The procedure involved dipping a 60-µm radius Teflon coated platinum wire into a buffered solution containing glutamate oxidase and *o*-phenylenediamine (PPD), followed by a solution containing phosphatidylethanolamine (PEA) and bovine serum albumin (BSA). The glutamate oxidase was entrapped by the electropolymerization of PPD on the surface of the electrode. The PPD and PEA was used to block out interferences.

An interesting entrapment approach employing polymers to encapsulate GluOx onto a gold electrode has been reported [14]. The first step involved the immersion of a gold disc electrode in 3-mercaptopropionic acid (MPA) solution, followed by drop-coating layers of poly-L-lysine and poly(4-styrenesulfonate). Once dry, a mixture of GluOx and glutaraldehyde was drop-coated on to the surface to form a bilayer. The authors suggested that MPA increases the adhesion of the polyion complex to the gold surface by the electrostatic interaction between the carboxyl groups present on the MPA and the amino groups present on the poly-L-lysine. A response time of only 3 seconds was achieved after an addition of 20nM glutamic acid, which gave a current of 0.037 nA (1.85 nA/μM). A linear response was observed between 20μM and 200μM. Both the response time and limit of detection are superior to previously discussed biosensors. It was suggested that the rapid response was due to the close proximity of the enzymatic reaction to the surface of the electrode. For this method of fabrication of glutamate oxidase based biosensors, the latter approach leads to the lowest limit of detection.

The increased interest in glutamate measurement has led to the commercial development of an *in vivo* glutamate biosensor by Pinnacle Technology Inc. [15]; this has been successfully used for monitoring of real-time changes of glutamate concentrations in rodent brain. The biosensor employs an enzyme layer composed of GluOx and an "inner-selective" membrane, composed of an undisclosed material that eliminates interferences. The enzymatically generated hydrogen peroxide is monitored using a platinum-iridium electrode. The biosensor possesses a linear-range up to 50μM. The manufacturers indicate that the miniaturised biosensor requires calibration upon completion of an experiment in order to ensure the selectivity and integrity of the sensors.

2.2.2 Covalent-bonding

The application of a glutamate oxidase based biosensor for the measurement of glutamate in the serum of healthy and epileptic patients has been described [16]. The fabrication method

consists of electrodepositing chitosan (CHIT), gold nanoparticles (AuNP) and multiwalled carbon nanotubes (MWCNTs) on the surface of a gold electrode.

The serum sample was diluted with phosphate buffer solution (PBS) before analysis. The concentration of the glutamate in the sample was determined using a standard calibration curve constructed from the amperometric responses obtained with glutamate in PBS. The results compared favourably with a colorimetric test kit. A low operating potential of +0.135 V vs. Ag/AgCl for measuring the enzymatically generated H_2O_2 was significantly lower than other biosensors based on GluOx [13,17], The time taken to reach 95% of the maximum steady state response was 2 seconds after the initial injection. This method of fabrication whilst complex, possesses a significantly lower operating potential when compared to other biosensors fabricated using entrapment techniques.

2.2.3 Cross-linking

Enzyme immobilization can be achieved by intermolecular cross-linking of the protein structure of the enzyme to other protein molecules or within an insoluble support matrix. Jamal et. al. [17] have described a complex entrapment method which consisted of drop-coating a 10µL mixture of GluOx (25U in 205µL), 2mg of BSA, 20µL of glutaraldehyde (2.5% w/v) and 10µL of Nafion (0.5%) onto a platinum nanoparticle modified gold nanowire array (PtNP-NAE) and allowing it to dry overnight under ambient conditions. The fabrication technique is illustrated in Figure 2-2. The analytical response results from the oxidation of H_2O_2 at the gold nanowire electrode as illustrated in Equation 2.

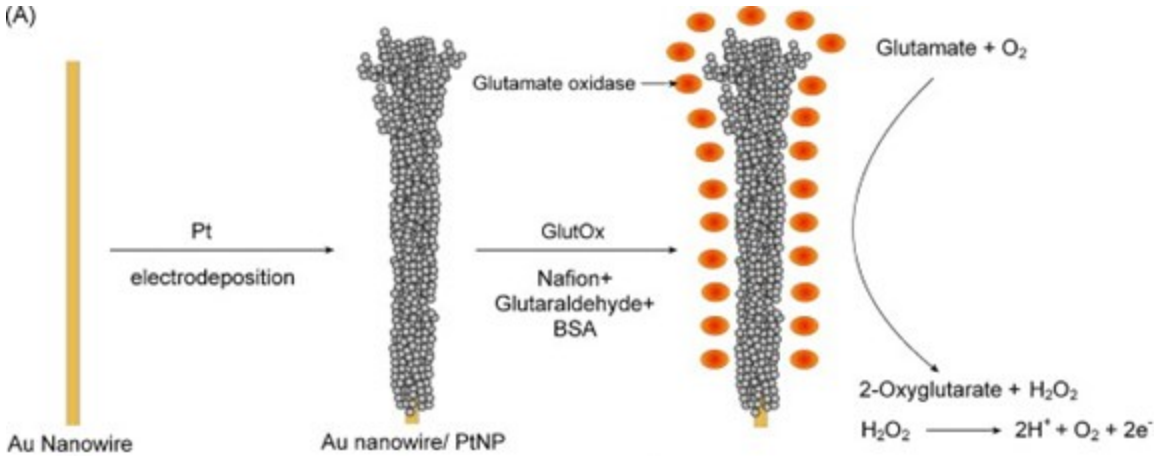

Figure 2-2: Schematic illustration of stepwise fabrication of the GlutOx/PtNP/NAEs electrodes. Reprinted with permission from [18], Elsevier.

The high sensitivity obtained appears to be related to the presence of the nanoparticles at the gold electrode surface. The nanoparticles act as conduction centres and facilitate the transfer of electrons towards the gold electrode. Additionally, a high enzyme loading was utilised, which in combination with the nanoparticles, resulted in increased enzyme immobilisation to the surface. However, given the high enzyme loading and use of both a gold nanowire electrode and platinum nanoparticles, the biosensor is unlikely to be commercially viable due to its high cost.

GluOx was immobilized to the surface of a palladium-electrodeposited screen printed carbon strip by a simple crosslinking immobilisation technique using a photo-crosslinkable polymer (PVA-SbQ) [18]. The biosensor exhibited a stable steady state response for six hours in a stirred solution indicating that the enzyme was fully retained within the polymer membrane.

A glutamate biosensor [19] was successfully applied to the determination of MSG in soy sauce, tomato sauce, chicken thai soup and chilli chicken. MSG levels compared very favourably with a spectrophotometric method (2 - 5% CoV based on n = 5). The biosensor was fabricated by mixing glutamate oxidase, BSA and glutaraldehyde, then spreading the mixture onto the surface of an O_2 permeable poly-carbonate membrane. The membrane was

then attached to an oxygen probe using a push cap system and oxygen consumption was measured at an applied potential of -0.7 V; this is a considerably more negative operating potential compared to previously discussed biosensors. In this case, the response is a result of the reduction reaction shown in Equation 3.

$$O_2 + 2e^- + 2H^+ \longrightarrow H_2O_2 \quad (3)$$

The lowest limit of detection achieved with a glutamate biosensor was fabricated by covalently immobilizing glutamate oxidase onto polypyrrole nanoparticles and polyaniline composite film (PPyNPs/PANI) [20]. Cyclic voltammetry was used to co-electropolymerize the compounds onto the surface. The PPyNPs act as an electron transfer mediator which allows a low operating potential to be employed (+85 mVs), that reduces the likelihood of oxidising interferences. The authors also claim that this leads to an increase in the sensitivity of the biosensor. The biosensor was successfully applied to the determination of glutamate in food samples including tomato soup and noodles. High recoveries of 95% - 97% were achieved which compares favourably with values attained by previously discussed biosensors [19].

2.3 Biosensors based on glutamate dehydrogenase

This section is subdivided in a similar way to section 2, ie: according to the method of immobilization. The electrochemical response can generally be described by the following equations:

$$\text{Glutamate} + NAD^+ \xrightarrow{\text{GLDH}} NADH + \alpha\text{-ketoglutarate} \quad (4)$$

$$NADH + \text{Mediator}_{ox} \longrightarrow NAD^+ + \text{Mediator}_{red} \quad (5)$$

$$\text{Mediator}_{red} \longrightarrow ne^- + mH^+ + \text{Mediator}_{ox} \quad (6)$$

Equation 4 represents the enzymatic reduction of the cofactor NAD^+ to NADH and the oxidation of glutamate to α-ketoglutarate. Equation 5 represents the electrochemical reduction of the oxidised mediator to the reduced form (Mediator_{red}). Equation 6 describes the electrochemical oxidation of Mediator_{red} at the base transducer which generates the

analytical response; the regenerated mediator $_{ox}$, can then undergo further reactions with NADH. Equations 4 and 5 represent the electrocatalytic oxidation of NADH, which occurs at lower applied potentials than obtained by the direct electrochemical oxidation of NADH at an unmodified electrode.

2.3.1 Entrapment

A simple fabrication method based on the integration of a liver mitochondrial fraction containing glutamate dehydrogenase was employed for the fabrication of a novel glutamate biosensor. The liver mitochondrial fraction was utilised in an attempt to reduce the cost of the biosensor, however, the activity of the biosensor appeared to be compromised in comparison to the biosensor incorporating purified glutamate dehydrogenase. The biological recognition element was mixed with a carbon paste, packed into an tube, and used in the determination of MSG in chicken bouillon cubes [21]. The enzymatically generated NADH was oxidised using ferricyanide as a electrochemical mediator. High recoveries of MSG were achieved. Several amino acids, commonly found in food products, did not interfere with the determination. Extensive pre-treatment of the food sample, consisting of dissolving, vacuum-filtering, washing and then further diluting the sample in buffer, was required before analysis, in contrast to simpler food preparation methods previously discussed [19].

A novel biosensor fabrication technique was developed by Tang et. al. [22] which consisted of entrapping GLDH between layers of alternating poly(amidoamine) dendrimer-encapsulated platinum nanoparticles (Pt-PAMAM) with multi-walled carbon nanotubes. PAMAM's were used to modify the surface of the glassy carbon electrode due to their excellent biocompatibility and chemical fixation properties. The procedure was repeated using positively charged Pt-PAMAM and negatively charged GLDH which were alternatively adsorbed onto the CNTs in a layer-by-layer process. The assembly process and enzyme immobilisation process is illustrated in Figure 2-3.

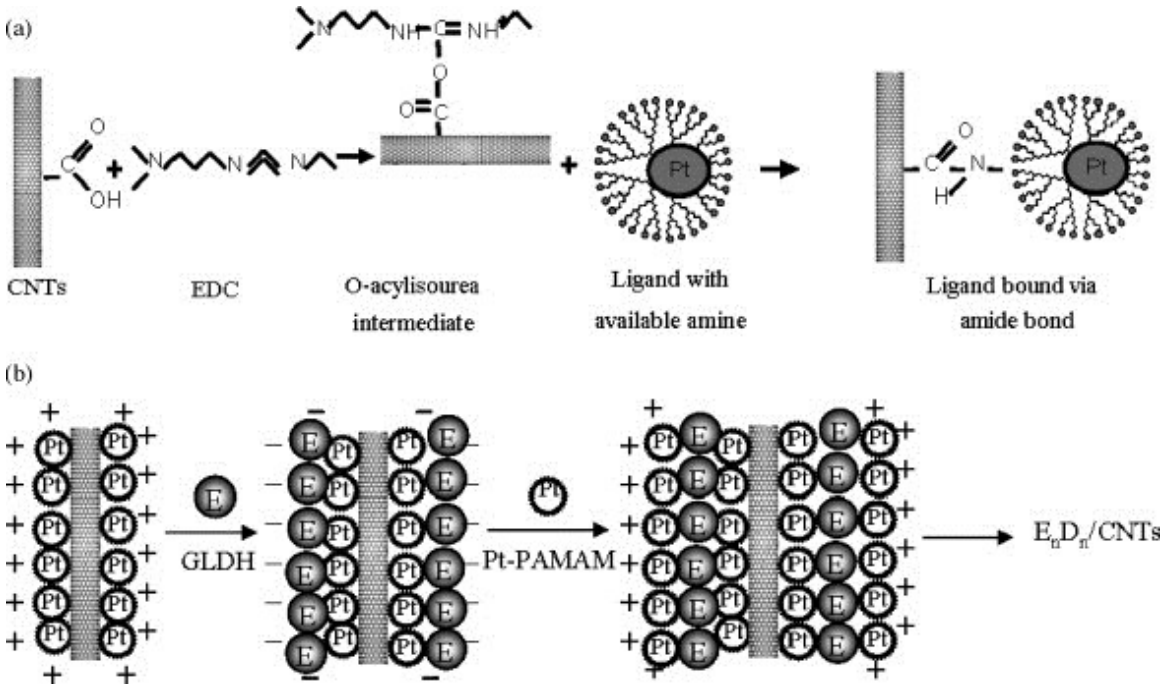

Figure 2-3: Schematic showing the procedure of immobilizing Pt-PAMAM onto CNTs (a) and the layer-by-layer self-assembly of GLDH and Pt-PAMAM onto CNTs (b). Pt-PAMAM/CNTs heterostructures were attached covalently via EDC, Pt-PAMAM and GLDH were alternately deposited. Reprinted with permission from [24], Elsevier.

Whilst the fabrication procedure is complex, the biosensor possesses superior sensitivity to previously discussed biosensors.

In contrast to the above, a simpler and less time consuming method of fabricating a glutamate biosensor has been described [23] which involved incorporating GLDH and NAD^+ into carbon paste. The mixture was inserted in a holder, placed in to a solution containing O-phenylenediamine and subsequently electropolymerized. The o-phenylenediamine film is simultaneously able to prevent interferences and facilitate the amperometric detection of NADH at low applied potentials by acting as an electron mediator. The biosensor was used to determine glutamate in chicken bouillon cubes; the results compared favourably to those obtained using a spectrophotometric method (12.6 ± 0.3% (n = 5) and 12.3% respectively). Despite the simpler fabrication method, the linear

range and sensitivity of the biosensor was lower than the sensor described by Tang et. al. [22].

In recent years, the biopolymer known as chitosan has been investigated in a variety of studies as a method of entrapping enzymes for biosensor construction [24]. CHIT appears to offer improved enzyme stability and is easy to immobilize onto a variety of materials. A biosensor for glutamate [25] has been constructed by depositing a mixture of purified CNTs, CHIT and MB onto a glassy carbon electrode and dried. The surface was then treated with an aliquot of GLDH in PBS, and dried at 4ºC. The cofactor was present in free solution at a concentration of 4mM. The selectivity of the biosensor was determined by the addition of interferences (AA, UA), with no apparent amperometric responses being generated. However, the application of the biosensor to clinical and food samples was not described in this paper.

Screen-printing technology has offered the possibility of the mass production at low cost of glutamate biosensors; these have been successfully applied to the measurement of glutamate in serum and food samples [26]. As screen-printed devices are inexpensive to manufacture they can be considered disposable, in comparison to glassy carbon electrodes, which are expensive and are not considered disposable devices. Consequently, the former are much convenient devices for fabricating biosensors and have become a popular route to commercialisation. The fabrication method involved drop-coating CHIT (0.05%) onto the surface of a Meldola's Blue (MB) SPCE (MB-SPCE), followed by an aliquot of glutamate dehydrogenase (3U/μL). This device is designated GLDH-CHIT-MB-SPCE. The biosensor was then left to dry under vacuum at 4ºC overnight. NAD^+ was present in free solution at a concentration of 4mM.

The electro-catalyst Meldola's Blue allowed an operating potential of only +100mV to be employed; the response occurred as a result of the electrocatalytic oxidation of enzymatically generated NADH. The biosensor was successfully applied to the

determination of MSG in Beef OXO cubes and endogenous glutamate in serum. The beef OXO cube was dissolved by sonication in PBS and the endogenous content of both the OXO cube and serum were determined. Recoveries of 91% were attained for the spiked OXO cube (n = 6) and 96% for the spiked serum test (n = 6). These results compare favourably to those reported by Alvarez-Crespo et. al. [23] and Basu et.al [19]. This device improves upon the linear range of previously discussed biosensors, [23,25].

In order to further develop this biosensor for potential commercial development, all of the components needed to be immobilized onto the surface of the transducer. The layer-by-layer fabrication process is described in the paper [27]. The schematic shown in Figure 4 summarises the important steps involved in this process.

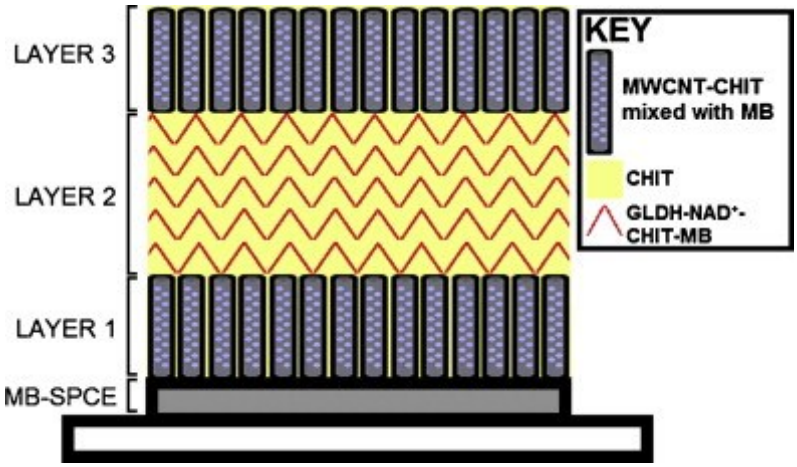

Figure 2-4: A schematic diagram displaying the layer-by-layer drop coating fabrication procedure used to construct the reagentless glutamate biosensor, based on a MB-SPCE electrode. Reprinted with permission from [27], Elsevier.

An amperometric plot using the reagentless biosensor are shown in Figure 5. The biosensor was successfully applied to the determination of glutamate in spiked serum. A recovery of 104% (n = 5, CoV: 2.91%) was determined, which compares favourably to previously discussed biosensors [19,23,26]. An interference study was conducted in both serum and food samples (stock cubes) and no interfering signals were generated. Such reagentless biosensors offer the advantage of being low cost, simple to use and requires no additional

cofactor to be added to the sample solution. Clearly, this is a prerequisite for commercial devices.

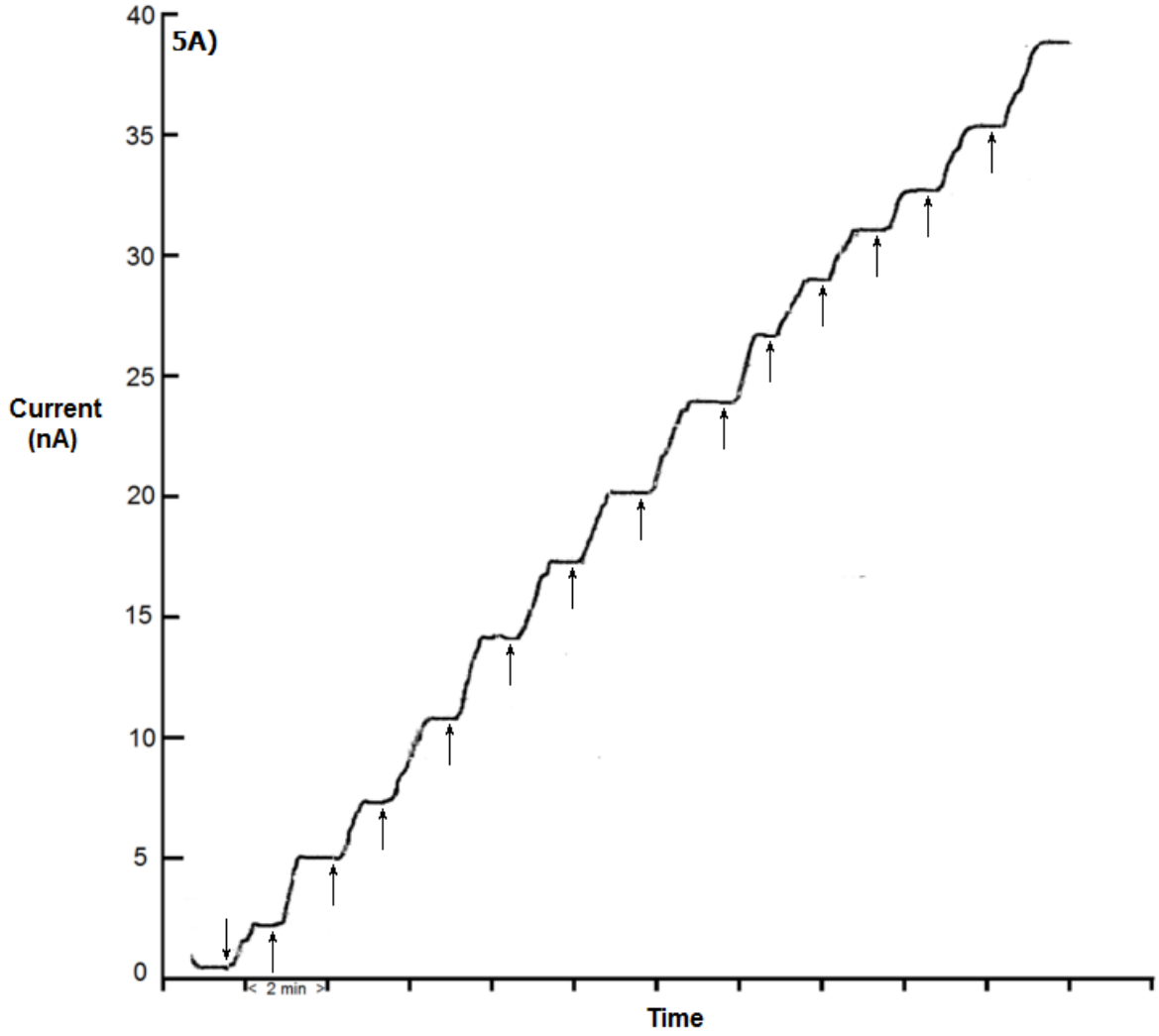

Figure 2-5: Amperogram conducted with the reagentless glutamate biosensor. Each arrow represents an injection of 3 µL of 25 mM glutamate in a 10 mL stirred solution containing supporting electrolyte; 75 mM, PB (pH 7.0), with 50 mM NaCl at an applied potential of +0.1 V vs. Ag/AgCl. Adapted with permission from [27], Elsevier.

2.3.2 Covalent Bonding

The electrochemical technique known as different pulse voltammetry was used in conjunction with a glutamate biosensor to develop a novel assay for measuring glutamate in a mixture of naturally occurring biomolecules commonly found in biological samples [28]. The biosensor fabrication procedure involves vertically aligned carbon nanotubes

(VACNTs) which are treated in order to convert the tips of the CNTs into carboxylic acid groups, in order to covalently bind the enzyme. GLDH was bound to the CNTs using 1-(3-dimethylamino propyl)-3-ethylcarbondiimide hydrochloride (EDC) and hydroxyl-sulfosuccinimide sodium salt (sulfo-NHS) to promote amide linkages between the carboxylic tips of the CNTs and the lysine residue present on the enzyme. This was achieved by immersing the electrode in a solution containing EDC/sulfo-NHS and mixed. Once dried, the enzyme was drop-coated onto the electrode, dried for 2 hours and washed with PBS/BSA mixture. The DPV obtained with the synthetic samples indicated that over the concentration range studied, no significant interferences should be expected. However, the biosensor was not applied to a real sample.

2.3.3 Crosslinking

Carbon nanotubes have been successfully employed to produce cross linking matrixes. Single wall carbon nanotubes have been treated with thionine (Th) to produce a Th-SWCNT nanocomposite on the surface of a glassy carbon electrode [29]. The nanocomposite acts as both an electron mediator and enzyme immobilization matrix. The GLDH was mixed with BSA and crossed linked with glutaraldehyde and coated onto the Th-SWCNT layer. An applied potential of +190mV was utilised for amperometric measurements. The linear range was found to superior to that which was achieved by Gholiazadeh et. al. [28] and Tang et. al. [22]. Ascorbic acid, uric acid and 4-acetamidophenol were examined as possible interferents; no discernible current responses were seen.

2.4 Conclusions

The review has highlighted some novel approaches to the fabrication of electrochemical glutamate biosensors. The performance characteristics of the glutamate biosensors discussed are summarised within Table 1. The most commonly reported method for the immobilization of both glutamate oxidase and dehydrogenase is entrapment.

The utilisation of glutamate oxidase offers an advantage over glutamate dehydrogenase as the latter requires the cofactor NAD^+ to be co-immobilised onto the appropriate transducer. In addition the response times are also generally shorter for glutamate oxidase based biosensors. However, there are several drawbacks with the use of these biosensors. Significantly higher applied potentials must be utilised in order to generate an amperometric response from the enzymatic generation of H_2O_2. In contrast low operational potentials of around 0 V can be applied with dehydrogenase based biosensors; which is advantageous when measuring glutamate in complex media.

Expensive electrode materials such as gold and platinum are often used in the development of glutamate biosensors utilising glutamate oxidase. In contrast, three glutamate biosensors employing GLDH immobilized onto SPCE's as the electrode material have been described. SPCE's offer an inexpensive approach to fabricating glutamate biosensors which is clearly an important consideration in the commercialisation of such devices.

Finally, the cost of glutamate dehydrogenase is far lower than that of glutamate oxidase (as of August 2015). 100mg (20U per mg) of glutamate dehydrogenase costs £175. By contrast, glutamate oxidase is sold by Sigma for £88.20 per 1U. This is clearly an important consideration for commercialisation.

Table 2-1: Details of the enzyme immobilisation technique and performance characteristics of amperometric glutamate biosensors based on glutamate oxidase and glutamate dehydrogenase

Legend: NS – Not specified, N/A – Not applicable * - Voltametric Measurement, ~ - Polarographic Measurement

Glutamate Oxidase based single enzyme systems									
Immobilisation Technique	Type	Ref	LOD	Optimum pH	V (vs. Ag/AgCl)	Sensitivity	Linear Range	Stability	Response Time
Poly(carbamoylsulphonate) (PCS) hydrogel mixed with GluOx	Entrapment	[11]	1.01µM	6.86	+400mV	1.94 nA/µM	100 - 5000µM	90% of activity retained after 2 weeks.	NS
Mixed ceria and titania nanoparticles for the detection of glutamate in hypoxic environments	Entrapment	[12]	0.594µM	7.4	+600mV	0.7937 nA/µM	5 – 50µM	75% of signal after 70 assays in aerobic environment. Anaerobic enviroment, stable for 8 assays.	~5
Biosensor for Neurotransmitter L-Glutamic Acid Designed for Efficient Use of L-Glutamate Oxidase and Effective Rejection of Interferences	Entrapment	[13]	0.27 µM	7.4	+700 mV	3.8 ± 1.3 nA cm^{-2} $mmol^{-1}$ L	0 - 100µM	NS	<10s

Polyion complex-bilayer membrane	Entrapment	[14]	0.2 nM	7.0	+800 mV	1.85 nA/μM	3 – 500 μM	Stable over 4 weeks with daily usage.	NS
Carboxylated multiwalled carbon nanotubes/gold nanoparticles/chitosan composite film modified Au electrode	Covalent-bonding	[16]	1.6μM	7.4	+135mV	155 nA/μM/cm^2	5 – 500 μM	4 months, no data shown.	2s
Pt nanoparticles modified Au nanowire array electrode	Entrapment	[17]	14μM	7.4	+650mV	194.6 μA mM^{-1} cm^{-2}	200 - 800 μM	98% of its initial response retained after 2 weeks.	4.8s
Photo-crosslinkable polymer membrane on a palladium-deposited screen-printed carbon electrode	Cross linking	[18]	0.05μM	7.0	+400mV	12.8 nA/μM	0.05μM - 100μM	Stored dry – 5 months, no change in response.	30 – 50s Not stated.
Cross linking with Glutaraldehyde and BSA as a spacing agent. ≃	Cross linking	[19]	N/A	7.0	-700mV	NS	NS	84% of initial signal after 48 days of use every 3 days.	120s
Polypyrrole nanoparticles/polyaniline modified gold electrode.	Cross linking	[20]	0.1nM	7.5	-130mV	533 nA/ μM/cm^2	0.02 - 400μm	60 days at 4ºC	3s

Glutamate Dehydrogenase based single enzyme systems										
Immobilisation Technique	Type	Ref	LOD	pH	V (vs. Ag/AgCl)	[NAD+/NAD(P)+]	Sensitivity	Linear Range	Stability	Response Time
A mixture of carbon paste, octadecylamine and mitochondria fraction, packed into the working electrode.	Entrapment	[21]	100µM	7.5	+350mV	1mM	0.189µA/mM	0.4 – 10mM	60% after 10 days of use.	N/A
Alternatively assembling layers of glutamate dehydrogenase and Pt-PAMAM.	Entrapment	[22]	100 µM	7.4	+200mV	0.1mM	433 µA/mM^{-1} cm^{2}	0.2 - 250 µM	85% after four weeks	3s
Unmodified carbon paste mixed with lyophilized enzyme and coenzyme, packed into the well of a working electrode.	Entrapment	[23]	3.8µM	8.0	+150 mV	N/A	4·6×10^{5} nA l mol^{-1}	5 - 78 µM	Signal decrease by 50% after 3 days	120s
GLDH dropcoated onto the surface of a CNT-CHIT-MDB modified GC electrode.	Entrapment	[25]	2 µM	7.0	-140mV	4mM	0.71 ± 0.08 nA/µM	25 – 100 µM	NS	NS
Immobilisation of GLDH with CHIT, drop coated onto the surface of a SPCE.	Entrapment	[26]	1.5 µM	7.0	+100mV	4mM	0.44nA/µM	12.5 - 150µM	NS	2s

Reagentless biosensor. Immobilisation of both NAD^+ and GLDH by utilising a mixture CHIT/MWCNT/MB dropcoated onto the surface of a SPCE in a layer by layer fashion.	Entrapment	[27]	3μM	7.0	+100mV	N/A	0.39 nA/μM	7.5 - 105μM	100% of original response retained after 2 weeks	20 – 30s
GLDH attached to CNTs utilising EDC and sulfo-NHS, by immersing electrode in PBS containing both compounds then dropcoating GLDH. *	Covalent bonding	[28]	0.57 μM	7.4	NS	2mM	With mediator: 1.17 mA mM^{-1} cm^{-2} / 0.153 mA mM^{-1} cm^{-2} Without mediator: 0.976 mA mM^{-1} cm^{-2} / 0.182 mA mM^{-1} cm^{-2}	With mediator: 0.1 - 20μM / 20 - 500μM Without mediator 0.1 - 20μM / 20 - 300μM	80.5% of original response after two weeks of use.	NS
GLDH is mixed with BSA then coated onto the surface of a Th-SWNTs/GC electrode, then followed by glutaraldehyde.	Crosslinking	[29]	0.1 μM	8.3	+190mV vs NHE	0.1μM	137.3 μA mM^{-1}	0.5 – 400μM	93% after 2 weeks	5s

2.5 References

[1] D. Purves, G.J. Augustine, D. Fitzpatrick, L.C. Katz, A.-S. LaMantia, J.O. McNamara, et al., Glutamate, (2001). http://www.ncbi.nlm.nih.gov/books/NBK10807/ (accessed October 15, 2014).

[2] A. Lau, M. Tymianski, Glutamate receptors, neurotoxicity and neurodegeneration., Pflugers Arch. 460 (2010) 525–42. doi:10.1007/s00424-010-0809-1.

[3] D.A. Butterfield, C.B. Pocernich, The glutamatergic system and Alzheimer's disease: therapeutic implications., CNS Drugs. 17 (2003) 641–52. http://www.ncbi.nlm.nih.gov/pubmed/12828500 (accessed June 15, 2015).

[4] J.M. Berg, J.L. Tymoczko, L. Stryer, The First Step in Amino Acid Degradation Is the Removal of Nitrogen, (2002). http://www.ncbi.nlm.nih.gov/books/NBK22475/ (accessed April 9, 2015).

[5] J.T. Brosnan, Glutamate, at the interface between amino acid and carbohydrate metabolism., J. Nutr. 130 (2000) 988S–90S. http://www.ncbi.nlm.nih.gov/pubmed/10736367 (accessed April 2, 2015).

[6] J.T. Brosnan, K.C. Man, D.E. Hall, S.A. Colbourne, M.E. Brosnan, Interorgan metabolism of amino acids in streptozotocin-diabetic ketoacidotic rat., Am. J. Physiol. 244 (1983) E151–8. http://www.ncbi.nlm.nih.gov/pubmed/6401931 (accessed April 2, 2015).

[7] M. Mutlu, Biosensors in Food Processing, Safety, and Quality Control, CRC Press, 2010. https://books.google.com/books?id=4KQWKOFodAgC&pgis=1 (accessed September 8, 2015).

[8] T. POPULIN, S. MORET, S. TRUANT, L. CONTE, A survey on the presence of free glutamic acid in foodstuffs, with and without added monosodium glutamate, Food Chem. 104 (2007) 1712–1717. doi:10.1016/j.foodchem.2007.03.034.

[9] R. Liu, Q. Zhou, L. Zhang, H. Guo, Toxic effects of wastewater from various phases of monosodium glutamate production on seed germination and root elongation of crops, Front. Environ. Sci. Eng. China. 1 (2007) 114–119. doi:10.1007/s11783-007-0021-5.

[10] L. Cao, Carrier-bound Immobilized Enzymes: Principles, Application and Design, John Wiley & Sons, 2006. https://books.google.com/books?id=h_78o7-0hrQC&pgis=1 (accessed June 16, 2015).

[11] A.W.K. Kwong, B. Gründig, J. Hu, R. Renneberg, Comparative study of hydrogel-immobilized l-glutamate oxidases for a novel thick-film biosensor and its application in food samples, Biotechnol. Lett. 22 (n.d.) 267–272. doi:10.1023/A:1005694704872.

[12] R.E. Özel, C. Ispas, M. Ganesana, J.C. Leiter, S. Andreescu, Glutamate oxidase biosensor based on mixed ceria and titania nanoparticles for the detection of glutamate in hypoxic environments, Biosens. Bioelectron. 52 (2014) 397–402. http://www.sciencedirect.com/science/article/pii/S0956566313006039 (accessed October 9, 2013).

[13] M.R. Ryan, J.P. Lowry, R.D. O'Neill, Biosensor for neurotransmitter L-glutamic acid designed for efficient use of L-glutamate oxidase and effective rejection of interference., Analyst. 122 (1997) 1419–24. http://www.ncbi.nlm.nih.gov/pubmed/9474818 (accessed May 20, 2015).

[14] F. Mizutani, Y. Sato, T. Sawaguchi, S. Yabuki, S. Iijima, Rapid measurement of transaminase activities using an amperometric l-glutamate-sensing electrode based on a glutamate oxidase–polyion complex-bilayer membrane, Sensors Actuators B Chem. 52 (1998) 23–29. doi:10.1016/S0925-4005(98)00251-2.

[15] Pinnacle Glutamate Biosensor for Mice and Rats, (n.d.). http://www.pinnaclet.com/glutamate.html (accessed April 22, 2015).

[16] B. Batra, C.S. Pundir, An amperometric glutamate biosensor based on immobilization of glutamate oxidase onto carboxylated multiwalled carbon nanotubes/gold nanoparticles/chitosan composite film modified Au electrode, Biosens. Bioelectron. 47 (2013) 496–501. http://www.sciencedirect.com/science/article/pii/S0956566313002339 (accessed October 9, 2013).

[17] M. Jamal, J. Xu, K.M. Razeeb, Disposable biosensor based on immobilisation of glutamate oxidase on Pt nanoparticles modified Au nanowire array electrode., Biosens. Bioelectron. 26 (2010) 1420–4. doi:10.1016/j.bios.2010.07.071.

[18] K.-S. Chang, W.-L. Hsu, H.-Y. Chen, C.-K. Chang, C.-Y. Chen, Determination of glutamate pyruvate transaminase activity in clinical specimens using a biosensor composed of immobilized l-glutamate oxidase in a photo-crosslinkable polymer membrane on a palladium-deposited screen-printed carbon electrode, Anal. Chim. Acta. 481 (2003) 199–208. doi:10.1016/S0003-2670(03)00093-X.

[19] A.K. Basu, P. Chattopadhyay, U. Roychudhuri, R. Chakraborty, Development of biosensor based on immobilized L-glutamate oxidase for determination of monosodium glutamate in food., Indian J. Exp. Biol. 44 (2006) 392–8. http://www.ncbi.nlm.nih.gov/pubmed/16708893 (accessed May 22, 2015).

[20] B. Batra, S. Kumari, C.S. Pundir, Construction of glutamate biosensor based on covalent immobilization of glutamate oxidase on polypyrrole nanoparticles/polyaniline modified gold electrode., Enzyme Microb. Technol. 57 (2014) 69–77. doi:10.1016/j.enzmictec.2014.02.001.

[21] S.T. Girousi, A.A. Pantazaki, A.N. Voulgaropoulos, Mitochondria-Based Amperometric Biosensor for the Determination ofL-Glutamic Acid, Electroanalysis. 13 (2001) 243–245. doi:10.1002/1521-4109(200103)13:3<243::AID-ELAN243>3.0.CO;2-J.

[22] L. Tang, Y. Zhu, L. Xu, X. Yang, C. Li, Amperometric glutamate biosensor based on self-assembling glutamate dehydrogenase and dendrimer-encapsulated platinum nanoparticles onto carbon nanotubes., Talanta. 73 (2007) 438–43. doi:10.1016/j.talanta.2007.04.008.

[23] S.L. Alvarez-Crespo, M.J. Lobo-Castañón, A.J. Miranda-Ordieres, P. Tuñón-Blanco, Amperometric glutamate biosensor based on poly(o-phenylenediamine) film electrogenerated onto modified carbon paste electrodes, Biosens. Bioelectron. 12 (1997) 739–747. doi:10.1016/S0956-5663(97)00041-9.

[24] B. Krajewska, Application of chitin- and chitosan-based materials for enzyme immobilizations: a review, Enzyme Microb. Technol. 35 (2004) 126–139. http://www.sciencedirect.com/science/article/pii/S0141022904001231 (accessed October 9, 2013).

[25] S. Chakraborty, C. Retna Raj, Amperometric biosensing of glutamate using carbon nanotube based electrode, Electrochem. Commun. 9 (2007) 1323–1330. doi:10.1016/j.elecom.2007.01.039.

[26] G. Hughes, R.M. Pemberton, P.R. Fielden, J.P. Hart, Development of a Disposable Screen Printed Amperometric Biosensor Based on Glutamate Dehydrogenase, for the Determination of Glutamate in Clinical and Food Applications, Anal. Bioanal. Electrochem. 6 (2014) 435–449. http://abechem.com/No. 4-2014/2014,6_4_,435-449.pdf.

[27] G. Hughes, R.M. Pemberton, P.R. Fielden, J.P. Hart, Development of a novel reagentless, screen–printed amperometric biosensor based on glutamate dehydrogenase and NAD+, integrated with multi–walled carbon nanotubes for the determination of glutamate in food and clinical applications, Sensors Actuators B Chem. (2015). doi:10.1016/j.snb.2015.04.066.

[28] A. Gholizadeh, S. Shahrokhian, A.I. zad, S. Mohajerzadeh, M. Vosoughi, S. Darbari, et al., Mediator-less highly sensitive voltammetric detection of glutamate using glutamate dehydrogenase/vertically aligned CNTs grown on silicon substrate., Biosens. Bioelectron. 31 (2012) 110–5. doi:10.1016/j.bios.2011.10.002.

[29] L. Meng, P. Wu, G. Chen, C. Cai, Y. Sun, Z. Yuan, Low potential detection of glutamate based on the electrocatalytic oxidation of NADH at thionine/single-walled carbon nanotubes composite modified electrode., Biosens. Bioelectron. 24 (2009) 1751–6. doi:10.1016/j.bios.2008.09.001.

CHAPTER THREE

Development of a disposable screen-printed amperometric biosensor based on glutamate dehydrogenase, for the determination of glutamate in clinical and food applications

3. Contents

Glutamate is one of the most abundant excitatory neurotransmitters and is involved in fundamental neurological processes such as the formation of memories and learning [1]. Deficiencies or abnormalities in the behaviour of neurological pathways that utilize glutamate and its receptors are associated with neurological disorders such as Alzheimers [2], schizophrenia [3] and depression [4].

Glutamate is also a key compound in nitrogen metabolism, protein synthesis and degradation, and is of great physiological importance. It is the most abundant intracellular amino acid with concentrations varying between 2 and 20 mM [5], whilst estimated extracellular levels of L-glutamate are around of 150 μM in plasma and 10 μM in cerebrospinal fluid [6][7].

Glutamate metabolism is linked with the citric acid cycle [8], GABA synthesis [9] and urea cycle [10]. It is also linked to amino acid degradation as glutamate dehydrogenase (GLDH) catalyses the elimination of amino groups from amino acids. GLDH catalyses the oxidative deamination of glutamate to 2-oxoglutarate, using nicotinamide adenine dinucleotide (NAD^+) as a cofactor (Figure 1-8) [11]. It is a reversible reaction, which typically favours glutamate formation in mammals [12].

Genetically expressed defects in glutamate metabolism have been recently discovered and lead to hyperinsulinism/hypermmonemia syndrome. [13]

L-glutamate, in the form of monosodium glutamate (MSG), also has widespread use as a flavour-enhancing food additive, commonly found in Chinese food and is linked to Chinese Restaurant Syndrome (CRS) [14]. Thus the analysis and determination of L-glutamate is important for both food and clinical applications.

The measurement of glutamate has been carried out using various analytical techniques such as HPLC [15], [16], capillary electrophoresis [17] and enzyme recycling in conjunction with microfluidic [18] and spectrophotometric [19] techniques. In the present

study we wished to explore the possibility of developing an amperometric biosensor for glutamate measurements. This device would offer reliability, convenience and low cost, particularly when fabrication was performed using screen-printing technology. We previously reported on the development of amperometric biosensors based on dehydrogenase enzymes, for lactate [20][21], alcohol [22], glucose [23] and NH_4^+ [24], [25]. These devices were based on a screen printed carbon electrode (SPCE) incorporating the electrocatalyst Meldola's Blue (MB-SPCE). MB reduces the overpotential for the detection of NADH, which is formed during the operation of the biosensor. Applied potentials close to 0 V vs. Ag/AgCl are possible. In a previous chapter [25] we reported on a electrochemical NH_4^+ biosensor based on the reaction of this species with 2-oxoglutarate and NADH in the presence of the enzyme GLDH. Consequently, we considered that the development of a glutamate biosensor should be feasible by immobilizing GLDH onto the surface of a MB-SPCE and driving the overall reaction in the opposite direction by incorporating the oxidised cofactor (NAD^+) with the enzyme.

In this study we have investigated an immobilising procedure involving chitosan (CHIT). As discussed in Chapter One, Section 1.3.3.3.1, chitosan is a linear hydrophilic polysaccharide composed of n-acetyl-D-glucosamine and D-glucosamine units which are linked with a ß-(1-4) glycosidic bonds. It is a biocompantible, inexpensive, non-toxic biopolymer with excellent film forming properties [26] and can therefore be employed for enzyme immobilisation. The application of chitosan as an enzyme immobilization matrix has been reported previously for many different enzymes [27].

In the present chapter we describe the development and application of a GLDH-CHIT-MB-SPCE biosensor for the determination of glutamate in serum and of glutamate as MSG in food (OXO cubes).

3.1 Materials and Methods

3.1.1 Chemicals and reagents

All chemicals were of analytical grade, purchased from Sigma Aldrich, UK, except glutamate dehydrogenase (CAT: 10197734001) which was purchased from Roche, UK. The 75 mM phosphate buffer (PB) was prepared by combining appropriate volumes of tri-sodium phosphate dodecahydrate, sodium dihydrogen orthophosphate dehydrate and disodium hydrogen orthophosphate dehydrate solutions to yield the desired pH. Glutamate and NADH/NAD^+ solutions were prepared in 75 mM PB. 0.05% of chitosan was dissolved in 0.05 M HCl following up to 10 minutes sonication. Bovine serum albumin (BSA) (obtained from AbD Serotec) was used to produce dummy electrodes by drop-coating the same equivalent protein mass as glutamate dehydrogenase. Fetal bovine serum (FBS) (South American Origin, CAT: S1810-500) obtained from Labtech Int. Ltd, was used for serum analysis. Food samples (Beef OXO cubes) were obtained from a local supermarket.

3.1.2 Apparatus

All electrochemical experiments were conducted with a three-electrode system consisting of a carbon working electrode containing MB-SPCE (Gwent Electronic Materials Ltd; Ink Code: C2030519P5), Ag/AgCl reference electrode (GEM Product Code C61003P7): printed onto PVC, and a separate Pt counter electrode. The area of the working electrode was defined using insulating tape, into a 3 x 3 mm square area. The electrodes were then connected to the potentiostat using gold clips. Solutions, when required, were stirred using a circular magnetic stirring disk and stirrer (IKA® C-MAG HS IKAMAG, Germany) at a fixed speed. A μAutolab II electrochemical analyser with general purpose electrochemical software GPES 4.9 was used to acquire data and experimentally control the voltage applied to the SPCE in the 10 ml electrochemical cell. An AMEL Model 466 polarographic analyser combined with a GOULD BS-271 chart recorder was used for some amperometric studies. Measurement and monitoring of the pH was conducted with a Fisherbrand Hydrus

400 pH meter (Orion Research Inc., USA). Sonications were performed with a Devon FS100 sonicator (Ultrasonics, Hove, Sussex, UK).

3.2 Procedures

3.2.1 Fabrication of glutamate biosensor

A 0.05% HCl solution containing CHIT was drop-coated onto the surface of the unmodified MB-SPCE 9mm^2 working electrode and left to dry under vacuum. Once dried the enzyme GLDH with the appropriate quantity of units was drop-coated directly onto the CHIT layer. The same procedure was used to obtain dummy biosensors by using CHIT and the same mass of BSA as that of the enzyme. Figure 3-1 illustrates the proposed GLDH-CHIT-MB-SPCE biosensor. The biosensors were stored in a desiccator, shielded from light at 4ºC overnight to allow the enzyme layer to dry.

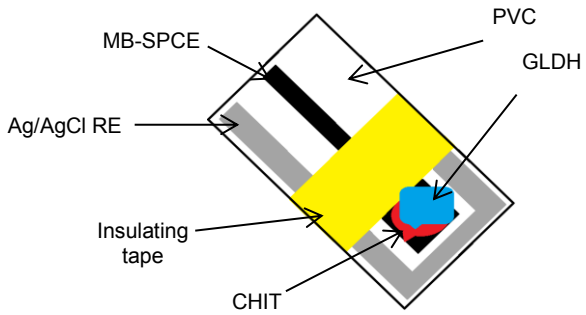

Figure 3-1) Diagram of proposed biosensor strip. The insulating tape defines both the WE and RE. CHIT is then drop-coated and allowed to dry, followed by GLDH. All studies were conducted using a separate Pt wire counter electrode.

Serum and food samples were analysed (n = 3) for interferences using dummy biosensors. If interferences were detected, the average signal generated was deducted from the enzyme biosensor response.

3.2.2 Calibration studies of the biosensor using amperometry in stirred solution.

All amperometric measurements were performed in stirred solutions using an applied potential of +0.1 V vs. Ag/AgCl. Measurements of glutamate were conducted in 75 mM PB (pH 7.0) containing 4 mM of NAD^+ and 50 mM NaCl using the GLDH-CHIT-MB-SPCE. The biosensor was immersed into a stirred 10 mL buffer solution, the potential applied and sufficient time was allowed for allowed a steady-state current to be obtained. The amperometric responses to additions of known concentrations of glutamate were then recorded. Amperometry was used to determine the effects of pH (5 – 9) and temperature (25 - 40°C) by examining the performance characteristics over the concentration range of 25 μM to 300 μM glutamate.

3.2.3 Application of optimised amperometric biosensor (GLDH-CHIT-MB-SPCE) to the determination of glutamate in food.

OXO cubes (5.9g, average mass of three OXO cubes) were prepared by dissolving one cube in 50 mL of PB and sonicating for 15 minutes. The endogenous concentration of MSG was determined by using the method of standard addition. An initial 10μl volume of the dissolved OXO cube was added to the stirred buffered solution (10 mL) in the voltammetric cell containing the biosensor, operated at +0.1 V (vs. Ag/AgCl) with subsequent standard additions of 10μL of 25 mM glutamate.

The reproducibility of the biosensor assay for MSG analysis in OXO cubes was determined by repeating the whole procedure six times with six individual biosensors. The effects of interferences from the OXO cube were established by using a dummy BSA biosensor and deducted from the enzyme biosensor signal.

The recovery of MSG added to OXO cubes was investigated by fortifying the solution containing one OXO cube with 100 mM of glutamate. The analysis of this solution was

performed in a similar manner to that described for the unfortified solution. In this case, an aliquot of only 2μL of the fortified OXO solution was added to 10mL volumes of buffer solution. Standard additions of 2.5uL of 100 mM glutamate were added to this mixture.

3.2.4 Application of optimised amperometric biosensor (GLDH-CHIT-MB-SPCE) to the determination of glutamate in serum.

To determine the original glutamate concentration, an initial volume of 100 μL of serum was added to 9.9mL of buffered solution. The serum solution was subjected to amperometry in stirred solution using an applied potential of + 0.1 V vs. Ag/AgCl. This was followed by additions of 10 μL aliquots of 25 mM standard glutamate solution to the voltammetric cell. The currents resulting from the enzymatic generation of NADH were used to construct standard addition plots, from which the endogenous concentration of glutamate was determined. The reproducibility of the biosensor was deduced by repeating the studies six times with six individual biosensors.

The procedure was repeated using serum spiked with 2 mM glutamate (n = 6) to determine to the recovery of the assay. The effects of the interference from serum were established by using a dummy BSA biosensor. A dummy biosensor was constructed by drop coating the equivalent weight of the enzyme with BSA.

3.3 Results and Discussion

3.3.1 Principle of Operation of the Biosensor

The overall principle of operation of the biosensor is shown in Figure 3-2. Glutamate in solution is oxidised to form 2-oxoglutarate in the presence of the immobilized enzyme glutamate dehydrogenase (GLDH) and NAD^+; the product NADH and NH_4^+ are formed during this reaction. The NADH diffuses through the CHIT layer to reach the electrode (Fig. 3-1), where it undergoes oxidation by the MB_{ox} which is reduced to MB_{red}. The electrochemical oxidation of MB_{red} to MB_{ox} occurs at an applied potential of +0.1 V vs.

Ag/AgCl and produces the analytical response (Fig. 3-2) The value of +0.1 V was deduced by constructing a hydrodynamic voltammogram and selecting the potential from the position of the plateau (Fig. 3-3).

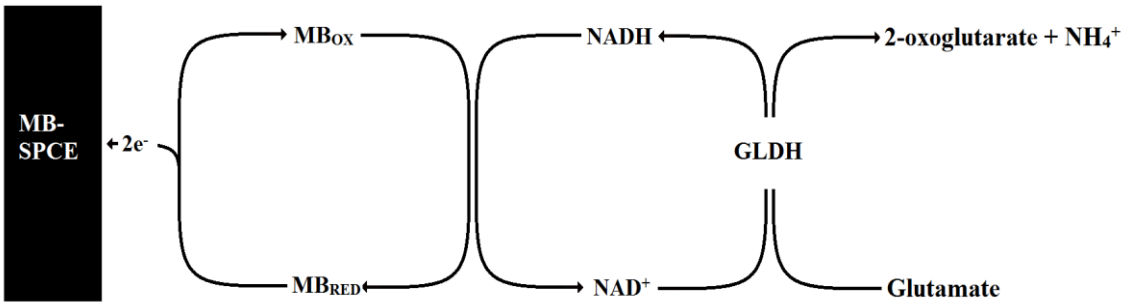

Figure 3-2: Schematic displaying the interaction between the immobilized enzyme GLDH and glutamate at the surface of the electrode and the subsequent generation of the analytical response.

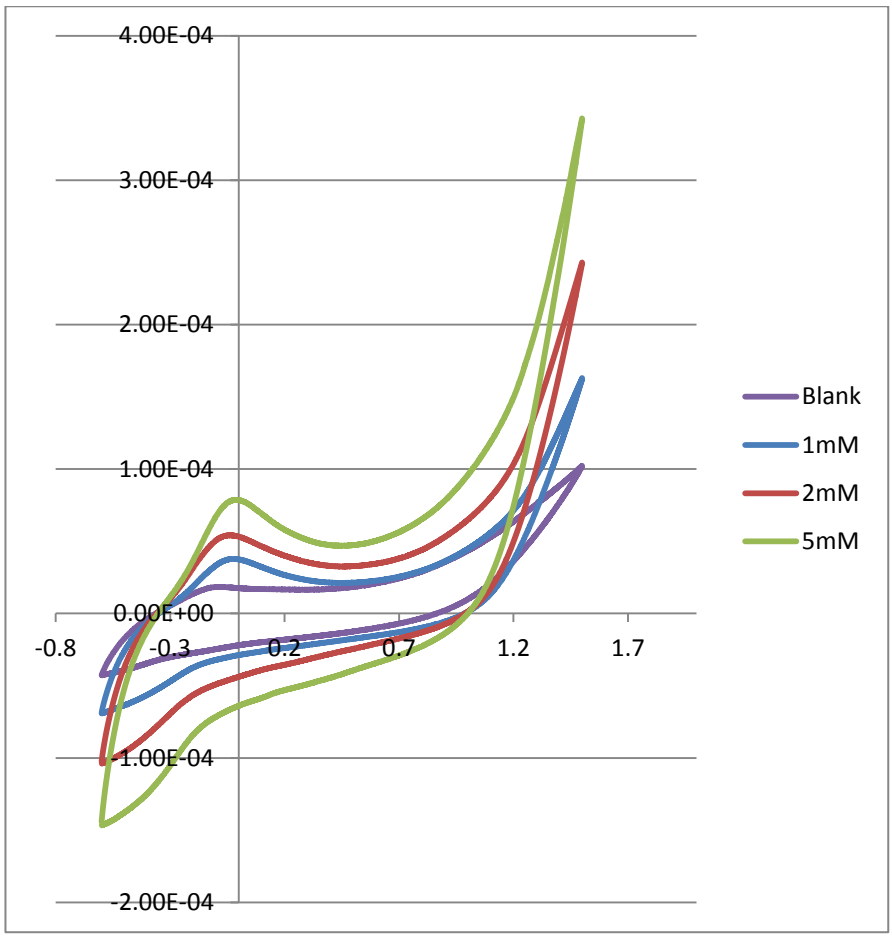

Figure 3-3 Cyclic voltammograms illustrating an increase in the current related to an increase in the concentration of NADH. Scan rate 20mVs, -0.5V - 1.3V scan range.

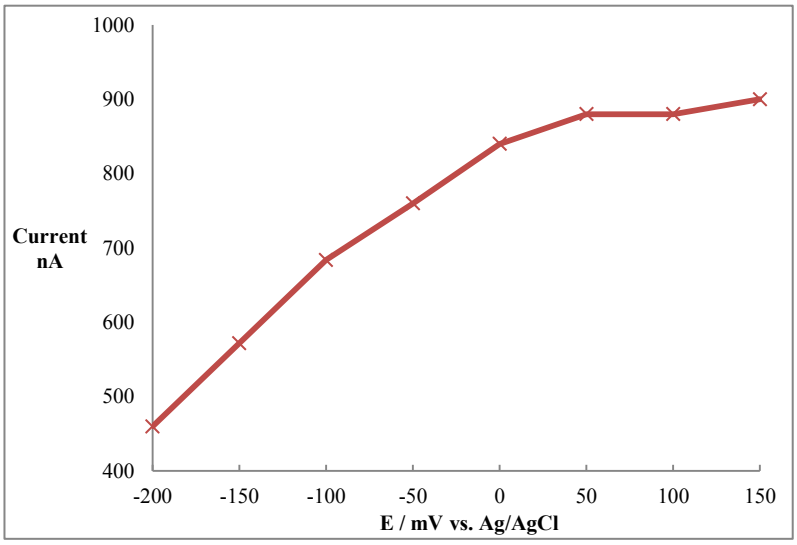

Figure 3-4: Hydrodynamic voltammogram plot of GLDH-CHIT-MB-SPCE in the presence of 1mM NADH, in 10mL of supporting electrolyte; 75mM, PB (pH 7.0) and 50 mM NaCl.

3.3.2 Immobilisation of GLDH using chitosan

During initial studies when drop-coating the GLDH onto the surface of the MB-SPCE alone, steady-state currents were not produced. Additions of glutamate produced inconsistent currents, suggesting that the GLDH may have been dissipating into the free solution, producing sporadic current responses. Studies conducted to investigate the use of glutaraldehyde and cellulose acetate; both commonly used enzyme binding agents, failed to generate steady-state currents or produced little to no signal response, indicating loss of enzyme into solution. CHIT was therefore applied to the surface of the biosensors to fabricate GLDH-CHIT-MB-SPCE devices; subsequent additions of glutamate produced consistent steady state responses with this approach.

3.3.3 Optimisation Studies

The response of the GLDH-CHIT-MB-SPCE biosensor to changes in temperature was investigated using concentrations of glutamate over the range 12.5 to 250 μM prepared in 75 mM phosphate solution (pH 7.0). The effect of temperatures between 25 to 40°C was studied. The maximum amperometric response was found to occur at 35°C (Figure 3-4). The decrease occurring above 35°C may be due to enzyme denaturing at higher temperatures. It may be noted that the linear range was highest using 30°C which could be beneficial in some applications.

The effect of pH was investigated over the pH range 5 – 9 (Figure 3-5). The highest sensitivity (0.18 nA/μM) was obtained at pH 9, with a near-linear decrease down to a pH of 5. However, the linearity of the responses showed an inverse trend with the greatest linear range occurring at pH 5, decreasing down to a pH of 9.

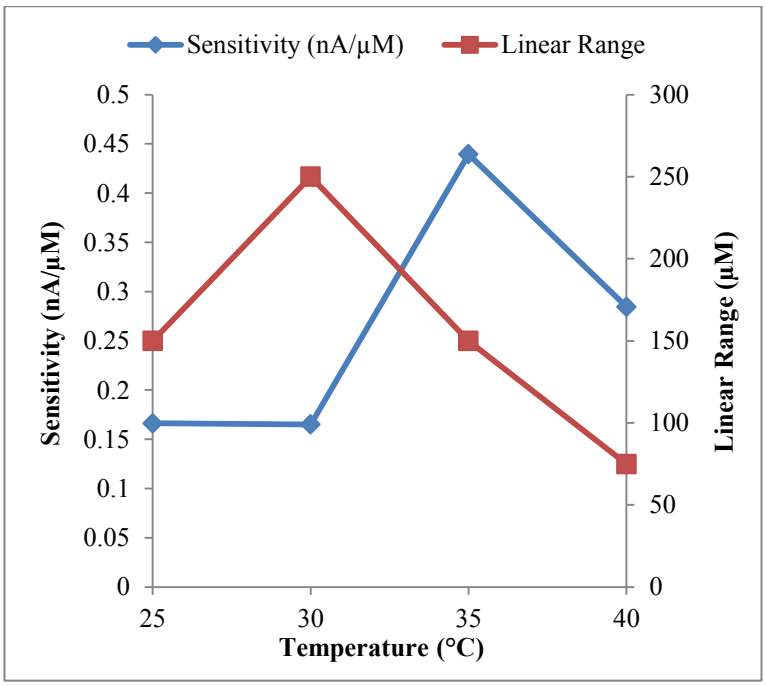

Figure 3-5: Illustrates the effects of temperature upon the current response of the biosensor to injections of glutamate up to 275 µM in 25µM steps

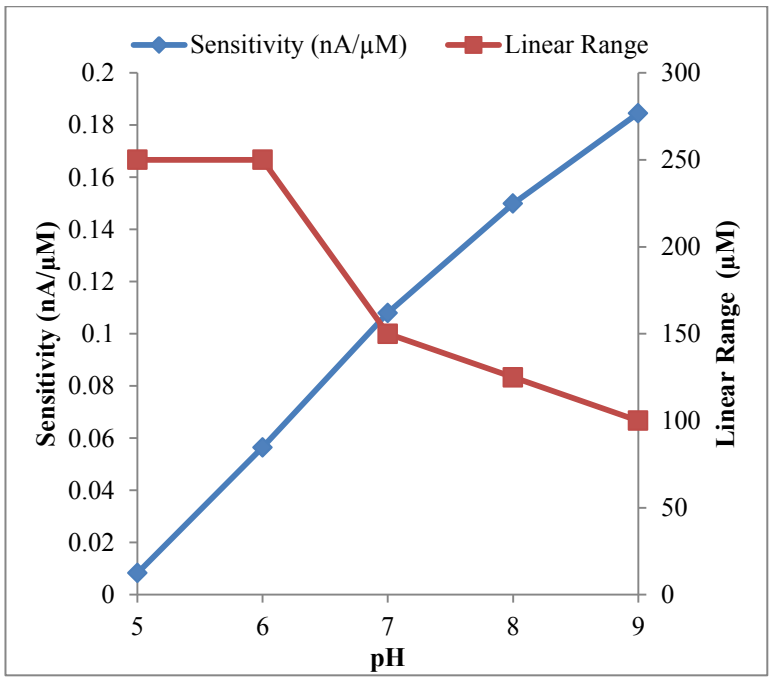

Figure 3-6: Illustrates the effects of pH upon the current response of the biosensor to the addition of glutamate. An applied potential +0.1V vs. Ag/AgCl in 10 ml of 75 mM phosphate buffer solution containing 50 mM NaCl was used.

3.3.4 Calibration Studies

Calibration studies with glutamate were conducted with the fully developed glutamate biosensor using the optimized experimental conditions over the concentration range 25µM – 275 µM . The biosensor exhibited a sensitivity of 0.44 nA/µM (n = 3). The calculated limit of detection (based on three times signal-to-noise) was 1.5 µM, thus the biosensor is clearly appropriate for analysing extracellular concentrations of glutamate in clinical applications.

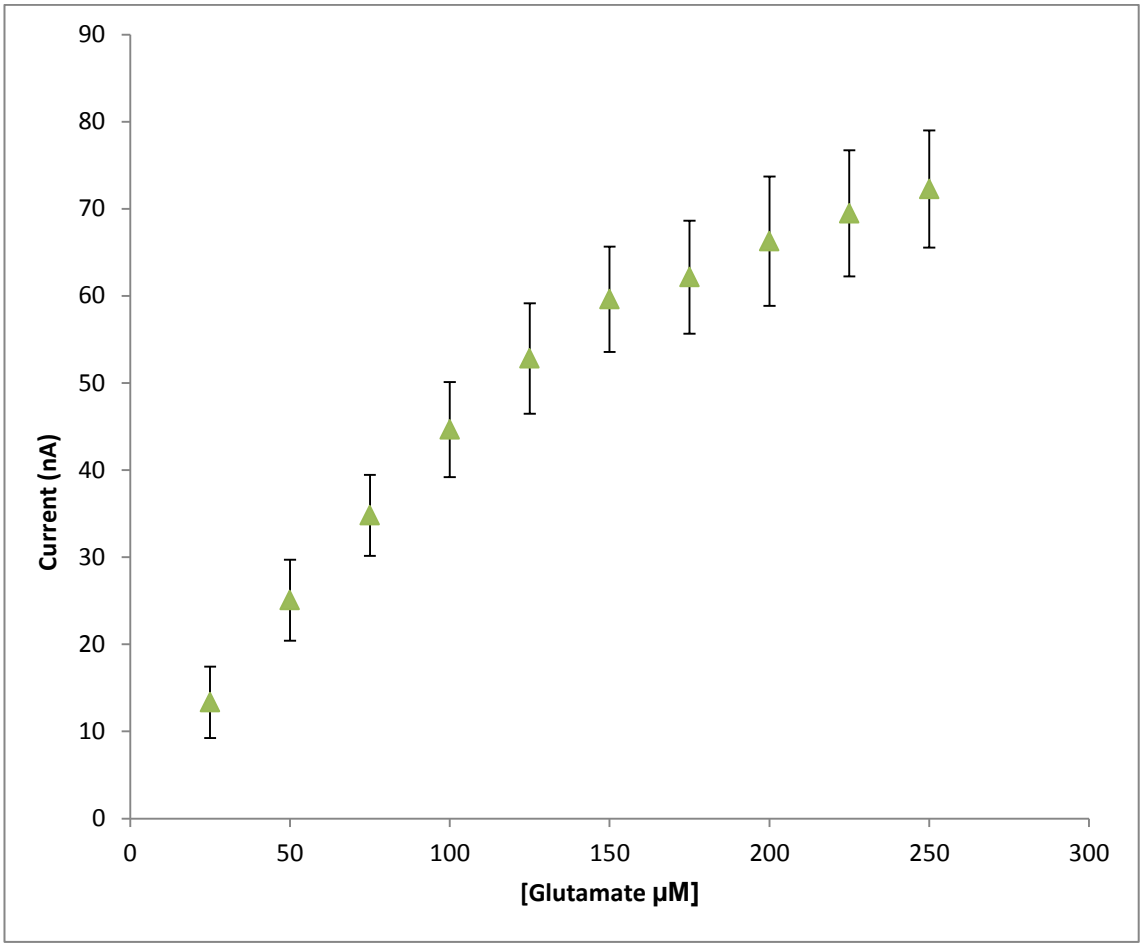

Figure 3-7: Calibration plot depicting the full range over which the calibration study was conducted with the glutamate biosensor. As illustrated by the plot, once the concentration of glutamate exceeds 150µM, the Km has been exceeded. Std deviations are based on n = 3. Conditions: 35ºC, pH 7.

3.3.5 Application of the optimum amperometric biosensor (GLDH-CHIT-MB-SPCE) to the determination of glutamate in unspiked and spiked food.

Many food products are known to contain MSG as a flavour enhancer, therefore, we decided to explore the possibility of applying our new glutamate biosensor to a known brand of beef stock cube.

A standard addition study was conducted by dissolving one OXO cube (5.916 g mass) in 50ml of PB using sonication for 15 minutes. Six replicate OXO cube samples were analysed using fresh biosensors for each measurement. The determination was performed by filling the cell with 9.99 mL of electrolyte, establishing a steady state current, and then injecting a 10µL volume of unfiltered OXO cube in PB solution with subsequent 10µL injections of 25 mM glutamate (Figure 3-6A). The mean quantity of glutamate discovered in unspiked OXO cubes (n = 6) was 125.43 mg/g with a coefficient of variation of 8.98%. Results are shown in Table 3-1. A standard addition calibration plot is shown in Figure 3-8.

GLDH-CHIT-MB-SPCE biosensors were used to determine glutamate in spiked OXO cubes. The OXO cube was spiked with 100 mM of glutamate, doubling the endogenous level of glutamate found in OXO cube stock. The standard addition method employed for the unspiked OXO cubes was altered by changing the initial injection of spiked OXO cube solution to 2µL. The mean recovery (n = 6) was a 91% with a CV of 6.39% (Table 3-1) This result indicated high reproducibility for biosensor in what was a complex, unfiltered medium.

Interestingly the endogenous content of MSG in OXO cubes measured by our gave similar values for stock cubes containing MSG analysed by both HPTLC [28] and an optical biosensor [29]; values of 133.50 mg/g and 182.9 mg/g were detected by the named methods respectively.

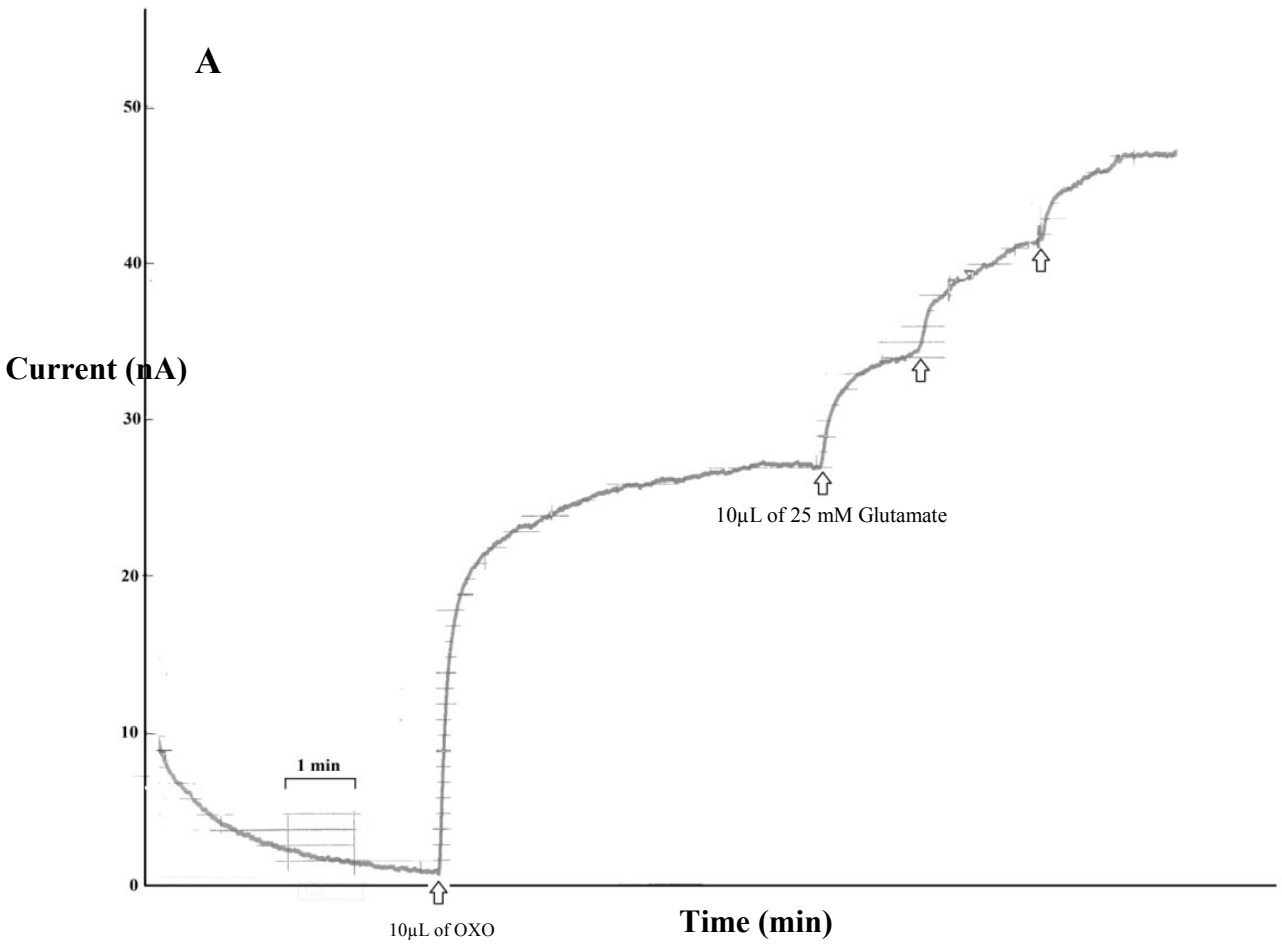

Figure 3-8) A. Amperogram obtained using a GLDH-CHIT-MB-SPCE with a solution containing 10µL of a dissolved OXO cube; arrows indicate additions of 10µL of 25 mM glutamate into a 10mL volume. Measurements taken 1.5 min after each addition.

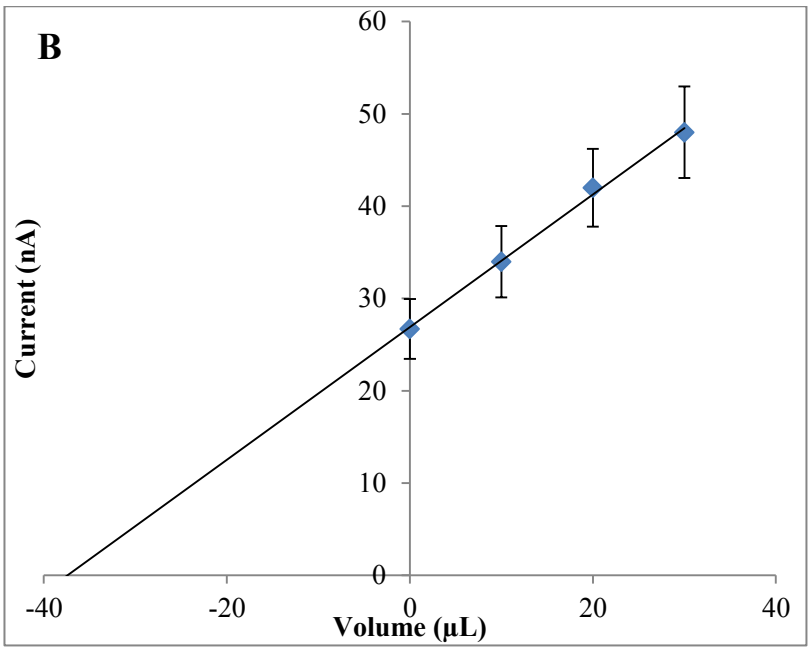

Figure 3-9: Typical standard addition calibration plot obtained with a solution containing a dissolved OXO cube using a GLDH-CHIT-MB-SPCE. Standard error bars based on n = 6.

Unspiked OXO Cube	
Sample	**Quantity of Glutamate Detected (mg/g)**
1	114.15
2	147.29
3	129.37
4	113.96
5	125.47
6	122.35
Mean (mg/g)	125.43
Std Dev	11.26
CV (%)	8.98

Table 3-1) Data obtained from the unspiked OXO cube/food study. The mean endogenous concentration was 125.43 mg /g (n = 6) in unspiked OXO cubes.

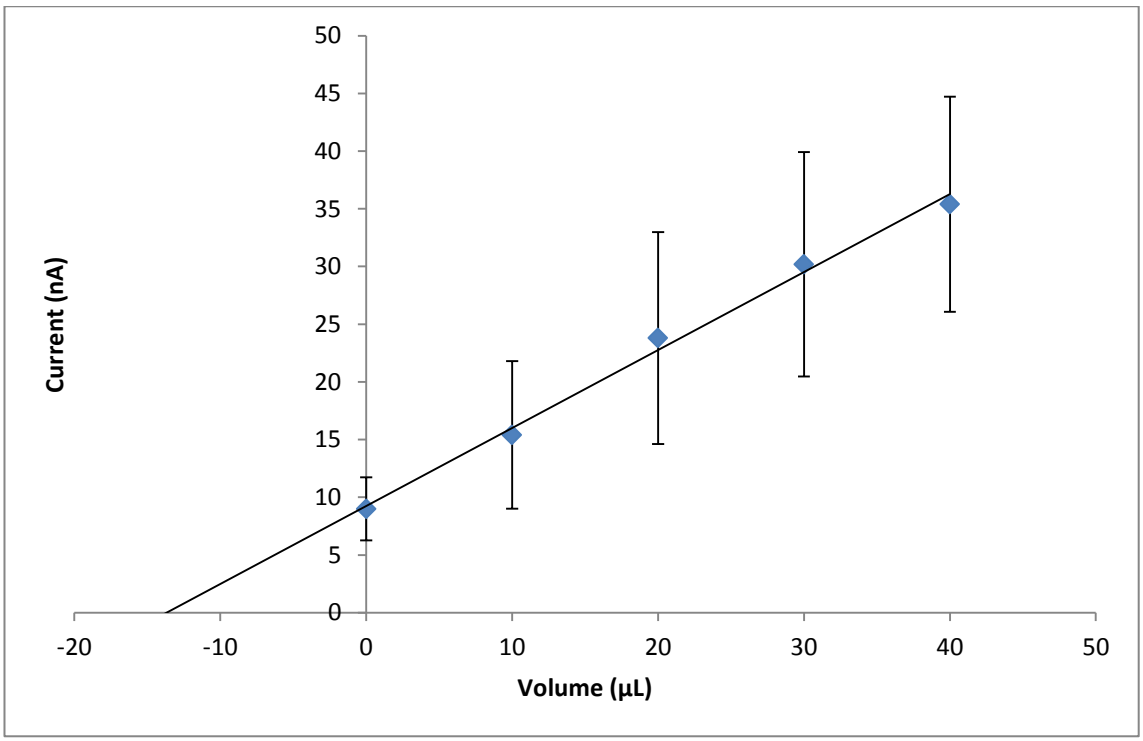

Figure 3-10: Typical standard addition calibration plot obtained with a solution containing a dissolved spiked OXO cube using a GLDH-CHIT-MB-SPCE. Standard error bars based on n = 6.

Spiked OXO Cube				
Sample	**Endogenous Concentration mg/g**	**Spike mg/g**	**Total Concentration Found mg/g**	**Recovery (%)**
1	125.43	158.03	266.05	86
2	125.43	158.03	268.20	88
3	125.43	158.03	280.11	97
4	125.43	158.03	279.03	96
5	125.43	158.03	273.73	92
6	125.43	158.03	262.15	83
Mean (%)	91			
Std Dev	6.00			
CV (%)	6.39			

Table 3-2) Data obtained from the spiked OXO cube/food study.

3.3.6 Application of the optimum amperometric biosensor (GLDH-CHIT- MB-SPCE) to the determination of glutamate in both unspiked and spiked serum.

Amperometry, in conjunction with the method of multiple standard additions was conducted to determine the endogenous levels of glutamate and the recovery for serum spiked with additional glutamate. The replicate serum samples were analysed using a fresh biosensor for each measurement.

The data obtained on serum samples using the glutamate biosensor are shown in Table 3-2. The endogenous levels of glutamate detected were 1.68 mM for the unspiked samples. The coefficient of variation was 4.09% for the six individual samples. This concentration is above that discovered by Ye and Sontheimer in 1998 [30] who discovered concentrations ranging from 808.2 μM to 1195.7 μM in fetal bovine (calf) sera (FBS) using a bioluminescence detection method. However, this study did not include the provider of serum nor the South American variety used in studies conducted using the GLDH-CHIT-MB-SPCE biosensor, thus glutamate concentrations may potentially be higher in different batches given the variation displayed. These results show promise due to the low coefficient of variation, small amount of serum required to carry out analysis and the lack of preparation steps.

The GLDH-CHIT-MB-SPCE biosensors were then used to determine glutamate in spiked serum. The serum was spiked with 2.00 mM glutamate so as to roughly double the endogenous levels of glutamate and to allow a distinction between the spike and endogenous levels. The results are shown in Table 3-3. The mean recovery (n = 6) was 96% with a CV of 3.29% indicating high reproducibility in serum. This method offers an economical and simple approach for the screening of glutamate levels in serum. It should be mentioned that the biosensors were stored in a desiccator in a refrigerator at 4°C before use; under these conditions they were found to be stable for at least one week.

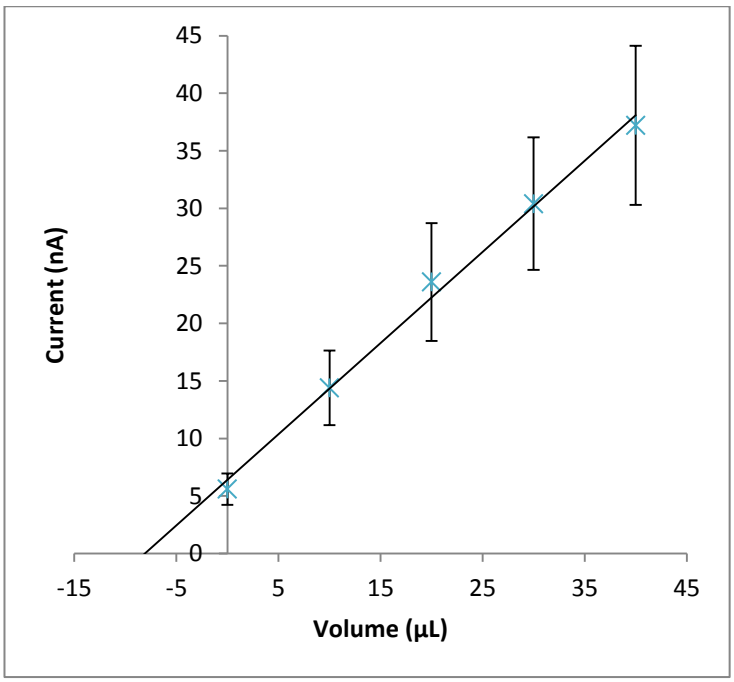

Figure 3-11: Typical standard addition calibration plot obtained with a serum solution using a GLDH-CHIT-MB-SPCE. Standard error bars based on n = 6.

Unspiked Serum

Sample	Concentration of Glutamate detected (mM)
1	1.70
2	1.54
3	1.67
4	1.76
5	1.69
6	1.71
Mean (mM)	1.68
Std Dev	0.07
CV (%)	4.10

Table 3-3) Data obtained from the unspiked serum study. In unspiked serum, 1.68 mM of glutamate was detected (n = 6) with a coefficient of variation of 4.1%.

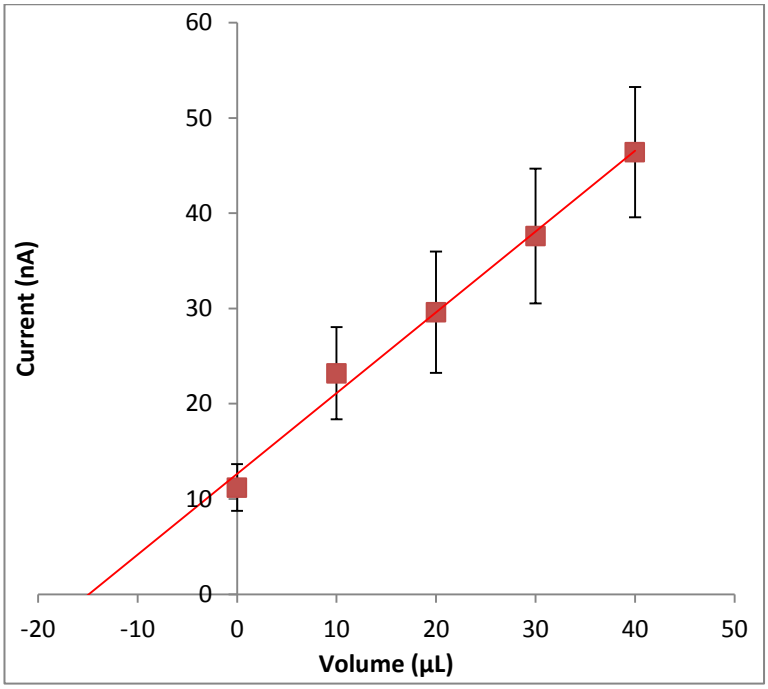

Figure 3-12: Typical standard addition calibration plot obtained with a serum solution using a GLDH-CHIT-MB-SPCE. Standard error bars based on n = 6.

Spiked Serum

Sample	Spike mM	Endogenous Concentration mM	Total Concentration Found mM	Recovery (%)
1	2.00	1.68	3.52	92
2	2.00	1.68	3.65	98
3	2.00	1.68	3.62	97
4	2.00	1.68	3.65	99
5	2.00	1.68	3.62	97
6	2.00	1.68	3.49	90
Mean (%)	96			
Std Dev	3.14			
CV (%)	3.29			

Table 3-4) In spiked serum, the mean recovery was 96%, coefficient of variation 3.29 % (n = 6).

The GLDH-CHIT-MB-SPCE biosensor described in this chapter possesses a superior limit of detection by comparison to other biosensors utilising glutamate dehydrogenase and can be fabricated simply in comparison to those reported previously (Table 3-5). Consequently, these devices hold promise for application quality control in clinical laboratories. It is interesting to note that a biosensor based on glutamate oxidase [31] has been reported for the determination of glutamate in soy sauce; a detection limit of 10nM was achieved. However, it should be mentioned that the operating potential required to detect H_2O_2 was +950mV, as a result the selectivity of the device may not be sufficient for the analysis of glutamate in serum.

Immobilization Method	Ref	LOD	pH	Applied Potential	[NAD^+]	Sensitivity	Linear Range	Response Time
GLDH attached to the inner surface of a 75µM i.d. capillary using biotin-avidin chemistry. NADH measured by fluorescence.	[32]	3 µM	8.5, but saline 7.3 also used.	-	3 mM	-	-	450ms
Glassy carbon covered in CNT-CHIT-MDB composite film. GLDH in PBS was caste on the CNT composite electrode.	[33]	2 µM	7.2	-100 mV	4 mM	0.71 ± 0.08 nA/µM	N/A	~10s
GLDH and diaphorase immobilized on a nanocompositie electrode.	[34]	5.4 µM	9.0	+300 mV	2 mM	28 nA µM $^{-1}cm^{-2}$	10 - 3495µM	-
Polymer-modifid electrode. MB entrapped into two polymers	[35]	2 µM	7.4	0 mV	1 mM	0.70 nA μM^{-1}	0 - 100µM	
Nanomolar Detection of Glutamate at a biosensor based on Screen-printed Electrodes modified with Carbon Nanotubes	[31]	10 nM	7.4	+950 mV	N/A	0.72nA ± 0.05 µA μM^{-1}	0.01 – 10 µM	<5s
GLDH-CHIT-MB- SPCE	**This study.**	**1.5 µM**	**7.0**	**+100 mV**	**4 mM**	**0.44 nA/µM**	**12.5 - 150 µM**	**~2s**

Table 3-3) A comparison of previously reported Glutamate biosensors, including the one described in this chapter.

3.4 Conclusions

This chapter has demonstrated the effective use of CHIT to immobilise GLDH onto the surface of a MB-SPCE for the fabrication of a glutamate biosensor and the successful application of the biosensor to the determination of glutamate, in both serum and food samples, without any sample pre-treatment, other than dilution.

This simple approach is attractive as it is based on an electrochemical biosensor fabricated by incorporating biological compounds with a chemically modified screen printed carbon electrode. SPCE's can be mass produced at low cost so biosensors based on this technology can be considered disposable. This latter feature may be of significance in biological fluid analysis where contamination may be an issue.

In summary our proposed biosensor approach offers the advantages of good selectivity owning to the combination of an enzyme integrated with a transducer operated at a low potential of only +100mV, coupled with the simplicity of fabrication and analytical operation.

3.5 References

[1] G. Riedel, B. Platt, and J. Micheau, (2003), "Glutamate receptor function in learning and memory," *Behav Brain Res*, **140**, 1–47.

[2] R. Rupsingh, M. Borrie, M. Smith, J. L. Wells, and R. Bartha, (2011), "Reduced hippocampal glutamate in Alzheimer disease.," *Neurobiol. Aging*, **32**, 802–10.

[3] J. R. Field, A. G. Walker, and P. J. Conn, (2011), "Targeting glutamate synapses in schizophrenia.," *Trends Mol. Med.*, **17**, 689–98.

[4] I. A. Paul and P. Skolnick, (2003), "Glutamate and depression: clinical and preclinical studies.," *Ann. N. Y. Acad. Sci.*, **1003**, 250–72.

[5] P. Newsholme, J. Procopio, M. M. R. Lima, T. C. Pithon-Curi, and R. Curi, (2003), "Glutamine and glutamate--their central role in cell metabolism and function.," *Cell Biochem. Funct.*, **21**, 1–9.

[6] N. C. Danbolt, (2001), "Glutamate uptake.," *Prog. Neurobiol.*, **65**, 1–105.

[7] D. E. Featherstone and S. A. Shippy, (2008), "Regulation of synaptic transmission by ambient extracellular glutamate.," *Neuroscientist*, **14**, 171–81.

[8] O. E. Owen, S. C. Kalhan, and R. W. Hanson, (2002), "The key role of anaplerosis and cataplerosis for citric acid cycle function.," *J. Biol. Chem.*, **277**, 30409–12.

[9] G. C. Mathews and J. S. Diamond, (2003), "Neuronal Glutamate Uptake Contributes to GABA Synthesis and Inhibitory Synaptic Strength," *J. Neurosci.*, **23**, 2040–2048.

[10] H. A. Krebs, R. Hems, P. Lund, D. Halliday, and W. W. Read, (1978), "Sources of ammonia for mammalian urea synthesis.," *Biochem. J.*, **176**, 733–7.

[11] E. Santero, I. Canosa, F. Govantes, and A. B. Hervás, *Dehydrogenases*. InTech, (2012).

[12] R. C. Hudson and R. M. Daniel, (1993), "L-glutamate dehydrogenases: distribution, properties and mechanism.," *Comp. Biochem. Physiol. B.*, **106**, 767–92.

[13] A. Kelly and C. Stanley, (2001), "Disorders of glutamate metabolism," *Ment. Retard. Dev. ...*, **295**, 287–295.

[14] I. Mosby, (2008), "'That Won-Ton Soup Headache': The Chinese Restaurant Syndrome, MSG and the Making of American Food, 1968-1980," *Soc. Hist. Med.*, **22**, 133–151.

[15] T. P. Piepponen and A. Skujins, (2001), "Rapid and sensitive step gradient assays of glutamate, glycine, taurine and gamma-aminobutyric acid by high-performance liquid chromatography-fluorescence detection with o-phthalaldehyde-mercaptoethanol derivatization with an emphasis on microdialysis sam," *J. Chromatogr. B. Biomed. Sci. Appl.*, **757**, 277–83.

[16] K. Buck, P. Voehringer, and B. Ferger, (2009), "Rapid analysis of GABA and glutamate in microdialysis samples using high performance liquid chromatography and tandem mass spectrometry.," *J. Neurosci. Methods*, **182**, 78–84.

[17] L. A. Dawson, J. M. Stow, and A. M. Palmer, (1997), "Improved method for the measurement of glutamate and aspartate using capillary electrophoresis with laser

induced fluorescence detection and its application to brain microdialysis.," *J. Chromatogr. B. Biomed. Sci. Appl.*, **694**, 455–60.

[18] W. Laiwattanapaisal and J. Yakovleva, (2009), "On-chip microfluidic systems for determination of L-glutamate based on enzymatic recycling of substrate," *Biomicrofluidics*, **3**, 14104.

[19] W. Khampha, V. Meevootisom, and S. Wiyakrutta, (2004), "Spectrophotometric enzymatic cycling method using l-glutamate dehydrogenase and d-phenylglycine aminotransferase for determination of l-glutamate in foods," *Anal. Chim. Acta*, **520**, 133–139.

[20] S. D. Sprules, J. P. Hart, R. Pittson, and S. a Wring, (1996), "Evaluation of a new disposable screen-printed sensor strip for the measurement of NADH and its modification to produce a lactate biosensor employing microliter volumes," *Electroanalysis*, **8**, 539–543.

[21] S. D. Sprules, J. P. Hart, S. A. Wring, and R. Pittson, (1995), "A reagentless, disposable biosensor for lactic acid based on a screen-printed carbon electrode containing Meldola's Blue and coated with lactate dehydrogenase, NAD+ and cellulose acetate," *Anal. Chim. Acta*, **304**, 17–24.

[22] M. Boujtita, J. P. Hart, and R. Pittson, (2000), "Development of a disposable ethanol biosensor based on a chemically modified screen-printed electrode coated with alcohol oxidase for the analysis of beer.," *Biosens. Bioelectron.*, **15**, 257–63.

[23] R. M. Pemberton, T. Cox, R. Tuffin, I. Sage, G. a Drago, N. Biddle, J. Griffiths, R. Pittson, G. Johnson, J. Xu, S. K. Jackson, G. Kenna, R. Luxton, and J. P. Hart,

(2013), "Microfabricated glucose biosensor for culture welloperation," *Biosens Bioelectron*, **42**, 668–677.

[24] J. P. Hart, S. Serban, L. J. Jones, N. Biddle, R. Pittson, and G. A. Drago, (2006), "Selective and Rapid Biosensor Integrated into a Commercial Hand- Held Instrument for the Measurement of Ammonium Ion in Sewage Effluent," *Anal. Lett.*, **39**, 1657–1667.

[25] J. P. Hart, A. K. Abass, D. C. Cowell, and A. Chappell, (1999), "Development of a Disposable Amperometric NH Biosensor Based on a Chemically Modified Screen-Printed Carbon Electrode Coated with Glutamate Dehydrogenase, 2-Oxoglutarate, and NADH," *Electroanalysis*, **11**, 406–411.

[26] B. Krajewska, (2004), "Application of chitin- and chitosan-based materials for enzyme immobilizations: a review," *Enzyme Microb. Technol.*, **35**, 126–139.

[27] M. N. . Ravi Kumar, (2000), "A review of chitin and chitosan applications," *React. Funct. Polym.*, **46**, 1–27.

[28] V. N. Krishna, D. Karthika, D. M. Surya, M. Rubini, M. Vishalini, and Y. Pradeepa, (2010), "Analysis of Monosodium l-Glutamate in Food Products by High-Performance Thin Layer Chromatography.," *J. Young Pharm.*, **2**, 297–300.

[29] N. Z. Md Muslim, M. Ahmad, L. Y. Heng, and B. Saad, (2012), "Optical biosensor test strip for the screening and direct determination of l-glutamate in food samples," *Sensors Actuators B Chem.*, **161**, 493–497.

[30] Z. C. Ye and H. Sontheimer, (1998), "Astrocytes protect neurons from neurotoxic injury by serum glutamate.," *Glia*, **22**, 237–48.

[31] R. Khan, W. Gorski, and C. D. Garcia, (2011), "Nanomolar Detection of Glutamate at a Biosensor Based on Screen-Printed Electrodes Modified with Carbon Nanotubes.," *Electroanalysis*, **23**, 2357–2363.

[32] R. J. Cosford and W. G. Kuhr, (1996), "Capillary biosensor for glutamate.," *Anal. Chem.*, **68**, 2164–2169.

[33] S. Chakraborty and C. Retna Raj, (2007), "Amperometric biosensing of glutamate using carbon nanotube based electrode," *Electrochem. commun.*, **9**, 1323–1330.

[34] R. Monošík, M. Streďanský, and E. Šturdík, (2013), "A Biosensor Utilizing l-Glutamate Dehydrogenase and Diaphorase Immobilized on Nanocomposite Electrode for Determination of l-Glutamate in Food Samples," *Food Anal. Methods*, **6**, 521–527.

[35] R. Doaga, T. McCormac, and E. Dempsey, (2009), "Electrochemical Sensing of NADH and Glutamate Based on Meldola Blue in 1,2-Diaminobenzene and 3,4-Ethylenedioxythiophene Polymer Films," *Electroanalysis*, **21**, 2099–2108.

CHAPTER FOUR

The development and application of a reagentless glutamate microband biosensor for real-time monitoring of cell toxicity.

4. Contents

4.1. Introduction

In Chapter 3, a non-reagentless biosensor was described for the determination of glutamate. Glutamate dehydrogenase was bound to the surface of the biosensor utilising CHIT, whilst NAD^+ was present in free solution. As described in Chapter 1, microband electrodes possess unique properties which could be utilised and applied to real time toxicity testing.

The development of pharmaceutical compounds is a costly and extensive process, with product development costing up to 30 – 35% of bringing a new drug to the market [1]. Early development candidates for drug development are selected based on their pharmacological and toxicological properties which are investigated through early-stage in vitro cell based assays [2]. Cytotoxicity assays such as neutral red, MTT, LDH leakage and protein assays are used to evaluate the number of dead cells [3]. Pemberton et. al. [4], [5] have described the development and application of a glucose microband biosensor for the real time monitoring of glucose uptake in HepG2 cells, that have been exposed to different concentrations of paracetamol in real time. The authors have shown the possibility of using cell monitoring in conjunction with electrochemical biosensor towards the eventually replacing of animals in toxicity testing in drug development. This cell line has previously been applied as a model for the real time monitoring of toxic challenge by measuring the inhibition of the uptake of glucose [5], the release of lactate [6] and both glucose and lactate simultaneously [7].

The concentration of intracellular glutamate is typically higher than that of extracellular glutamate. For example, within the brain, extracellular glutamate concentrations are normally within the 1 – 10μM range [8], [9] whilst intracellular glutamate concentrations are typically in the micromolar range [10]. Similar micromolar levels have been observed intracellularly in rat livers [11], [12].

The use of electrochemistry for the real time acquisition of metabolic data, towards the potential reduction of animal testing, is highly desirable both ethically and to improve the

reliability of drug testing using human cells. Toxicity testing in environmental monitoring and food safety has become of increasing interest [13], [14]. Electrochemical biosensors are capable of high specificity towards the target analyte of interest when utilising a low operating potential and incorporating the appropriate enzyme and cofactors to the surface of the electrode.

This small dimension results in advantageous properties such as low ohmic drop, increased mass transport via radial diffusion and small double layer capacitance thereby improving the signal to noise ratio [15]. The microband biosensor was fabricated by drop coating a "bio-cocktail" of chitosan (CHIT), nicotinamide adenine dinucleotide (NAD^+) and glutamate dehydrogenase (GLDH), onto the working area of a Meldola's Blue screen-printed carbon electrode (MB-SPCE). The working area of the biosensor, once the biological components had dried, was covered with insulating tape. The microelectrode biosensors were fabricated by cutting through the covered working expose an edge that measures in micrometers in one dimension. This simple fabrication procedure is utilised to construct a reagentless glutamate microband biosensor.

As mentioned in Chapter 3 a non-reagentless glutamate biosensor has previously been developed by drop-coating the required components onto the working electrode of screen-printed carbon electrodes [16]. This chapter discusses the development of a reagentless glutamate microband biosensor, employing CHIT, NAD^+, GLDH and MB-SPCE in a simple fabrication method. The application of this microband biosensor is for the real time monitoring of glutamate flux from cells in response to toxic challenge is described. The scientific novelty is present in both in the simplicity of fabrication of the reagentless microband biosensor and its application to post-exposure and real time toxicity testing in cell media.

4.2. Materials and Methods

4.2.1. Chemicals and Reagents

Foetal bovine serum (FBS), Minimum Essential Medium Eagle (MEM) and all other chemicals were purchased from Sigma-Aldrich. All chemicals were of analytical grade, purchased from Sigma Aldrich, UK, except glutamate dehydrogenase (CAT: 10197734001) which was purchased from Roche, UK. The 75 mM phosphate buffer (PB) was prepared by combining appropriate volumes of tri–sodium phosphate dodecahydrate, sodium dihydrogen orthophosphate dihydrate and disodium hydrogen orthophosphate anhydrous solutions to yield the desired pH. Glutamate and NADH/NAD^+ solutions were dissolved directly in 75 mM PB. Chitosan (CHIT) was dissolved in 0.05 M HCl (pH < 3.0) to produce a 0.05% solution following up to 10 minutes sonication. A 25mM stock solution of glutamate (monosodium glutamate, MSG) was utilised for glutamate calibrations. A 100mM stock of paracetamol in 100% ethanol was diluted by $1/5^{th}$ with cell culture media and filtered sterilised (0.2µm) before use.

4.2.2. Apparatus

All electrochemical studies were conducted with a two electrode system consisting of a carbon working electrode containing MB (MB–SPCE, Gwent Electronic Materials Ltd; Ink Code: C2030519P5), a Ag/AgCl reference electrode (GEM Product Code C61003P7); both printed onto PVC. The electrodes were then connected to the potentiostat using gold clips. Microband electrodes/biosensors and reference electrodes were held by gold clips attached to cork lids which were push-fitted into 6-well plate wells. Electrodes were connected to a PG580RM 5-channel potential (Uniscan Instruments Ltd, Buxton, UK; www.uniscan.com) which was controlled using UiEChem software (Version 2.02), for both single and multiple parallel well studies. All cell culture work such as feeding, splitting the cells and dosing with paracetamol was conducted under a sterile fume hood. The cork lid electrode holders was sterilised with 70% ethanol spray in order to reduce contamination. The electrodes

themselves were not sterilised as the ethanol would potentially damage the enzyme and cofactor. Studies utilising MEM and HepG2 cells were carried out in an incubator with a 5% CO_2 atmosphere at 37ºC in order to maintain the pH of the cell media. Solutions, when required, were stirred using a IKA MS 1 Minishaker. Measurement and monitoring of the pH was conducted with a Fisherbrand Hydrus 400 pH meter (Orion Research Inc., USA). Sonications were performed with a Devon FS100 sonicator (Ultrasonics, Hove, Sussex, UK).

4.2.3. Biosensor Fabrication

The biosensor fabrication procedure is illustrated in Figure 4-1 (a-e). Briefly, microband biosensors were fabricated by drop coating (a) 5µL of CHIT (0.05% in 0.05M HCl) onto the surface of a 3mm^2 working electrode, followed by (b) 9µL of GLDH (3U/µL) and 1µL of NAD^+ (106µg). (c) The biosensor was then left to dry overnight at 4ºC. (d) Once dried, insulating tape was used to cover the working area and some of the electrode track. (e) The covered area of the working electrode was cut through using a scissors to expose a 3mm-long working electrode edge. The technique has previously been utilised to successfully fabricate microband electrodes for the measurement of glucose [17] and hydrogen peroxide [6].

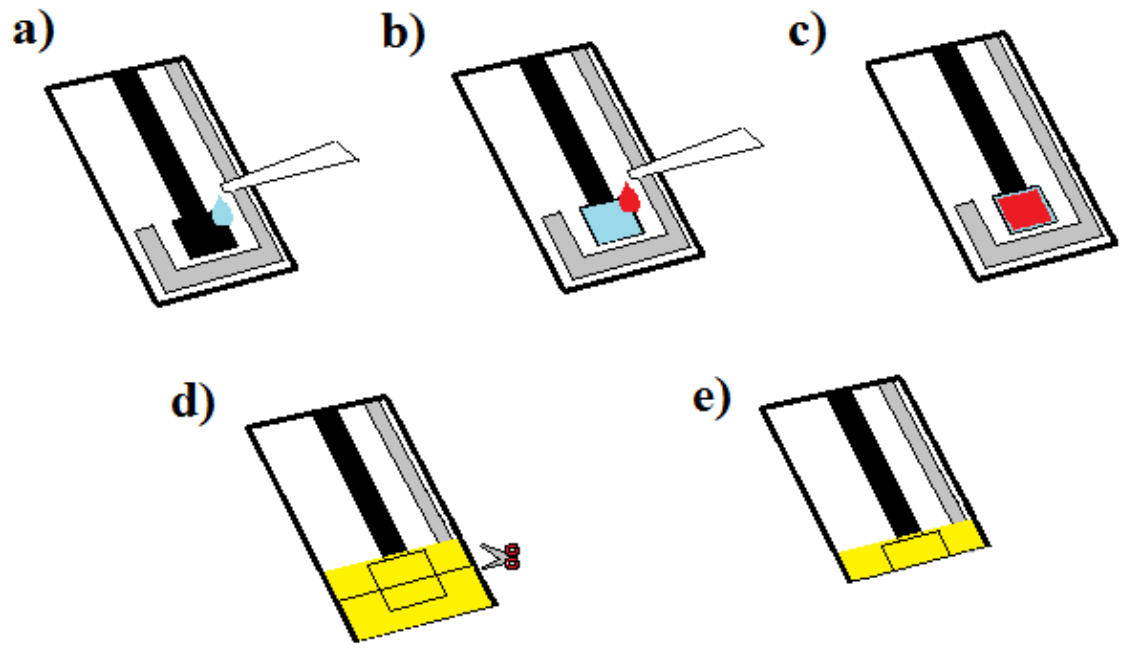

Figure 4-1: A step-by-step diagram of the fabrication of the reagentless glutamate biosensor. a) Drop coating of CHIT b) drop coating of GLDH and NAD^+ c) drying d) application of insulating tape across working area of electrode e) cutting through working electrode to expose the microband biosensor.

4.2.4. Electron Microscopy

The microband biosensor was attached to a 9 mm-diameter double sided adhesive carbon disc on a 45º angled aluminium stub. A cross section of the edge of the electrode was examined using a Philips XL30 environmental scanning electron microscope (ESEM).

4.2.5. Voltammetry and amperometry

Each cyclic voltammogram or amperogram, was obtained by lowering a microband biosensor, in combination with a screen-printed Ag/AgCl reference electrode, into the voltammetric cell containing a quiescent 10 ml solution of 0.75 M phosphate buffer containing 5mM NADH, plain 0.75 M phosphate buffer or culture medium. For the voltammetric characterisation of NADH the following procedure was employed; phosphate buffer solution was degassed with nitrogen for 5 minutes, 15 s equilibration at open circuit voltage, working electrode potential scanned from -0.5 V to +0.6V to -0.5V at a scan rate of 5mV/s

For amperometric calibration studies the voltage was switched directly from open circuit to the appropriate applied potential (+0.1 V vs. Ag/AgCl). Solutions were agitated with a gyrorotator at a fixed speed for both phosphate buffer and cell media studies. This was in order to facilitate diffusion and improve the homogeneity of the solution.

Initially, studies were carried out with the biosensor in phosphate buffer solutions containing glutamate in order to determine whether the performance was suitable for the subsequent monitoring of cells. Amperometry, over prolonged times in cell culture, was performed by applying a potential of +0.1 V to the micro-band biosensor immersed in a 6 ml volume of cell culture medium in the well of a 6-well plate, containing HepG2 cells and paracetamol where appropriate. The resulting real time current responses were recorded over a period of 8 hours.

4.2.6. HepG2 cell culture

The HepG2 (Human Caucasian Hepatocyte Carcinoma) cell line (obtained from ECACC) was cultured as a monolayer in 75 cm^2 flasks, in a 5% CO_2-in-air atmosphere at 37 °C, at an initial density of $2*10^5$ cells cm^{-2}. Cells were counted using a haemocytometer. The medium was MEM containing 10% FBS, 1% non-essential amino acids (NEAA), 200 nM L-glutamine. When confluent, the cells were detached by trypsinisation, and resuspended in MEM containing FBS, NEAA and glutamine at the same initial density. For the assays described, cells were plated at a density of 2 x 10^6 cells mL^{-1} in 6 mL volumes into 6-well tissue culture plates.

4.2.7. Real time monitoring of glutamate in cell culture media in the presence/absence of cells and toxic compounds.

HepG2 cells grown in T75 flasks, once 80% confluent were trypsinized and transferred to six well tissue culture plates, along with 6mls of cell media under sterile conditions. 24 hours were allowed to pass to allow the cells to fully adhere to the bottom of the cell well. Once adhered, appropriate aliquots of paracetamol (100mM in 20% ethanol, diluted with cell culture medium) were added to the wells in order to achieve the desired concentration. The cork lids carrying a microband glutamate biosensor and reference electrode were push-fitted into each well. A small (1 mm diameter) hole in the top surface of each sensor cork lid allowed air to escape, avoided pressure build-up during the push-fitting step and allowed for gaseous exchange to maintain the pH of the media. The non-essential amino acids (NEAA) added to the cell culture media was found to contain a small concentration of glutamate (0.31μM) which may have contributed to the background current.

Electrical contact was made through the temperature seal of the incubator and connected to respective channels of the multichannel potentiostat. The 6-well plate was rotated utilising a mini-shaker within an incubator at 37 °C, 5% CO_2 in the air atmosphere. An operating potential of +0.1 V vs Ag/AgCl was applied to each working electrode, and the instrument was run in amperometric mode 8 hours for the real time studies. The resulting data were exported into Microsoft Excel and plotted as current-versus time graphs.

4.3. Results and discussion

4.3.1. Microband biosensors

An SEM image of the edge of the microband electrodes based on MB-SPCE are shown in Figure 4-2. Each layer of the biosensor is labelled, with each layer visible. The thickness of the original MB-SPCE working electrode is about 20 µm, thus the sensor is defined as a microband biosensor. The exposed edge of the microband electrode possesses an area of 60,000 square µm (3mm x 20µm).

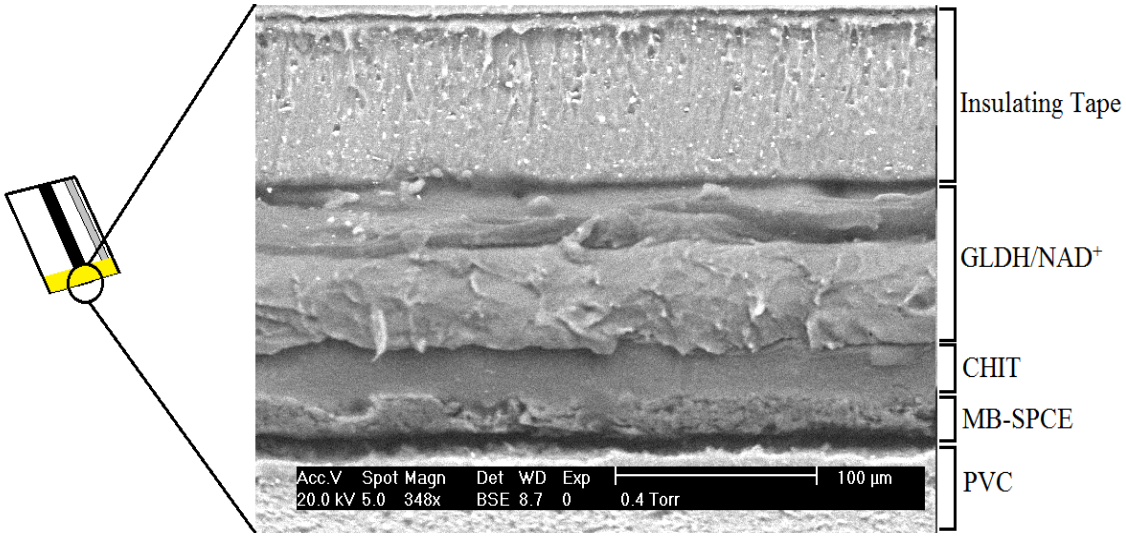

Figure 4-2. SEM image of the cross section of the microband biosensor electrode.

4.3.2. Electrochemical Characterisation in NADH utilising Cyclic Voltammetry

The cyclic voltammogram for the Meldola's Blue microband electrode in a solution containing 0.75mM PBS, 0.50 mM NaCl, pH 7 and 5mM NADH, the resulting cyclic voltammogram (Figure 4-3A) showed sigmoidal behaviour, with an increased current response, which confirms that the response is due to the electro-catalytic oxidation using the MB-SPCE [18]. This electrocatalytic response for NADH is a prerequisite for the operation of the amperometric glutamate microband biosensor. The blank carried out in the same solution in the absence of NADH showed a peak shape response indicative of a surface confined layer of Meldola's Blue (Figure 4-3, B, C).

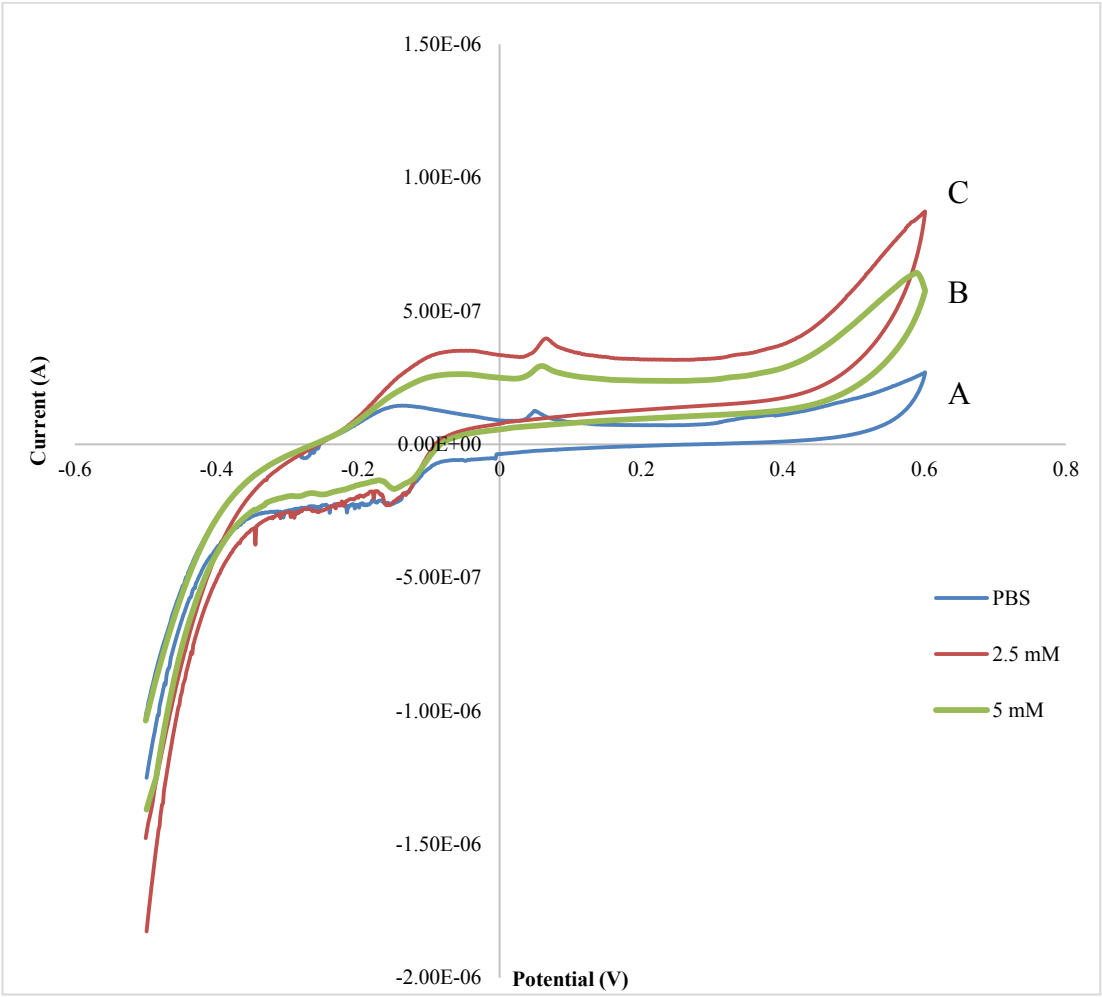

Figure 4-3: Cyclic voltammograms of a reagentless glutamate biosensor in the presence (A) and absence of 2.5 (B) and 5mM NADH (C) (PBS, pH 7.0). Scan rate at 5mVs.

4.3.3. Calibration studies of glutamate in phosphate buffer solution.

Amperograms obtained with the microband biosensors in agitated phosphate buffer solutions (0.75mM with additional 0.5mM NaCl) at an applied potential +0.1V (Ag/AgCl) are shown in Figure 4-4. The corresponding calibration plot is shown in Figure 4-5. Arrows indicate aliquots of 6μL of a 25mM glutamate stock solution into 6mLs of buffer. The standard deviations represented are based on n = 5. The biosensor, operating in phosphate buffer possessed the following characteristics; linear range; 25 - 125μM, sensitivity; 0.0636 nA/μM and a theoretical limit of detection of 1.20μM (based on 3*S/N). All studies were carried out at 37ºC, pH 7.0. We considered that these characteristics were suitable for further studies with cell media. The current density for the biosensor in phosphate solution was calculated to be 5μA/cm^2, which is quite low for a microband biosensor. A study investigating the voltammetric behaviour of the microband biosensor in the presence of 5mM ferricyanide resulted in a current density of 740μA/cm^2, indicating that the Meldola's Blue is the rate limiting step.

4.3.4. Amperometric studies of glutamate in cell media.

Amperograms obtained with the microband biosensors in agitated MEM cell media at an applied potential +0.1V (Ag/AgCl) are shown in Figure 4-6. The arrows indicate aliquots of 6μL of a 25mM glutamate stock solution into 6mLs of buffer The corresponding calibration plot is shown in Figure 4-7. The standard deviations rare based on n = 3. The biosensor, functioning in cell media, possessed the following characteristics; linear range; 25 – 150 μM, sensitivity; 0.128 nA/μM and a theoretical limit of detection of 4.2μM (based on 3*S/N). All studies were carried out 37ºC, pH 7.0, in-air-atmosphere of 5% CO_2. At this point the biosensor assay appeared to be suitable for our proposed real time cell toxicity studies.

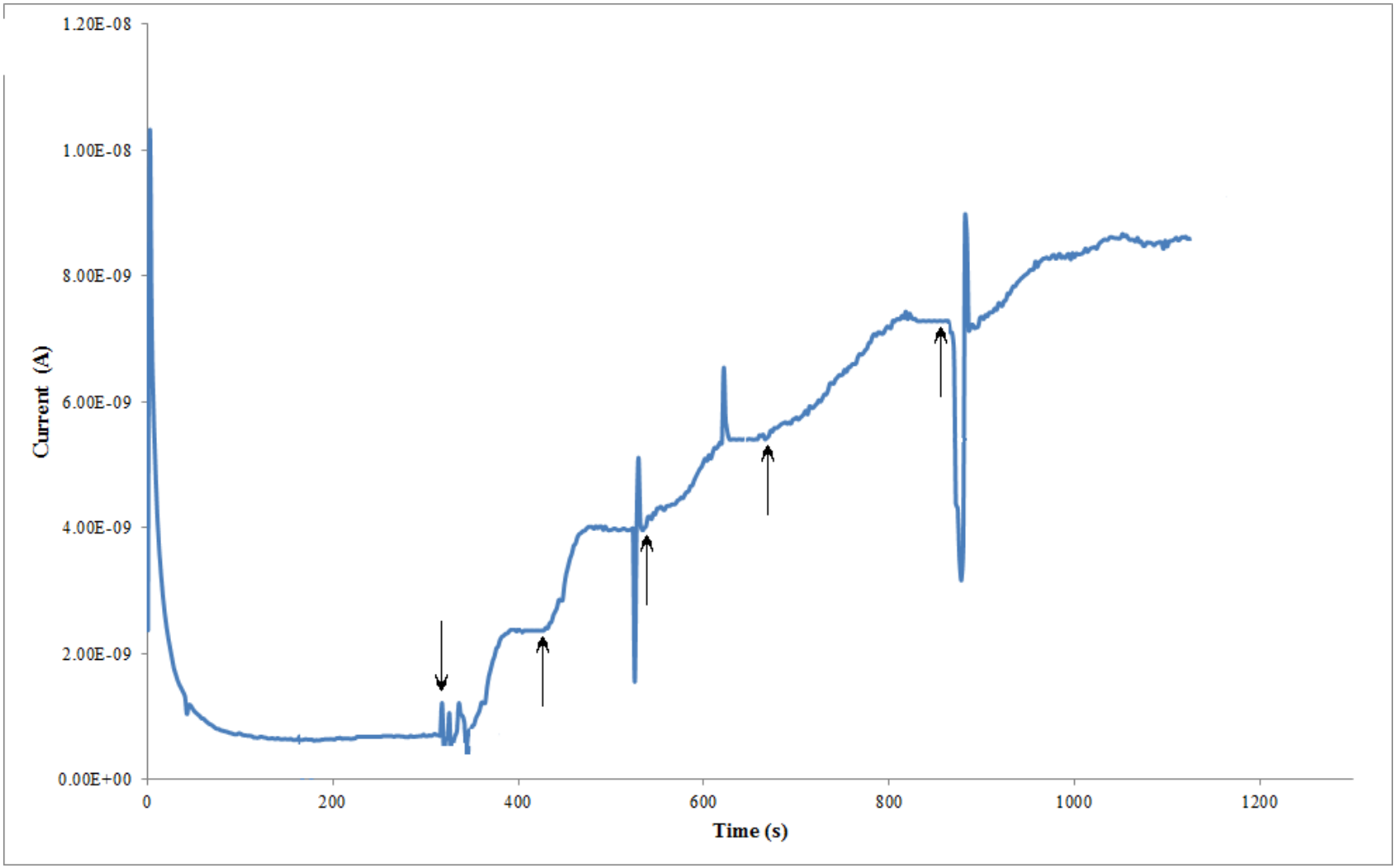

Figure 4-4: A) Amperogram conducted with the reagentless glutamate microband biosensor in phosphate buffer (pH 7). Each arrow indicates an aliquot of 6µL of a 25mM glutamate stock solution into 6mLs of buffer.

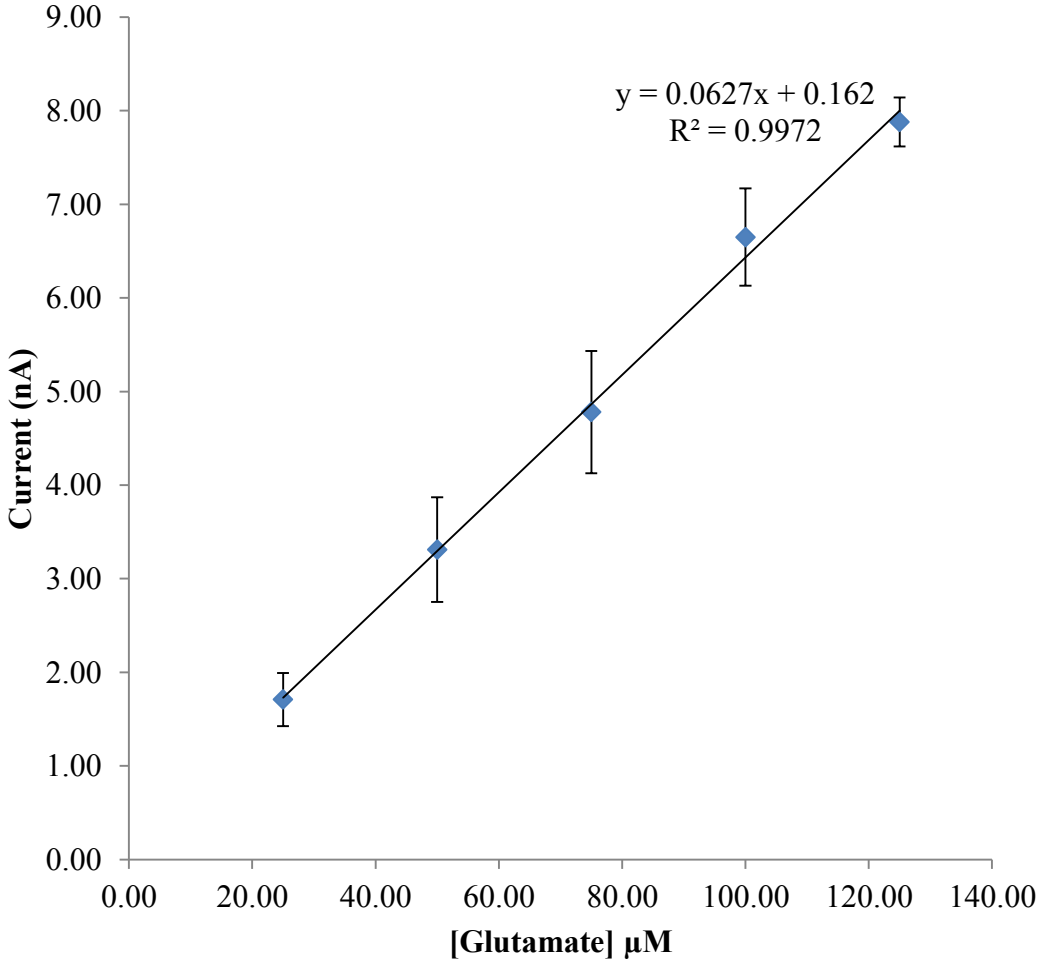

Figure 4-5: Resulting calibration plot. Standard deviation bars are based on n = 5). Sensitivity: 0.0627nA/µM

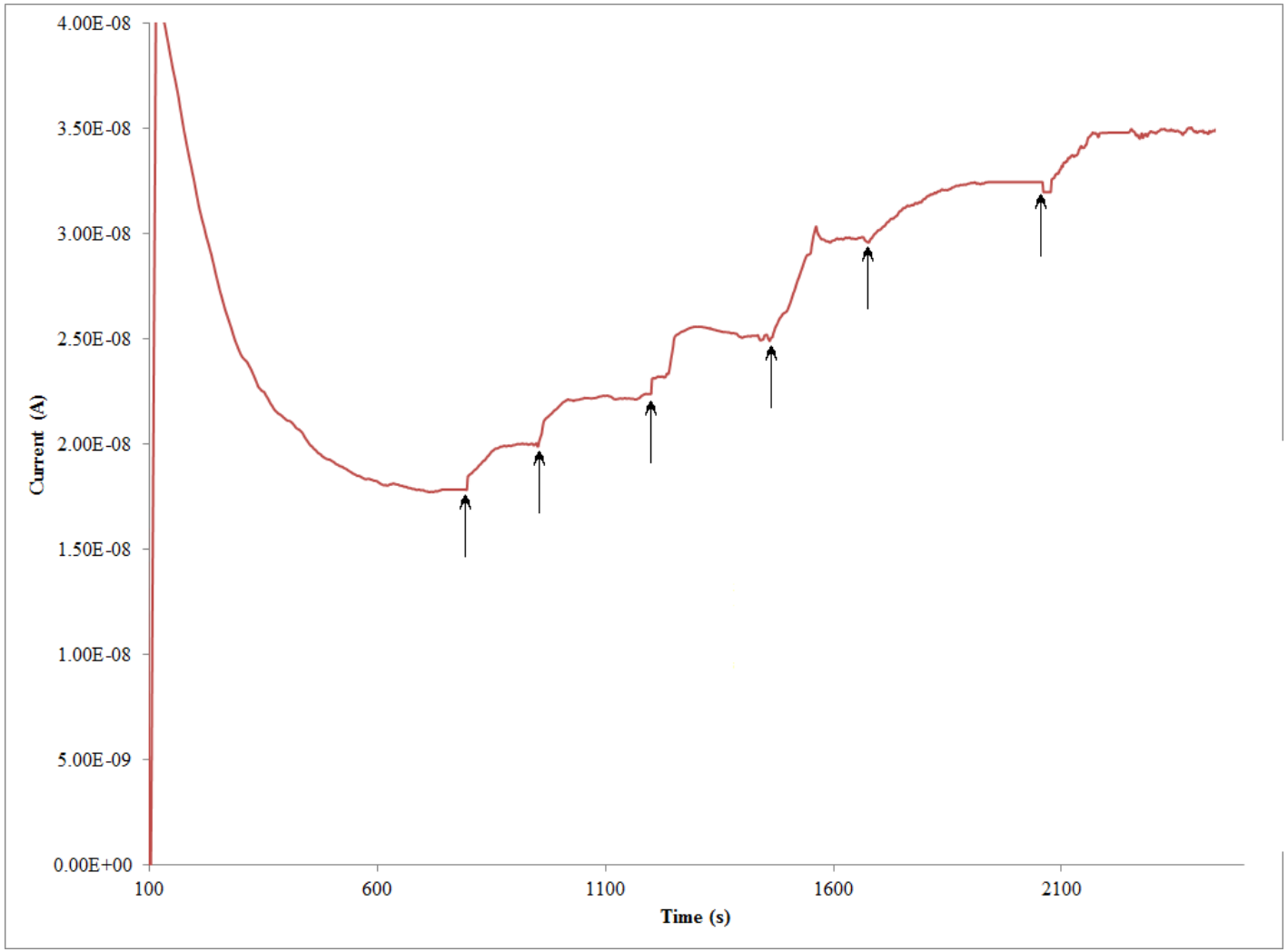

Figure 4-6: A) Amperogram conducted with the reagentless glutamate microband biosensor in cell media. Each arrows indicate an aliquot of 6µL of a 25mM glutamate stock solution into 6mLs of cell media.

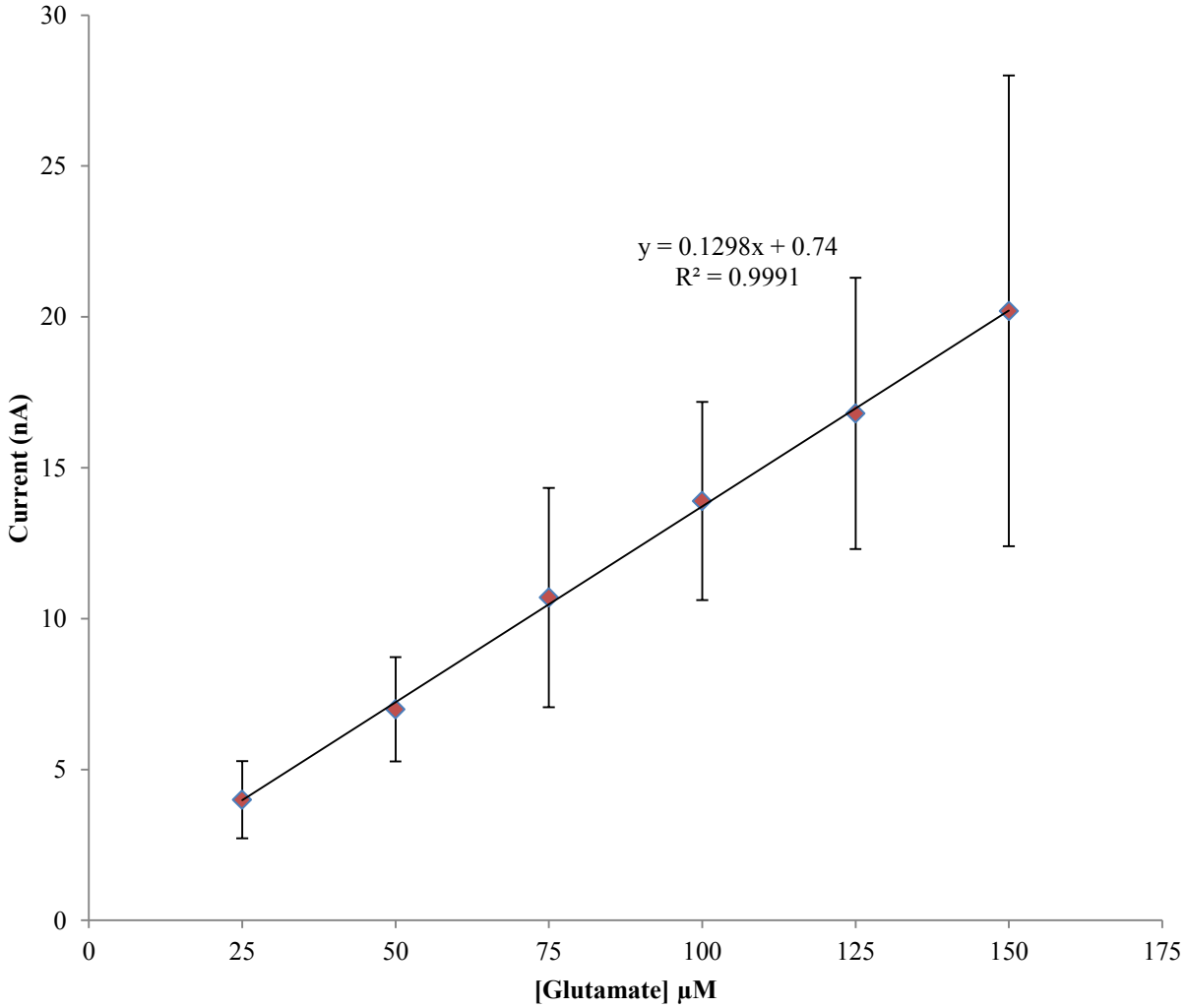

Figure 4-7: Resulting calibration plot. Standard deviation bars are based on n = 5. Sensitivity: 0.1298nA/µM

Fully confluent HepG2 cells were exposed to various concentrations of paracetamol (1mM, 5mM and 10mM) for 24 hours. After exposure, the cell media was collected and the cells were discarded. The microband biosensor was initially submerged in blank untreated cell media, then once steady state was reached the biosensor was transferred to the post-exposure cell media. This resulted in an increase in current as a result of the additional glutamate released from inside the HepG2 cells after exposure to paracetamol exposure. Once steady state had been reached, aliquots of 25mM glutamate were added to the cell. The response generated by the endogenous glutamate present in the cell media was substrate and the resulting current increases from the additions of glutamate were plotted against concentration. A standard addition calibration plot was constructed in order to determine the original concentration of glutamate found in the cell media.

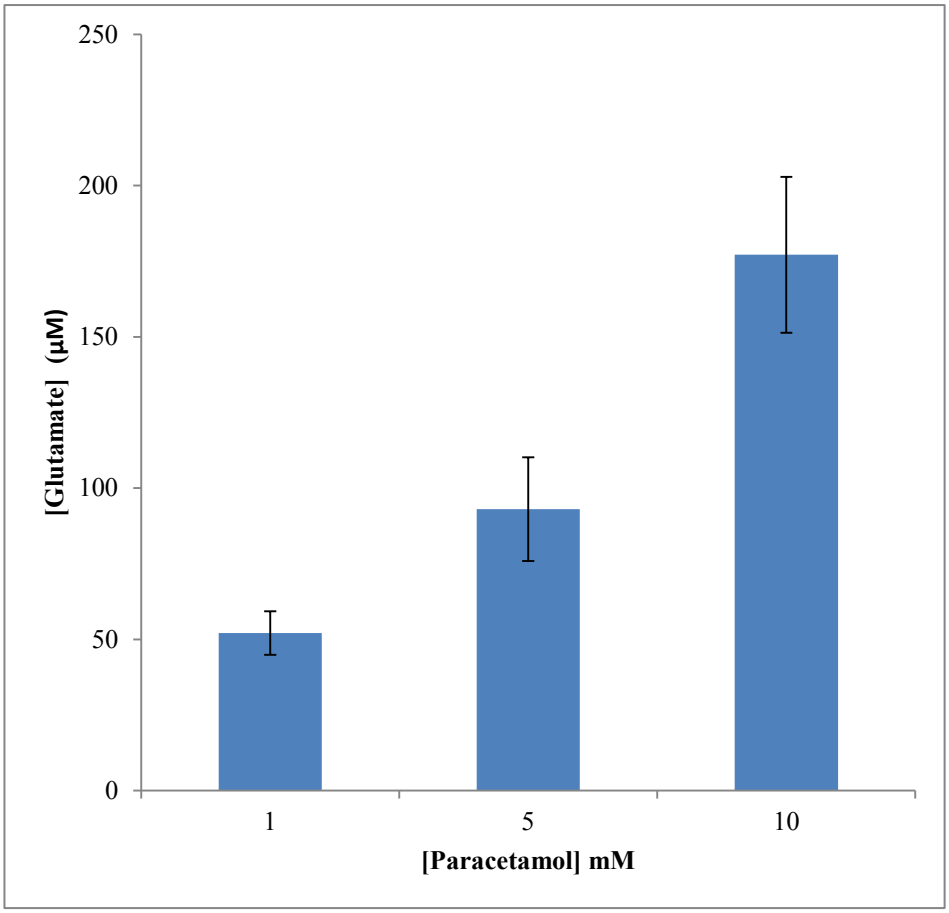

Figure 4-8: Bar chart illustrating the concentrations of glutamate present in cell media 24 hours post incubation in the presence of various concentrations of paracetamol. Std deviations based on n = 3.

The average endogenous concentrations for glutamate released from the HepG2 cells was 52.07μM (CoV: 13.74%, n = 3), 93.30μM (CoV: 18.41%, n = 3) and 177.14μM (CoV: 14.54% n = 3) for 1mM, 5mM, 10mM doses of paracetamol respectively. A t-test to analyse the significance of the values for 1mM and 5mM doses of paracetamol. A p value of less than 0.05 was generated, implying the difference between the two values is significant (Appendix Table 1). The resulting dose response plot is shown in Figure 4-8. The standard deviations shown are based on n = 3. Typical intracellular glutamate levels are 2 – 5 mM/L [19][20].

4.4. Real-time monitoring of glutamate release from HepG2 cells exposed to various concentrations of paracetamol.

Microband biosensors were placed into six-well plates containing fully confluent HepG2 cells exposed to various concentrations of paracetamol (1mM, 5mM and 10mM) for 8 hours. Microband biosensors were placed into the wells which monitored the release of glutamate and other constituents from the cells in real time by amperometry. Figure 4-9 illustrates the electrode holder, six well plate and minishaker setup within an incubator for the real time studies. The minishaker was utilised in order to assist diffusion and decrease the response time. The electrode holder consists of a cork lid which has been pierced with gold electrode clips. The exposed ends of the gold clips are connected to a “chocolate” block connector, which is wired directly one of the ports on the potentiostat. This enables the biosensor to be attached to the gold clips on the underside of the cork lid and be submerged in the cell media solution.

This method offers numerous advantages over a typical electrode holder setup. Firstly, the cork-lids reduce the evaporation of the cell media, thereby reducing potential drifts in current due to a false increase in concentration. Secondly, the lid is porous allowing for gaseous exchange, thereby maintaining the cell media pH. A pipette lid is also inserted through the cork, to assist gaseous exchange and allow for an entry port for the addition of

aliquots of glutamate. Thirdly, the cork lids allow for the real time analysis of multiple wells simultaneously, as they fit securely into the six well plates. Finally, it reduces the likelihood of shorting as the connections to the potentiostat are separated from the cell media solution.

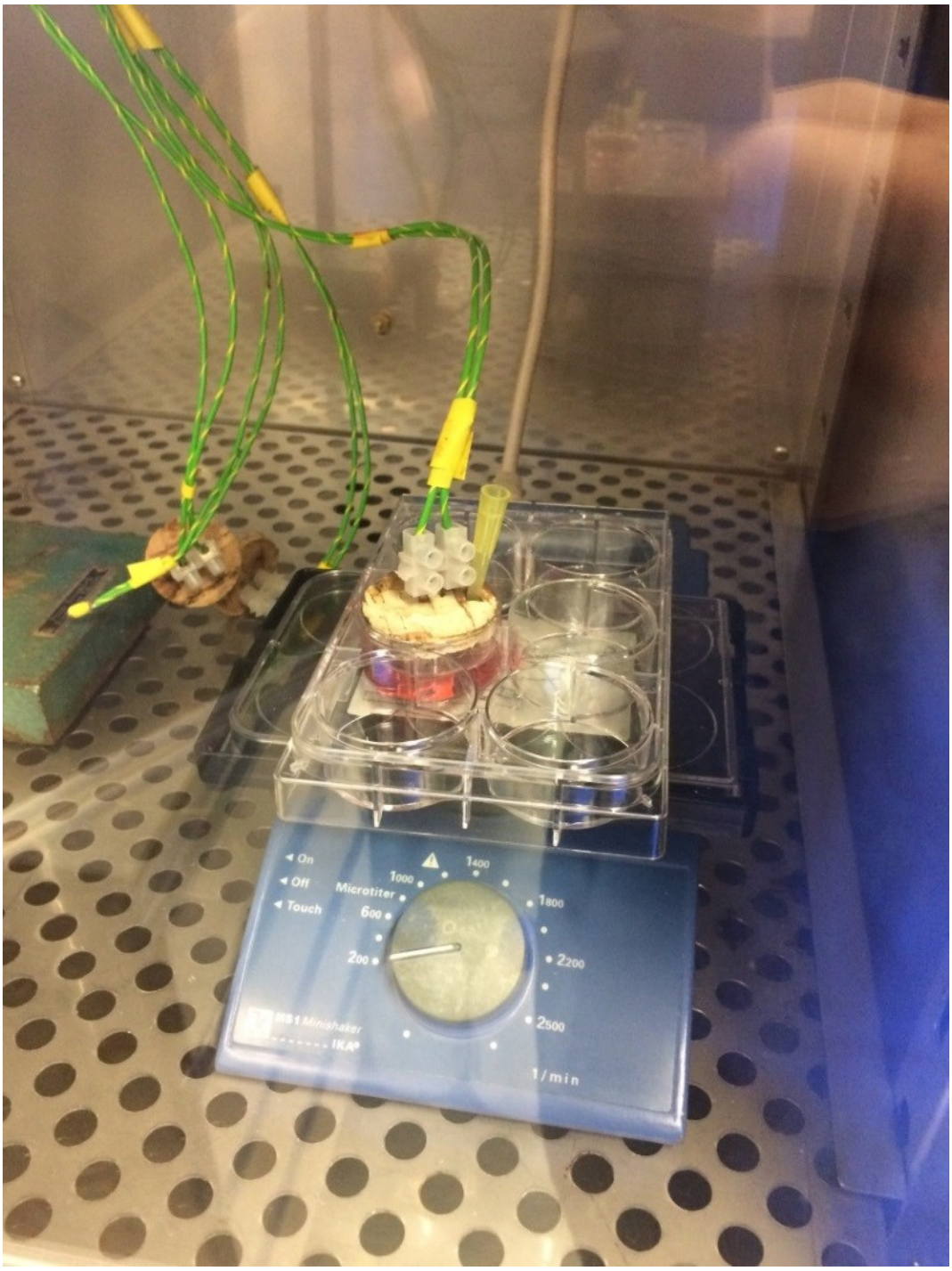

Figure 4-9: Image depicting the experimental setup used for the real time studies.

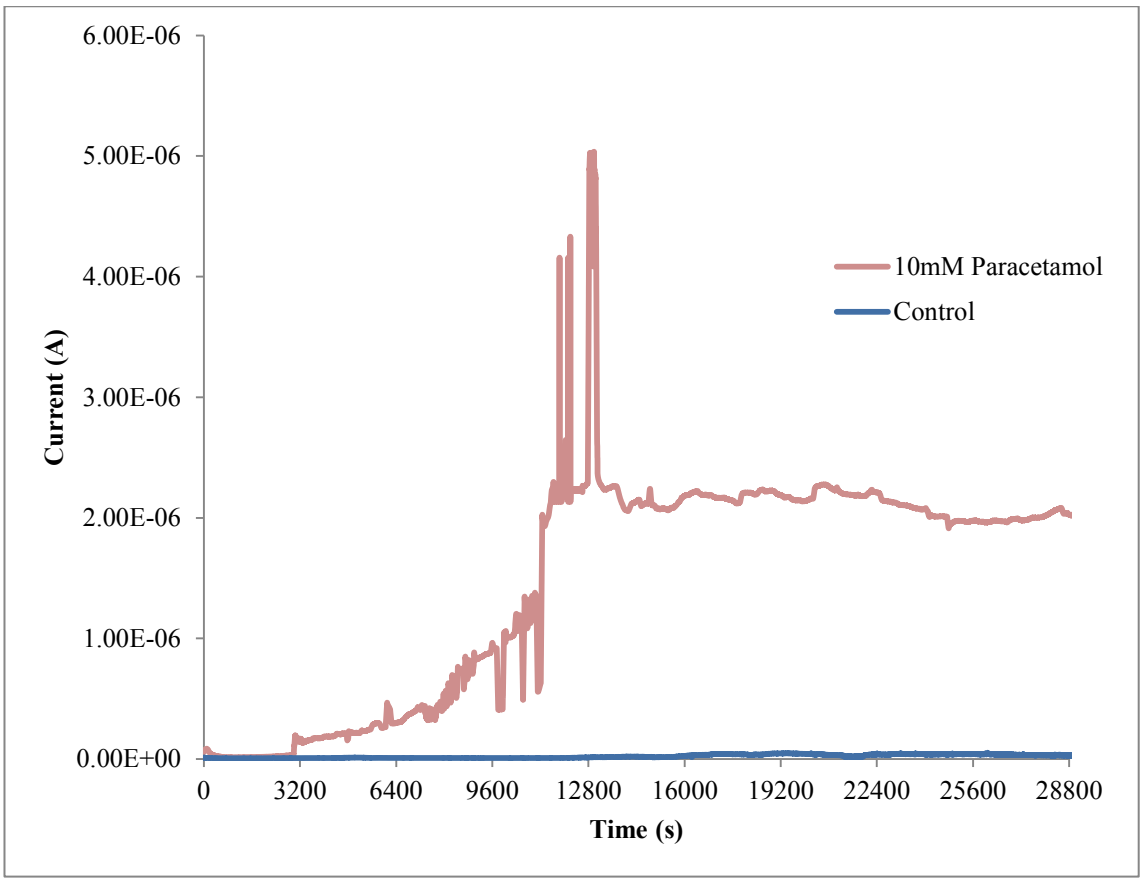

Figure 4-10: Typical real time amperometric response produced by glutamate released from HepG2s cells exposed to 10mM of paracetamol over 8 hours. 3600s = 1 hour.

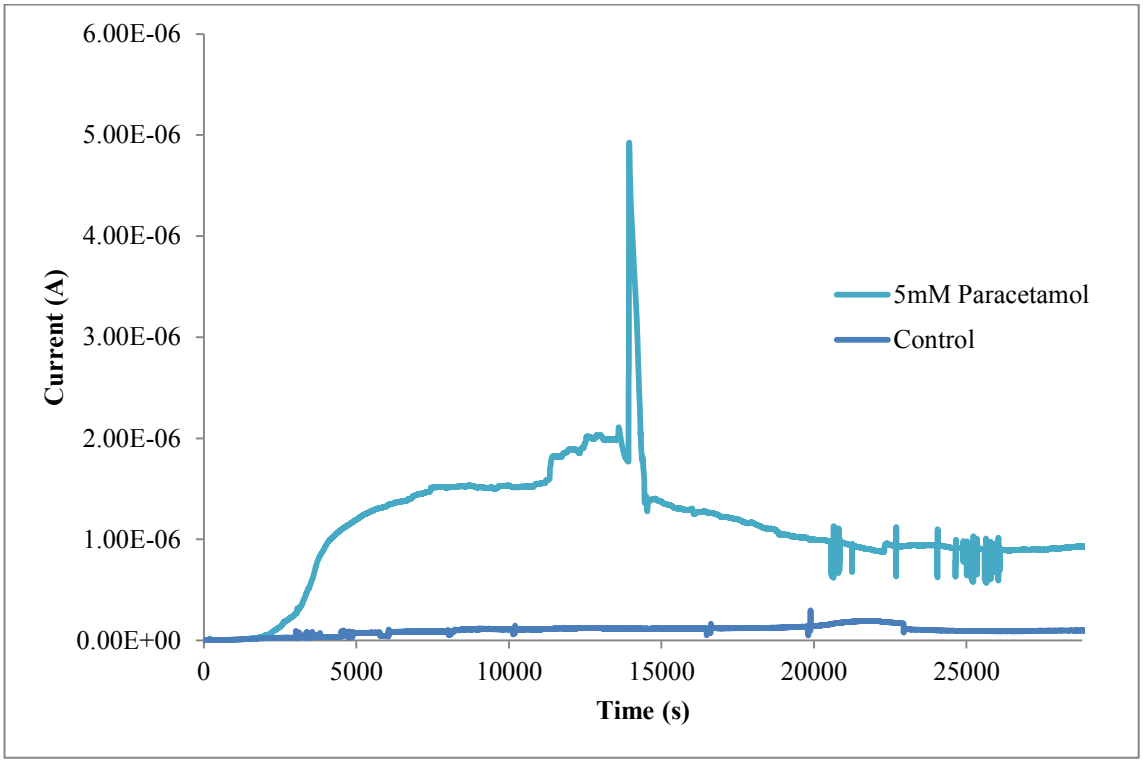

Figure 4-11: Typical real time amperometric response produced by glutamate released from HepG2s cells exposed to 5mM of paracetamol over 8 hours.

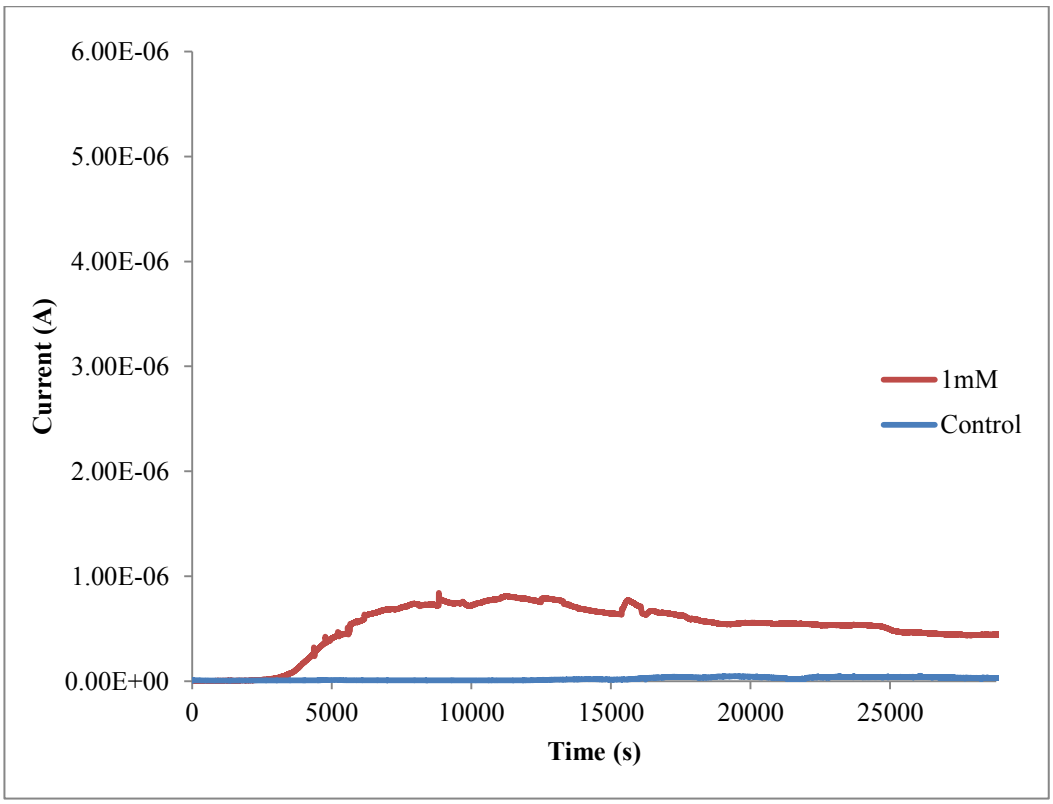

Figure 4-12: Typical real time amperometric response produced by glutamate released from HepG2s cells exposed to 5mM of paracetamol over 8 hours.

The resulting typical real time dose response plots for each concentration is shown in Figure 4-10, Figure 4-11 and Figure 4-12. The amperometric responses demonstrate the ability of the microband biosensor to monitor the release of glutamate from the HepG2 cells as a result of paracetamol induced toxicity. As a result, the observation of early metabolic reactions, cellular recovery from the initial exposure to paracetamol, and the rate at which cellular damage occurs, is possible.

It should be noted that the currents generated by the biosensor, while monitoring the HepG2, cells in real time exceeds the current corresponding to the K_m attained in non-treated culture media. This observation is probably as the result of the release of additional NAD^+ from the HepG2 cells, as well as additional glutamate, resulting in higher currents.

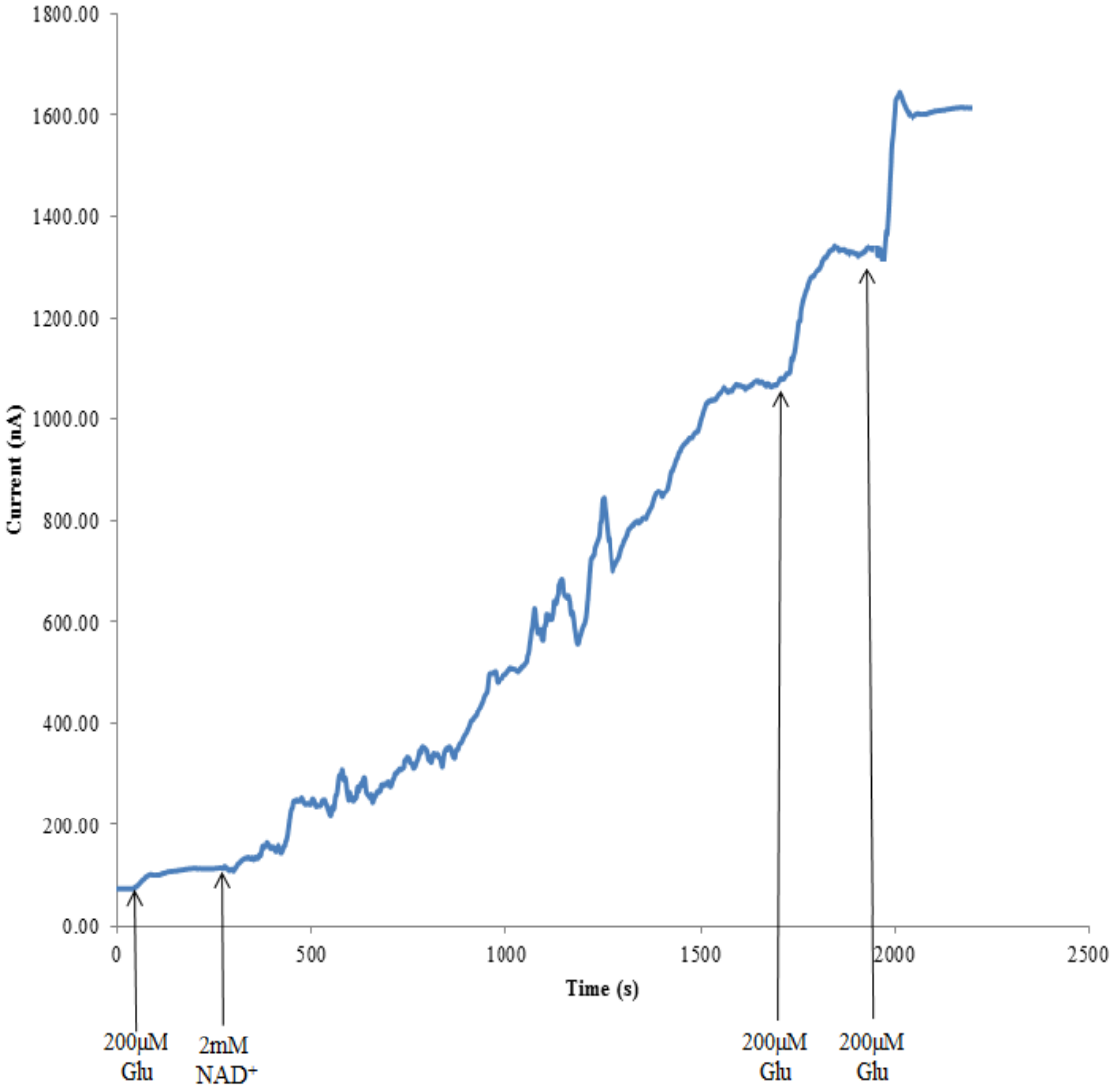

Figure 4-13: Amperogram illustrating additions of 200µM glutamate and 2mM NAD^+ into a cell containing 6mLs of cell media, in the absence of HepG2 cells.

In order to provide evidence for this observation, a study was performed with the biosensor in cell media containing glutamate without cells, but with the addition of NAD^+ solution. Figure 4-11 illustrates the current generated by an initial addition of 200µM of glutamate (42nA) to the cell-free medium, followed by the addition of 2mM NAD^+ solution, clearly, a large increase in current occurs following NAD^+ addition. A further two additions of 200µM glutamate were made which resulted in higher currents being generated than for the initial addition of NAD^+ (265nA and 270nA respectively). This study suggests that the NAD^+ released by the cells into free solution results in the increase in current beyond that previously observed with the end-point assay.

An explanation for this effect is as follows. Paracetamol (I) in sub-lethal concentrations is typically processed in the liver through Phase I and Phase II metabolism by CYP450 enzymes, whereby paracetamol is converted to n-acetyl-p-benzoquinone imine (NAPQI) (II). Subsequently, glutathione conjugates the NAPQI to form a non-harmful product (III) under small doses, however, at higher concentrations the glutathione is unable to regenerate at a sufficient rapid rate to sequester the NAPQI [21]. The excess NAPQI subsequently binds to membrane proteins (IV) [22][23], resulting in hepatic necrosis, which leads to the rupture of the cell membrane and release of its contents.

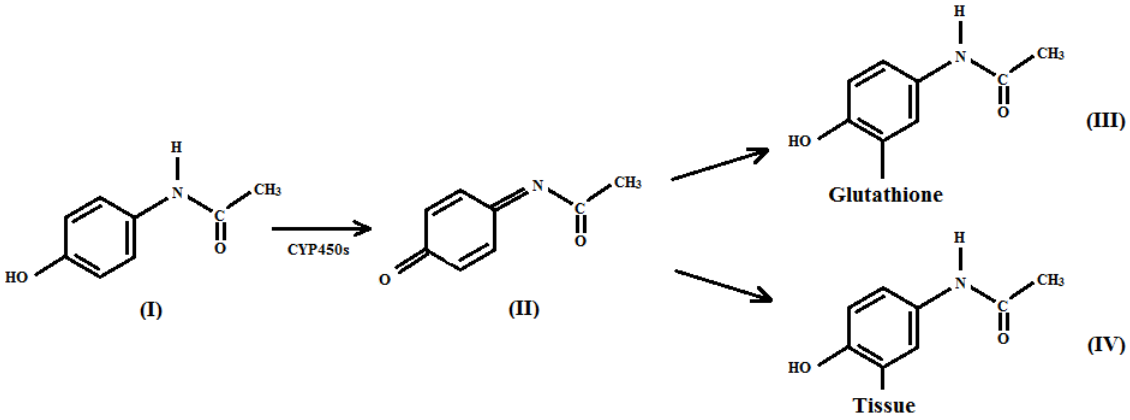

Figure 4-14: Mechanism of Action for Paracetamol and the conjugation of NAPQI.

Glutamate dehydrogenase is found in high concentrations in rat liver [24] and adult human liver [25] due to its association with amino acid metabolism. As a result, increased concentrations of paracetamol are likely to lead to increased hepatic necrosis, subsequently leading to an increase in glutamate concentration, which together with glutamate dehydrogenase and NAD^+ are released from the cells. The currents generated scale accordingly with the increasing concentrations of paracetamol utilised, highlighting that the biosensor is continuously monitoring changes in glutamate released by the cells.

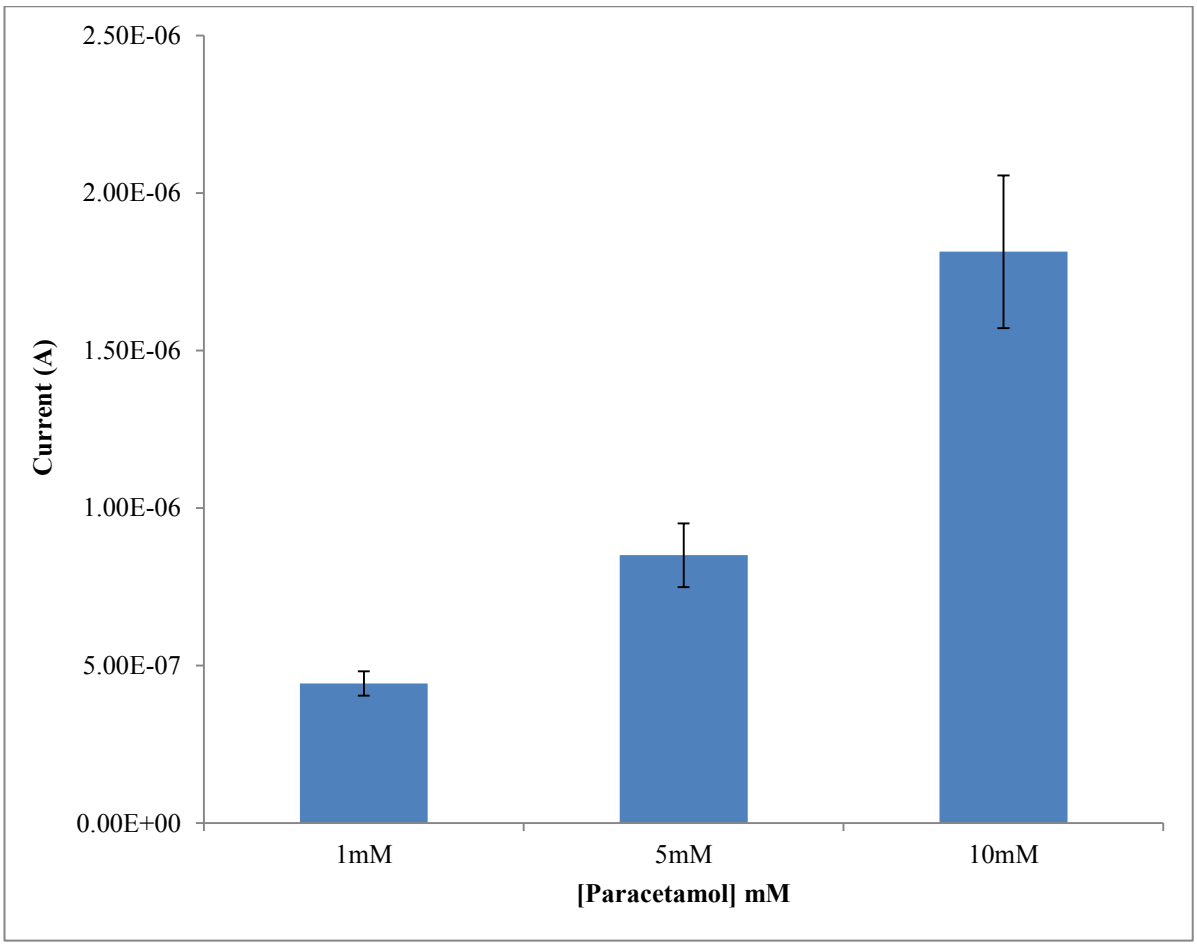

Figure 4-15: Bar chart illustrating the currents generated as a result of glutamate released by the HepG2 cells after 8 hours of incubation in the presence of various concentrations of paracetamol. Std deviations based on n = 3.

Figure 4-15 illustrates the currents generated with respect to the concentration of paracetamol. The standard deviations shown are as follows; 1mM (coefficient of variation (CoV): 3.3%), 5mM (CoV: 9.056%) and 10mM (CoV: 13.18%). It should be mentioned that the effect of paracetamol monitored in real time agrees closely with the end point assay described in section 4.3.5.

4.5. Conclusions

Based on the findings presented in this chapter, it appears that the application of a reagentless glutamate biosensor to both real-time monitoring and post-exposure of mammalian cells in response to toxic challenge from various concentrations of paracetamol can provide a means of assessing metabolic activity.

In repeat studies, the toxicity induced release of glutamate from the HepG2 cells resulted in currents which corresponded with the concentrations of paracetamol utilised. By standardising the experimental setup (37ºC in an incubator with a 5% CO_2 atmosphere, all studies carried out in cell media) reduced the potential for error by maintaining a favourable environment for the cell media/cells. This ensures all metabolic effects are caused by the addition of paracetamol.

Electrochemical microband biosensor monitoring in real time for metabolic events holds great potential for further development. The simple drop coating fabrication procedure and the simple cutting technique to fabricate the microband biosensor, could be a potential platform for developing other microband biosensors based on dehydrogenase enzymes. Future studies towards incorporating a series of reagentless microband biosensors based on screen printed carbon electrodes into a multi-well array system for the simultaneous monitoring of multiple analytes released from mammalian cells in response to toxic challenge for the reduction or replacement of animal testing is currently ongoing.

4.6. References

[1] P. Suresh and P. K. Basu, (2008), "Improving Pharmaceutical Product Development and Manufacturing: Impact on Cost of Drug Development and Cost of Goods Sold of Pharmaceuticals," *J. Pharm. Innov.*, **3**, 175–187.

[2] A. Astashkina, B. Mann, and D. W. Grainger, (2012), "A critical evaluation of in vitro cell culture models for high-throughput drug screening and toxicity.," *Pharmacol. Ther.*, **134**, 82–106.

[3] G. Fotakis and J. A. Timbrell, (2006), "In vitro cytotoxicity assays: comparison of LDH, neutral red, MTT and protein assay in hepatoma cell lines following exposure to cadmium chloride.," *Toxicol. Lett.*, **160**, 171–7.

[4] R. Pemberton, T. Cox, R. Tuffin, I. Sage, G. Drago, N. Biddle, J. Griffiths, R. Pittson, G. Johnson, J. Xu, S. Jackson, G. Kenna, R. W. Luxton, and J. P. Hart, "Microfabricated glucose biosensor for culture well operation," *Biosensors and Bioelectronics*. Elsevier, (15-Apr-2013).

[5] R. M. Pemberton, J. Xu, R. Pittson, G. A. Drago, J. Griffiths, S. K. Jackson, and J. P. Hart, (2011), "A screen-printed microband glucose biosensor system for real-time monitoring of toxicity in cell culture.," *Biosens. Bioelectron.*, **26**, 2448–53.

[6] R. M. Pemberton, F. J. Rawson, J. Xu, R. Pittson, G. A. Drago, J. Griffiths, S. K. Jackson, and J. P. Hart, (2010), "Application of screen-printed microband biosensors incorporated with cells to monitor metabolic effects of potential environmental toxins," *Microchim. Acta*, **170**, 321–330.

[7] R. Pemberton, T. Cox, R. Tuffin, G. Drago, J. Griffiths, R. Pittson, G. Johnson, J. Xu, I. Sage, R. Davies, S. K. Jackson, G. Kenna, R. W. Luxton, and J. P. Hart, "Fabrication and evaluation of a micro(bio)sensor array chip for multiple parallel measurements of important cell biomarkers," *Sensors*. (01-Nov-2014).

[8] N. C. Danbolt, (2001), "Glutamate uptake.," *Prog. Neurobiol.*, **65**, 1–105.

[9] C. F. Zorumski, S. Mennerick, and J. Que, (1996), "Modulation of excitatory synaptic transmission by low concentrations of glutamate in cultured rat hippocampal neurons.," *J. Physiol.*, **494**, 465–477.

[10] R. Dingledine and P. J. Conn, (2000), "Peripheral glutamate receptors: molecular biology and role in taste sensation.," *J. Nutr.*, **130**, 1039S–42S.

[11] W. J. C. Geerts, A. Jonker, L. Boon, A. J. Meijer, R. Charles, C. J. F. Van Noorden, and W. H. Lamers, (1997), "In Situ Measurement of Glutamate Concentrations in the Periportal, Intermediate, and Pericentral Zones of Rat Liver," *J. Histochem. Cytochem.*, **45**, 1217–1229.

[12] R. Hems, M. Stubbs, and H. A. Krebs, (1968), "Restricted permeability of rat liver for glutamate and succinate.," *Biochem. J.*, **107**, 807–15.

[13] F. Botrè, E. Podestà, B. Silvestrini, and C. Botrè, (2001), "Toxicity testing in environmental monitoring: the role of enzymatic biosensors.," *Ann. Ist. Super. Sanita*, **37**, 607–13.

[14] M. Campàs, B. Prieto-Simón, and J.-L. Marty, (2007), "Biosensors to detect marine toxins: Assessing seafood safety.," *Talanta*, **72**, 884–95.

[15] M. I. Montenegro, M. A. Queirós, and J. L. Daschbach, Eds., *Microelectrodes: Theory and Applications*. Dordrecht: Springer Netherlands, (1991).

[16] G. Hughes, R. M. Pemberton, P. R. Fielden, and J. P. Hart, (2014), "Development of a Disposable Screen Printed Amperometric Biosensor Based on Glutamate Dehydrogenase, for the Determination of Glutamate in Clinical and Food Applications," *Anal. Bioanal. Electrochem.*, **6**, 435–449.

[17] R. M. Pemberton, R. Pittson, N. Biddle, and J. P. Hart, (2009), "Fabrication of microband glucose biosensors using a screen-printing water-based carbon ink and their application in serum analysis.," *Biosens. Bioelectron.*, **24**, 1246–52.

[18] S. D. Sprules, J. P. Hart, R. Pittson, and S. a Wring, (1996), "Evaluation of a new disposable screen-printed sensor strip for the measurement of NADH and its modification to produce a lactate biosensor employing microliter volumes," *Electroanalysis*, **8**, 539–543.

[19] J. T. Brosnan, (2000), "Glutamate, at the interface between amino acid and carbohydrate metabolism.," *J. Nutr.*, **130**, 988S–90S.

[20] J. T. Brosnan, K. C. Man, D. E. Hall, S. A. Colbourne, and M. E. Brosnan, (1983), "Interorgan metabolism of amino acids in streptozotocin-diabetic ketoacidotic rat.," *Am. J. Physiol.*, **244**, E151–8.

[21] J. R. Mitchell, D. J. Jollow, W. Z. Potter, J. R. Gillette, and B. B. Brodie, (1973), "Acetaminophen-induced hepatic necrosis. IV. Protective role of glutathione.," *J. Pharmacol. Exp. Ther.*, **187**, 211–7.

[22] M. Moore, H. Thor, G. Moore, S. Nelson, P. Moldéus, and S. Orrenius, (1985), "The toxicity of acetaminophen and N-acetyl-p-benzoquinone imine in isolated hepatocytes is associated with thiol depletion and increased cytosolic Ca2+.," *J. Biol. Chem.*, **260**, 13035–40.

[23] Y. Dai and A. I. Cederbaum, (1995), "Cytotoxicity of acetaminophen in human cytochrome P4502E1-transfected HepG2 cells.," *J. Pharmacol. Exp. Ther.*, **273**, 1497–505.

[24] D. H. Williamson, P. Lund, and H. A. Krebs, (1967), "The redox state of free nicotinamide-adenine dinucleotide in the cytoplasm and mitochondria of rat liver.," *Biochem. J.*, **103**, 514–27.

[25] A. Herzfeld, V. M. Rosenoer, and S. M. Raper, (1976), "Glutamate dehydrogenase, alanine aminotransferase, thymidine kinase, and arginase in fetal and adult human and rat liver.," *Pediatr. Res.*, **10**, 960–4.

CHAPTER FIVE

Development of a novel reagentless, screen–printed amperometric biosensor based on glutamate dehydrogenase and NAD^+, integrated with multi–walled carbon nanotubes for the determination of glutamate in food and clinical applications.

5. Contents

5.1. Introduction

In chapter 3 we have reported on an approach to glutamate biosensor development, based on a screen–printed biosensor incorporating a redox mediator and glutamate dehydrogenase (GLDH). In that approach the required enzyme cofactor, nicotinamide adenine dinucleotide (NAD^+), was added into the analyte solution containing glutamate; the disposable biosensor was successfully applied to the analysis of serum and stock cubes [1]. While successful, the main drawback of this approach for a commercial biosensor is the requirement to add the cofactor into the sample solution. In chapter 4, a reagentless microband biosensor was fabricated and applied to both post-exposure and real time toxicity studies. The fabrication process consisted of utilising CHIT, NAD^+ and GLDH, dropcoated onto the surface of the working electrode of the MB-SPCE. Once dried, the surface was covered with insulating tape and the microband was defined by cutting through the WE with scissors. In this chapter, the fabrication of a conventional sized biosensor utilising a layer-by-layer drop coating procedure is described.

Carbon nanotubes (CNTs) are renowned for their unique electronic and mechanical properties [2]. They possess a high active surface area, excellent biocompatibility [3] and the ability to facilitate redox reactions with fast electron–transfer rates [4]. These abilities have popularised CNTs in the development of electrochemical biosensors.

Two forms of CNT exist; single walled CNT (SWCNTs) and multi–walled CNT (MWCNTs). SWCNTs possess a singular graphite sheet rolled into a tube to produce a cylindrical nanostructure, whereas MWCNT consist of several shells of cylindrical tubes. Integration of redox dyes such as Meldola's Blue (MB) into MWCNT matrices, has been previously demonstrated with well–defined voltammetric responses [5]–[7]. It should be mentioned that the electrocatalyst MB greatly reduces the over-potential for the oxidation of NADH [8].

The low solubility of unmodified MWCNTs leads to poor homogenous dispersion, thus in the present study the MWCNTs were suspended in a solution containing chitosan (CHIT). CHIT is a natural polysaccharide derived from crustaceans, which enhances enzyme stability and possesses good film forming properties [9], [10]. The dispersion of CNTs was possible due to the low pH required to solubilise the CHIT (pH < 3.0) [11], which was achieved using HCl. It was reported that the dispersion of MWCNTs in CHIT/HCl compared with other solvents gave the smallest particle sizes and resulted in the formation of a greater surface area without the need for functionalization.

It has previously been reported that NAD^+ was readily integrated into a glucose dehydrogenase biosensor and did not leach from the MWCNT matrix when coated onto the surface of a glassy carbon electrode [12]. This was achieved utilising a layer-by-layer assembly procedure. Other researchers have reported on the layer-by-layer immobilisation method using modified CNTs to immobilise glutamate oxidase [13], [14] and horse radish peroxidase [15]. This procedure is regarded as a simple, inexpensive and highly versatile method for the incorporation of components into film structures [16]. The advantages of a reagentless device fabricated using this approach is that it leads to a low cost biosensor which is convenient to use as no additional cofactor is required to be added to the sample solution [17], [18].

This chapter describes the steps involved in the layer-by-layer development of a fully reagentless amperometric biosensor for glutamate. The strategy employed to achieve this goal has involved the integration of the biological components (enzyme and cofactor) with multi–walled carbon nanotubes (MWCNTs) on the surface of a Meldola's Blue screen–printed carbon electrode (MB–SPCE). The biosensor has been applied to the determination of glutamate in serum sample and stock cubes.

Based on the literature, it is believed that this is the first report on the development and application of a reagentless amperometric glutamate biosensor, based on GLDH and NAD^+ integrated with a disposable screen-printed electrode.

5.2. Materials and Methods

5.2.1. Chemicals and reagents

All chemicals were of analytical grade, purchased from Sigma Aldrich, UK, except glutamate dehydrogenase (CAT: 10197734001) which was purchased from Roche, UK. The 75 mM phosphate buffer (PB) was prepared by combining appropriate volumes of tri–sodium phosphate dodecahydrate, sodium dihydrogen orthophosphate dihydrate and disodium hydrogen orthophosphate anhydrous solutions to yield the desired pH. Glutamate and NADH/NAD^+ solutions were dissolved directly in 75 mM PB. Chitosan (CHIT) was dissolved in 0.05 M HCl (pH < 3.0) to produce a 0.05% solution following up to 10 minutes sonication. The multi-walled carbon nanotubes (MWCNT)/CHIT solution was prepared by mixing 0.6 mg of MWCNT into 300 µL solution of 0.05% of CHIT, with 15 minutes of sonication and stirring for 24 hours. Meldola's Blue (MB) in solution was prepared by dissolving the appropriate weight in distilled water. Fetal bovine serum (FBS) (South American Origin, CAT: S1810–500) obtained from Labtech Int. Ltd, was used for serum analysis. Food samples (Beef OXO cubes) were obtained from a local supermarket.

5.2.2. Apparatus

All electrochemical experiments were conducted with a three–electrode system consisting of a carbon working electrode containing MB, (MB–SPCE, Gwent Electronic Materials Ltd; Ink Code: C2030519P5), a Ag/AgCl reference electrode (GEM Product Code C61003P7); both printed onto PVC, and a separate Pt counter electrode. The area of the working electrode was defined using insulating tape, into a 3 x 3 mm square area. The electrodes were then connected to the potentiostat using gold clips. Solutions, when required, were stirred using a circular magnetic stirring disk and stirrer (IKA® C–MAG HS

IKAMAG, Germany) at a uniform rate. A μAutolab II electrochemical analyser with general purpose electrochemical software GPES 4.9 was used to acquire data and experimentally control the voltage applied to the SPCE in the 10 ml electrochemical cell which was used for hydrodynamic voltammetry. An AMEL Model 466 polarographic analyser combined with a GOULD BS–271 chart recorder was used for all amperometric studies. Measurement and monitoring of the pH was conducted with a Fisherbrand Hydrus 400 pH meter (Orion Research Inc., USA). Sonications were performed with a Devon FS100 sonicator (Ultrasonics, Hove, Sussex, UK).

5.3. Procedures

5.3.1. Fabrication of the reagentless MWCNT–CHIT–MB/GLDH–NAD+–CHIT/MWCNT–CHIT biosensor.

Fabrication was carried out using a layer-by-layer approach to produce a total of three layers. Solutions were drop-coated onto the $3mm^2$ carbon working electrode. Initial studies were performed to deduce the composition of layers 1 and 3. Figure 5-1 represents the layer-by-layer biosensor.

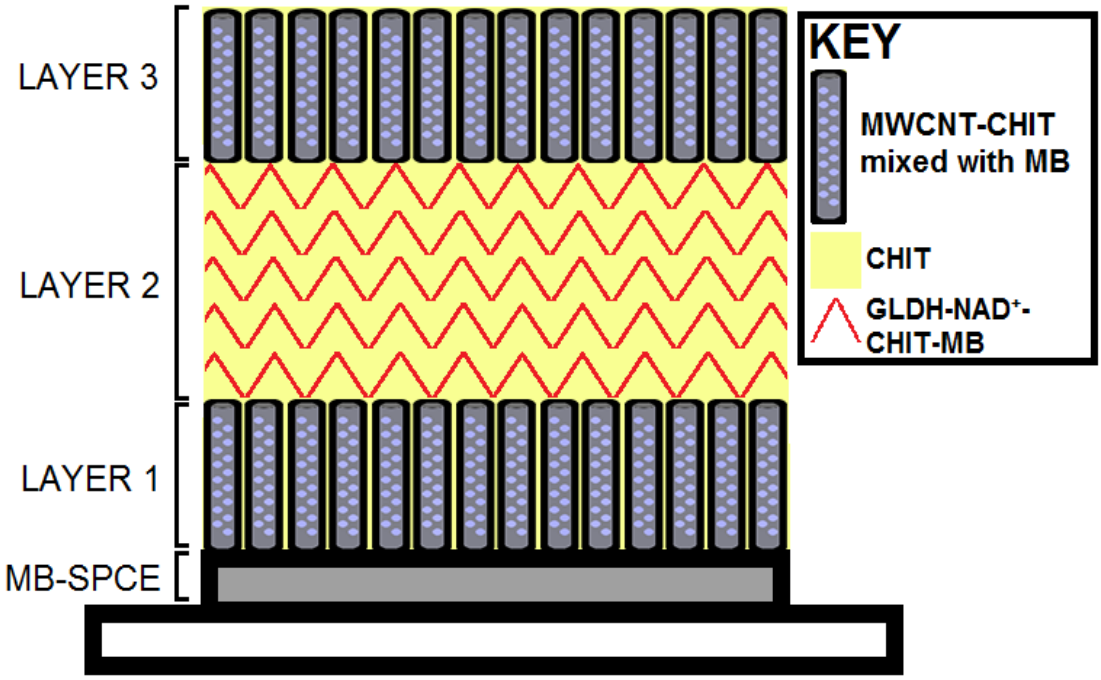

Figure 5-1: A schematic diagram displaying the layer-by-layer drop coating fabrication procedure used to construct the reagentless glutamate biosensor, based on a MB-SPCE electrode.

Layer 1 was formed by drop coating a 10µL mixture of MWCNTs suspended in a solution containing 0.05% CHIT in a 0.05M HCl solution. This layer was allowed to partially dry at 4°C under vacuum for 10 minutes.

Layer 2 was optimised by carrying out amperometric studies with biosensors constructed using different mass combinations of CHIT, NAD^+ with a fixed GLDH content of 27U (Table 1). This layer was allowed to dry at 4°C under vacuum for 3 hours.

Layer 3 was formed in the same manner as Layer 1. This layer was allowed to dry at 4°C under vacuum for 2 hours.

A further study into the effect of including additional MB was also performed. This was done by mixing in 1 µL of 0.01M MB in H_2O with the MWCNTs in layers 1 and 3. For layer 2, an additional 1 µL of 0.01M MB in H_2O was deposited at the composite surface. Biosensors were stored under a vacuum at 4°C when not in use. A photograph of the final biosensor is provided (Figure 5-2).

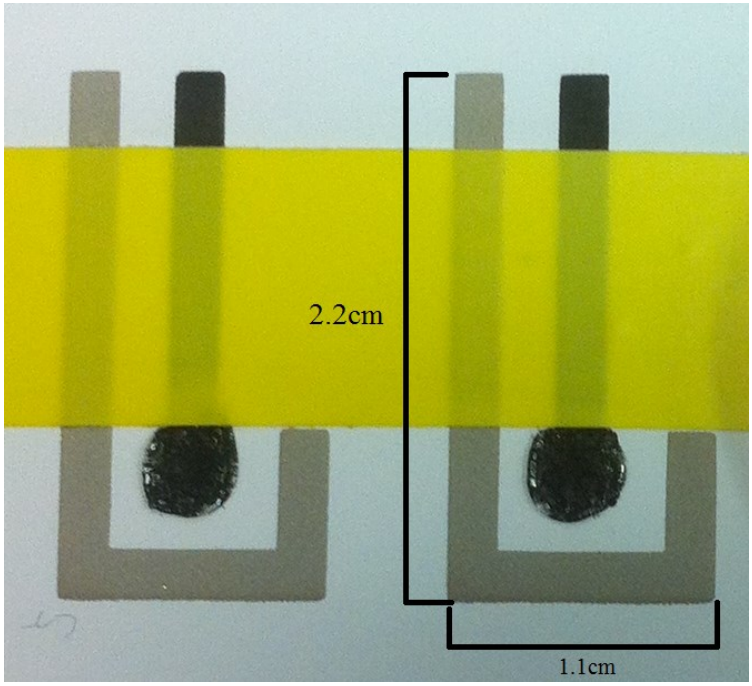

Figure 5-2: Photograph of the final complete biosensors with insulating tape attached.

5.3.2. Hydrodynamic Voltammetry

Hydrodynamic voltammetry was performed using the complete biosensor with 400 μM of glutamate, in 0.75 mM phosphate buffer (pH 7.0) containing 50mM NaCl , in order to enzymatically generate NADH so as to establish the optimum operating potential for the amperometric determination of glutamate in food and serum samples. An initial potential of -120mV was applied to the biosensor and the resulting steady state current was measured; the potential was then changed to -115mV and again a steady state current was measured. The procedure was continued by changing the potential by 50mV steps to a potential of +100mV, with subsequent steps increasing by 25mV up to a final potential of +150mV. The steady state currents were measured at each potential, then a hydrodynamic voltammogram was constructed by plotting the steady state currents against the corresponding potentials.

5.3.3. Optimisation studies with the proposed biosensor using amperometry in stirred solution.

All amperometric measurements were performed with stirred 10mL solutions of 75mM PB pH 7.0 with 50mM NaCl (PBS), using an applied potential of +0.1 V vs. Ag/AgCl. In order to optimise the conditions the biosensor was immersed in a stirred buffer solution, the potential applied and sufficient time was allowed for a steady–state current to be obtained. The optimisation of each component in layer 2 was performed by measuring the amperometric response to the additions of glutamate over the concentration range of 7.5 µM to 100 µM glutamate. The variations in the quantities of the components are shown in Table 5-1.

GLDH (Units)	NAD^+ (µg)	CHIT (µg)
27	13.5	5
27	27	5
27	54	5
27	106	5
27	214	5
27	106	5
27	106	10
27	106	15
27	106	20

Table 5-1: This table displays the combination of components found in layer 2.

After the optimisation of the NAD^+ and CHIT components, the integration of additional 0.01M Meldola's Blue into each layer of the biosensor was investigated by amperometry. Following optimisation of the individual biosensor components, studies into the effects of temperature and pH on the biosensor response were investigated. Optimum pH was

determined by carrying out calibration studies over the pH range 5 – 9 (Figure 5-3). A separate study was conducted to determine the optimum temperature (Figure 5-4). The temperature was varied over the range 25 – 40°C with the pH fixed at 7.

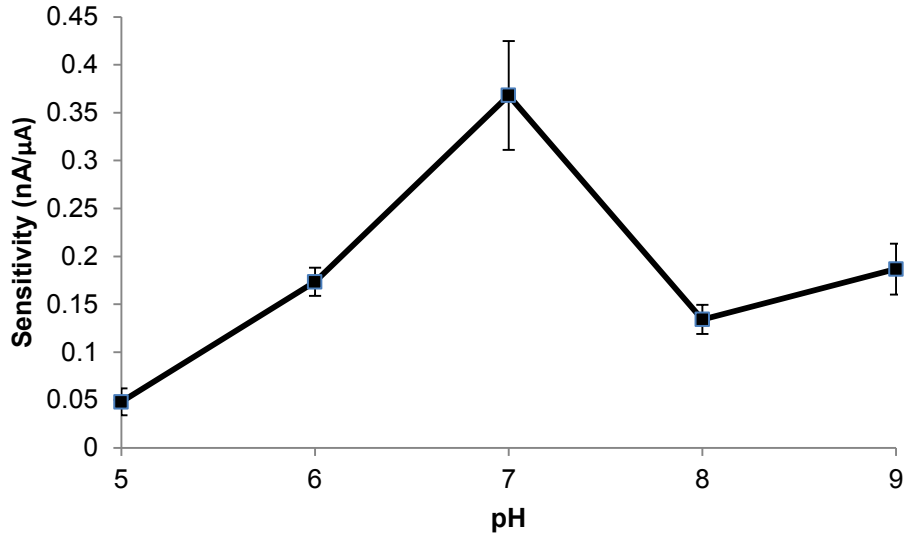

Figure 5-3: pH study conducted over the range of pH 5 to 9. n = 3

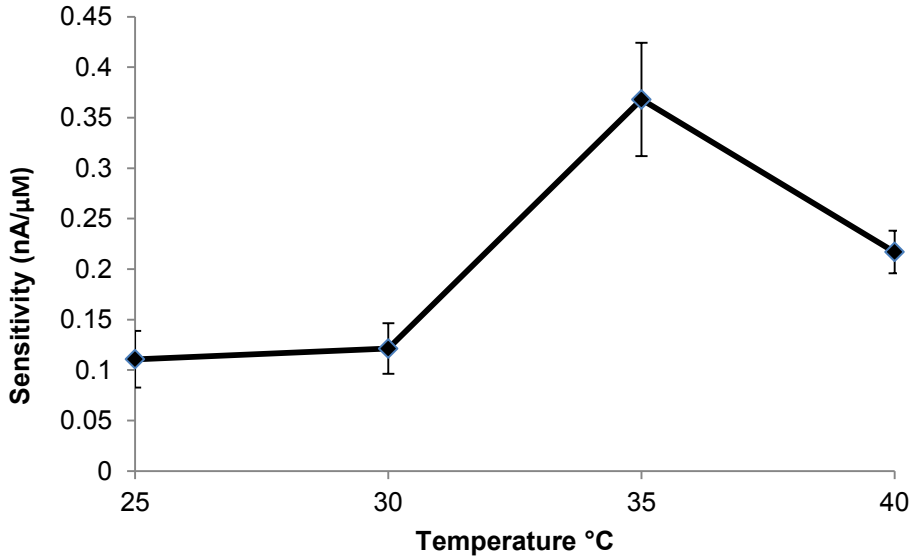

Figure 5-4: Temperature study conducted over the range of 25 to 40°C. n = 3

5.3.4. Application of optimised amperometric biosensor to the determination of glutamate in food.

An OXO cube was prepared by dissolving one cube in 50 mL of phosphate buffer and sonicating for 15 minutes. The endogenous concentration of MSG was determined by using the method of standard addition. An initial 5µl volume of the dissolved OXO cube was added to the stirred buffered solution (10 mL) in the voltammetric cell containing the biosensor, operated at +0.1 V (vs. Ag/AgCl) with subsequent standard additions of 3 µL of 25 mM glutamate.

The reproducibility of the biosensor assay for MSG analysis in OXO cubes was determined by repeating the whole procedure five times with five individual biosensors.

5.3.5. Application of optimised amperometric biosensor to the determination of glutamate in serum.

The endogenous glutamate concentration of serum was determined by injecting an initial volume of 150 µL of serum into 9.85mL of buffer solution. Amperometry in stirred solution using an applied potential of +0.1V vs. (Ag/AgCl) was conducted with the serum solution. This was followed by additions of 3 µL aliquots of 25 mM standard glutamate solution to the voltammetric cell. The currents resulting from the enzymatic generation of NADH were used to construct standard addition plots, from which the endogenous concentration of glutamate was determined (n = 5). The reproducibility of the biosensor measurement was deduced by repeating the studies five times on a freshly diluted solution of the same serum with a fresh biosensor for each measurement.

The procedure was repeated using 50µL of serum spiked with 1.5 mM glutamate (n = 5) to determine to the recovery of the assay.

Due to the complex nature of the samples investigated, interferences such as ascorbic acid, sugars and other amino acids may be present. The possible effects of naturally occurring

interferences from serum and OXO cubes were established using a dummy BSA biosensor. A dummy biosensor was constructed by drop coating the equivalent weight of the enzyme with BSA; however, no signals due to interfering substances were detected.

5.4. Results and Discussion

5.4.1. Characterisation of the biosensor using scanning electron microcroscopy (SEM) and amperometry

Figure 5-5 shows SEM images of the different layers deposited on top of the original Meldola's Blue SPCE (MB-SPCE). The only treatment of the biosensor specimens was a drying procedure.

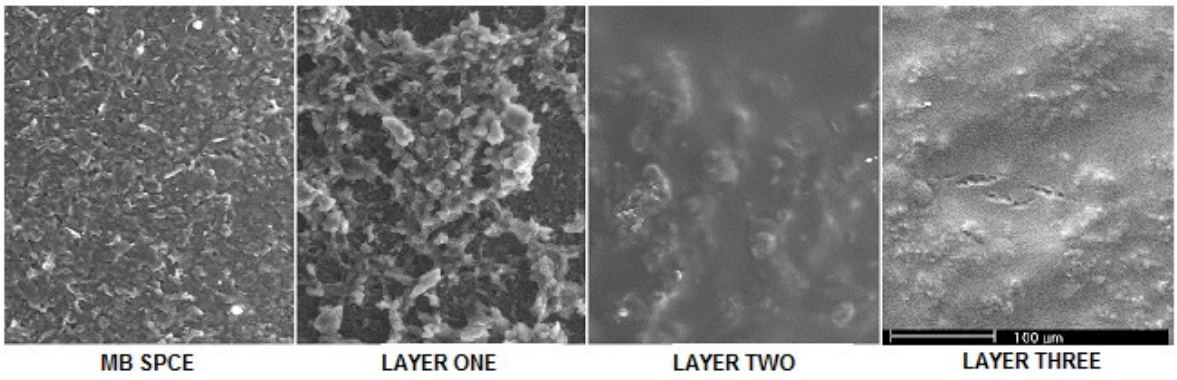

Figure 5-5: SEM imaging of each individual layer of the reagentless biosensor. The scale is the same for all SEM images.

Layer 1 (MWCNTs-CHIT-MB) is a porous open structure which shows the MWCNTs-CHIT deposited on the surface. The MB particles may be absorbed on both the exterior and interior of the MWCNTs.

Layer 2 appears to consist of a more cohesive film covering the added components (GLDH-NAD^+-CHIT-MB). The possibility of utilising this structure as a biosensor for glutamate was investigated, however, the amperograms did not display steady state currents. From this we deduced that the cofactor (NAD^+) and possibly the enzyme (GLDH) were not retained behind the film. This suggests that the film may actually be porous and that in solution the pores increase in size with egress of the biocomponents.

Layer 3 shows a more compact structure and the underlying biosensor components are less visible than in layer 2. The biosensor comprising all 3 layers produced steady state responses to the addition of glutamate, indicating successful immbolisation of all the components.

5.4.2. Hydrodynamic Voltammetry

Hydrodynamic voltammetry was performed using the reagentless biosensor with 400 µM of glutamate in 0.75mM phosphate buffer (pH 7.0) containing 50mM NaCl. The optimum potential was considered to be +0.1V vs. Ag/AgCl (Figure 5-6) as this potential was situated on the plateau of the voltammetric wave.

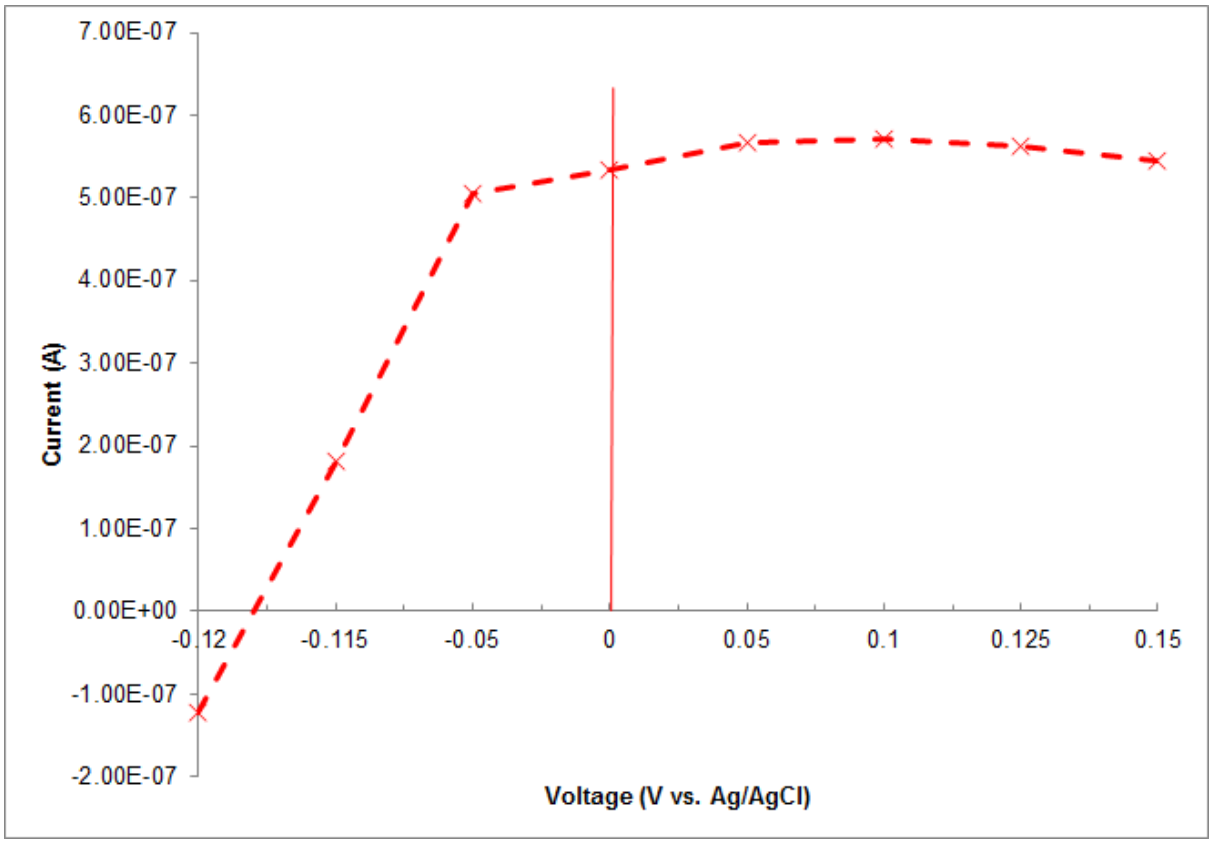

Figure 5-6: Hydrodynamic voltammograms obtained using MB-SPCE/MWCNT-CHIT-MB/GLDH-NAD+-CHIT-MB/MWCNT-CHIT-MB biosensor in the presence of 400µM glutamate in 75mM phosphate buffer (pH 7.0) containing 50 mM NaCl.

5.4.3. Optimisation Studies

GLDH (Units)	NAD^+ (µg)	CHIT (µg)	Linear Range (µM)	Sensitivity (nA/µM)
27	13.5	5	25 – 50	0.035
27	27	5	25 – 100	0.230
27	54	5	25 – 75	0.238
27	106	5	25 – 100	0.307
27	214	5	25 – 50	0.238
27	106	5	25 – 100	0.305
27	106	10	7.5 – 105	0.315
27	106	15	25 – 50	0.261
27	106	20	Steady states not achieved.	N/A

Table 5-2: Performance characteristics of the glutamate biosensor fabricated with different masses of NAD^+ and CHIT using a fixed quantity of GLDH.

Table 5-2 displays that the best performance for the glutamate biosensor was achieved with 106 µg NAD^+ and 10 µg of CHIT, together with 27U of GLDH in layer 2, in the absence of MB.

It has been noted by [19], that with increasing concentrations of CHIT, the particle size of untreated MWCNT's in aqueous solution is increased; consequently the larger particle size leads to increasingly entangled molecules of CNT/CHIT resulting in higher visocities. This change in visoscity would lead to a smaller diffusion coefficient, therefore leading to a decrease in the signal. This might explain why loadings of 15µg and 20µg resulted in less sensitivity than 10µg in the present study. This also suggests that 5µg may not have

sufficiently bound the biological components, in comparison to 10µg of CHIT. Consequently, a CHIT loading of 10µg was selected for further studies.

In order to asses the possibility of enchancing the effectiveness of the electron shuttling through the MWCNTs to the underlying MB electrode, the effect of adding additional MB into these layers was investigated. It was found that the sensitivity was increased from 0.315 nA/µM to 0.396 nA/µM and the linear range was unaltered. Consequently MB was incorporated into all layers of the biosensor for all further studies.

5.4.4. Linear Range, Sensitivity, Detection Limit and Lifetime of Biosensor

Figure 5-7A, shows a typical amperogram obtained with the optimised biosensor for different concentrations of glutamate. The resulting calibration plots (Appendix Figure 1) are linear over the range 7.5 – 105µM, the first calibration plot depicts Fig 5A; the detection limit was 3µM (based on n = 5, the coefficient of variation (CV) was 8.5%), based on three times the signal to noise, and the sensitivity was 0.39 nA/µM (based on n =5, the CV was 6.37%). It should be noted that the biosensor possesses sensitivity relative to surface area of 4.3µA/mM/cm^2. This behaviour demonstrates the possibility of applying this device to food and biological samples.

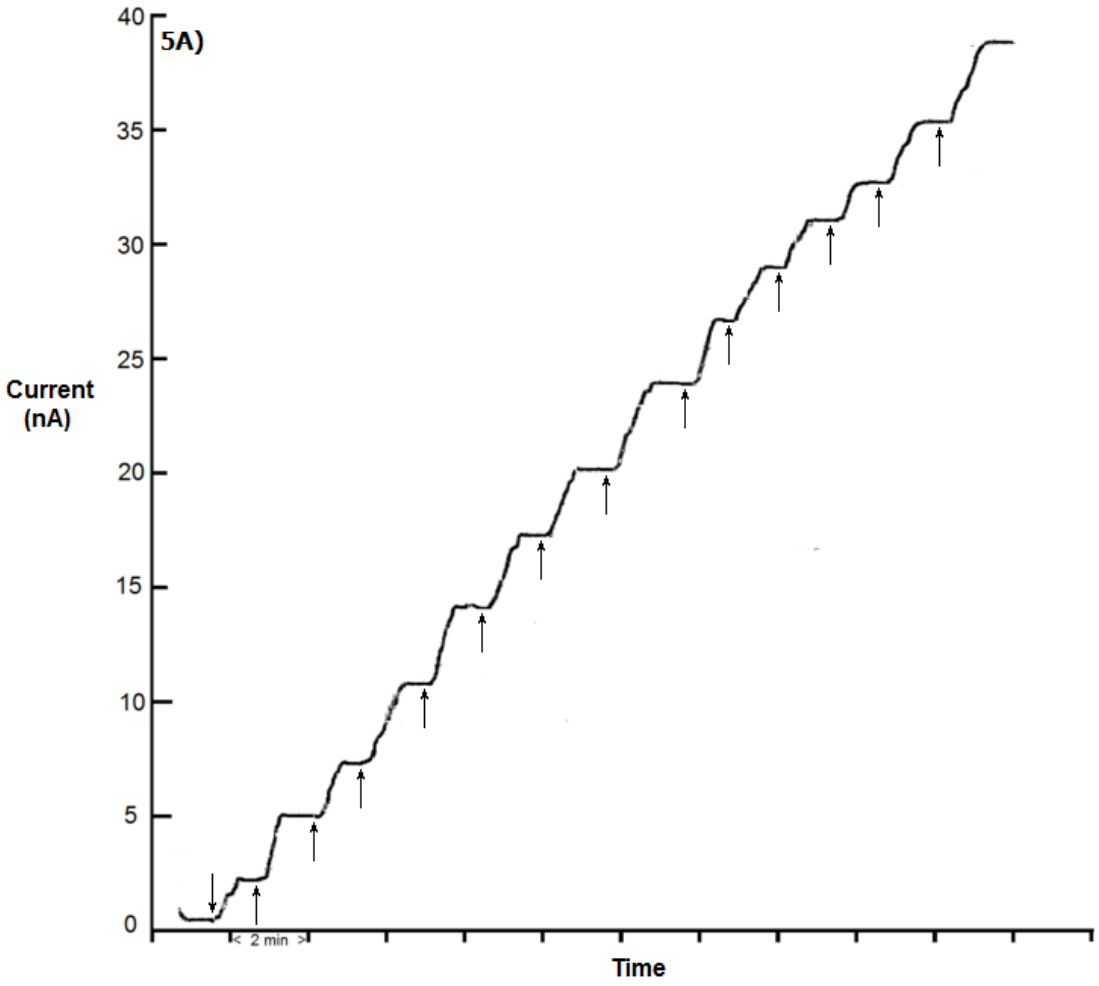

Figure 5-7 A) Amperogram conducted with the proposed final biosensor. Each arrow represents an injection of 3µL of 25mM glutamate in a 10mL stirred solution containing supporting electrolyte; 75mM, PB (pH 7.0), with 50mM NaCl at an applied potential of +0.1V vs. Ag/AgCl

The life time of the biosensor in continuous operation is 2 hours, whilst the shelf lifetime is at least 2 weeks without any change in sensitivity (Appendix Figure 2). For the latter study, biosensors were stored in a desiccator which was stored in a fridge at 4°C. It should be mentioned that biosensors based on the cofactor NAD^+ can be readily stabilised for over six months using commercially available enzyme stabilisers [20]. The life time of the biosensor was determined by calibration studies with known additions of glutamate in buffer (pH 7, 35°C). The sensitivity was then determined based on the slope of the subsequent calibration plots (n = 3).

5.4.5. Optimisation of Temperature and pH

The optimum pH was determined by carrying out calibration studies over the pH range 5 – 9 at a temperature of 25°C. The optimum pH was determined to be pH 7 as biosensors achieved the greatest sensitivity at this pH. A neutral pH also ensures that further studies investigating food and serum will not require the pH to be changed to achieve maximum sensitivity, thereby reducing sample preparation steps. A separate study was carried out to determine the optimum temperature. The temperature was varied over the range 25 – 40°C with the pH fixed at 7. The optimum temperature was determined to be 35°C.

5.4.6. Application of the optimum amperometric biosensor (MWCNT–CHIT–MB/GLDH–NAD–CHIT–MB/MWCNT–CHIT–MB) to the determination of glutamate in unspiked food.

Many food products are known to contain MSG as a flavour enhancer, therefore, we decided to apply our new reagentless biosensor to determine glutamate in a known brand of beef stock cube.

Standard addition was conducted by dissolving one OXO cube (5.9 g mass) in 50ml of PB and sonicating for 15 minutes until fully dissolved. Five replicate aliquots from this solution were analysed using fresh reagentless biosensors for each measurement. The determination was performed by adding an aliquot of PBS (9.95 mL) to the voltammetric cell, establishing a steady state current, and then injecting a 5μL volume of the OXO cube/PB solution into the cell. Sequential 3μL injections of 25 mM glutamate were then added to the cell, standard addition plots were constructed and from these the endogenous glutamate concentration was determined (n = 5). The mean quantity of glutamate recovered in unspiked OXO Cubes was 90.6 mg/g, with a CV of 7.52%; results are shown in Table 5-3. A typical amperogram obtained from the analysis of an OXO cube utilising the reagentless biosensor is shown in Figure 5-8.

OXO Cube Sample	Quantity of Glutamate Recovered (mg/g)		Unspiked Foetal Bovine Serum Sample	Concentration of Glutamate Detected (mM)
1	92.33		1	1.45
2	91.48		2	1.60
3	96.73		3	1.33
4	94.83		4	1.30
5	77.47		5	1.51
Mean (mg/g)	90.56		**Mean (mM)**	1.44
Std Dev	6.81		**Std Dev**	0.12
CV (%)	7.52		**Cov (%)**	8.54

Table 5-3: Quantity of glutamate determined in an unspiked beef OXO cube and in unspiked foetal bovine serum.

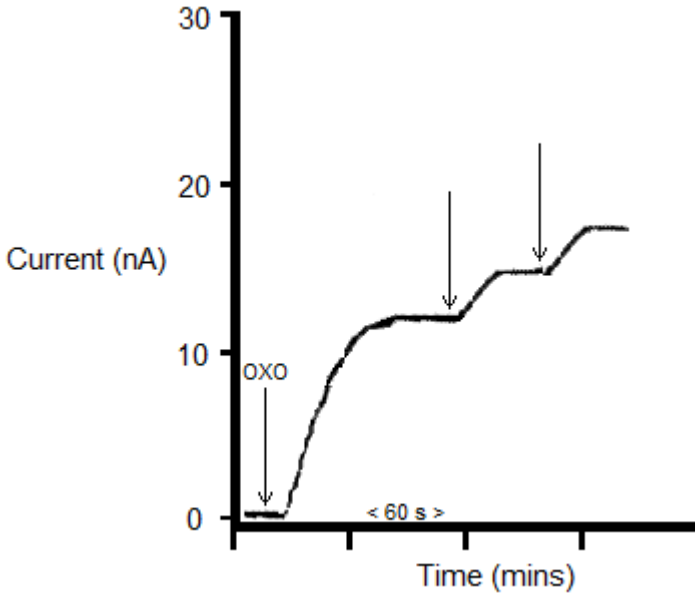

Figure 5-8: Amperogram displaying the determination by standard addition of an unspiked OXO cube, utilising the proposed final biosensor. 75mM, PB (pH 7.0), with 50mM NaCl at an applied potential of +0.1V vs. Ag/AgCl.

The average percentage of glutamate was calculated relative to the mass of an OXO cube and was found to be 18.1% (± 1.36%, n = 5). This compares favourably with a previously published value for MSG content in OXO cubes [1]. The quantity of glutamate recovered from the stock cube compares favourably with levels calculated with an optical biosensor, validated with HPLC [21] and utilising high performance thin layer chromatography [22]. The optical biosensor and HPLC analysis determined an L-glutamate level of 18.29% (± 0.66%) and 17.70% (± 0.34%) based on n = 3, whilst the high performance thin layer chromatography technique determined a level of 133.50 mg/g (± 0.84%, n = 3). These values compare favourably to the values we have determined utilising the reagentless biosensor.

5.4.7. Application of the optimum amperometric biosensor (MWCNT–CHIT–MB/GLDH–NAD–CHIT–MB/MWCNT–CHIT–MB) to the determination of glutamate in both unspiked and spiked serum.

Amperometry, in conjunction with standard addition, was used to determine the endogenous levels of glutamate and the recovery for serum spiked with additional glutamate. The replicate serum samples were analysed using a fresh biosensor for each measurement. A typical amperogram obtained from the analysis of unspiked serum utilising the reagentless biosensor is shown in Figure 5-9 in the supplementary material.

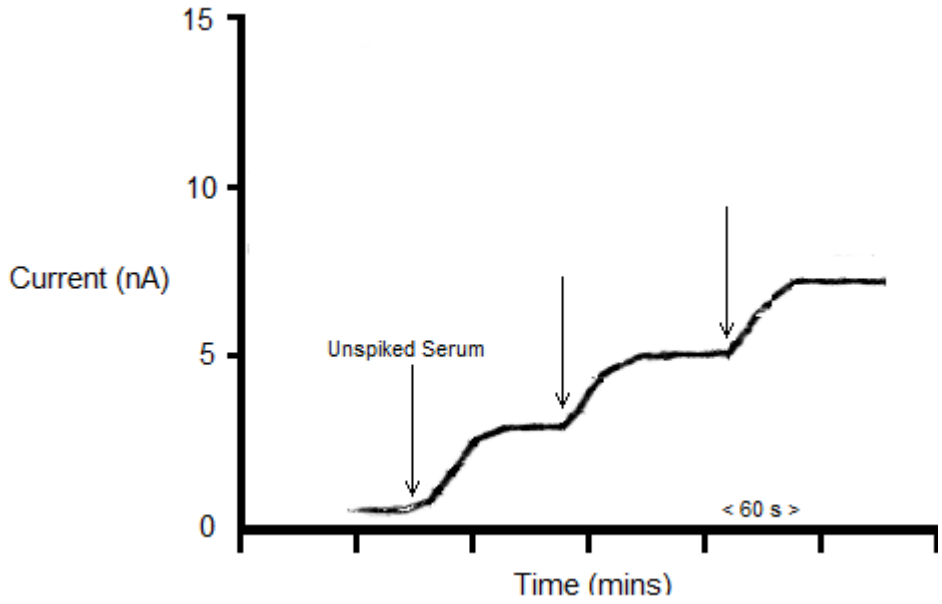

Figure 5-9: Amperogram displaying the determination by standard addition of an unspiked serum, utilising the proposed final biosensor. 75mM, PB (pH 7.0), with 50mM NaCl at an applied potential of +0.1V vs. Ag/AgCl.

The data obtained on serum samples using the glutamate biosensor are shown in Table 3. The mean endogenous level of glutamate detected was 1.44 mM for the unspiked samples. The coefficient of variation was 8.54% for the five individual samples. This value is comparable to our previous publication [1] in which we report a value of 1.68 mM. It is worth noting this also compares favourably to a value discovered by a bioluminescence method [23].

The biosensors were then used to determine glutamate in spiked serum by fortifying with 1.50 mM of glutamate. The results are shown in Table 5-4. The mean recovery (n = 5) was 104% with a CV of 2.91%.

Sample	Fortified Glutamate (mM)	Endogenous Concentration (mM)	Concentration of Glutamate Detected (mM)	Recovery (%)
1	1.50	1.44	2.96	101
2	1.50	1.44	3.01	105
3	1.50	1.44	3.02	105
4	1.50	1.44	2.97	102
5	1.50	1.44	3.07	109

Mean recovery (%)	104
Std Dev	3
Cov (%)	2.91

Table 5-4: Recovery of glutamate detected in spiked serum fortified with additional glutamate.

5.5. Conclusion

This chapter has described the development of a reagentless amperometric glutamate biosensor. This was achieved by incorporating the biocomponents using a layer-by-layer procedure involving chitosan and MWCNTs. The device produced well defined steady state currents over extended operating times indicating that the bio-components are securely immobilised onto the base transducer.

The reagentless glutamate biosensor, fabricated in this study, is to date the first of its kind; our biosensor detection limit compares favourably to those previously reported for non-reagentless glutamate sensors. The limit of detection of our biosensor is 3 μM, whereas detection limits of [24]–[33], respectively.

The device and its components have been fully optimised to produce a reproducible reagentless biosensor which has been applied to the analysis of glutamate in clinical and food samples. Notably, the samples required no pre-treatment, other than dilution. The content of glutamate determined in OXO cubes and in serum compares favourably to that determined with our previous glutamate biosensor [1].

This novel layer-by-layer approach to biosensor fabrication may hold promise as a generic platform for future biosensors based on dehydrogenase systems.

It should be mentioned that the analysis of neuronal cells for changes in glutamate flux is of significant biomedical interest. High levels of glutamate leads to excitotoxicity, which is associated with diseases previously mentioned in the introduction. For potential future studies and applications, it is of value to consider how our biosensor compares to previously reported sensors which determine neuronal glutamate.

Previously reported microelectrodes have been used to measure glutamate *in vivo* in rodent studies; these were fabricated by coating microelectrodes with glutamate oxidase [34]–[41]. These required high operating potentials (+600 - 700mV vs. Ag/AgCl), as the detection

system involved the measurement of hydrogen peroxide. High operating potentials can lead to the oxidisation of interferences such as ascorbic acid, which can interfere the measurement of glutamate. It is worth noting that Oldenziel et al., 2006, utilised a lower operating potential of +150mV vs. Ag/AgCl, by utilising the electron mediator horseradish peroxidase; which increased the complexity of biosensor fabrication.

Microelectrodes coated with glutamate dehydrogenase are uncommon; this is likely due to the requirement of integrating the cofactor NAD^+ onto the surface of the microelectrode without leeching, as mentioned previously. By miniaturizing our reagentless biosensor, the lower operating potential required to generate an analytical response would prove beneficial for the analysis of glutamate in real time, in neuronal cells. Our approach would negate the requirement for additional enzymes or use of charged membranes such as Nafion, to block out potential interferences. It should be feasible to incorporate the approach described in this chapter into an implantable system by dip coating a carbon fibre electrode (10μM diameter) into the formulation described in this chapter.

5.6. References

[1] G. Hughes, R. M. Pemberton, P. R. Fielden, and J. P. Hart, (2014), "Development of a Disposable Screen Printed Amperometric Biosensor Based on Glutamate Dehydrogenase, for the Determination of Glutamate in Clinical and Food Applications," *Anal. Bioanal. Electrochem.*, **6**, 435–449.

[2] J. Wang, (2005), "Carbon-Nanotube Based Electrochemical Biosensors: A Review," *Electroanalysis*, **17**, 7–14.

[3] M. Zhang, A. Smith, and W. Gorski, (2004), "Carbon nanotube-chitosan system for electrochemical sensing based on dehydrogenase enzymes.," *Anal. Chem.*, **76**, 5045–50.

[4] J. M. Nugent, K. S. V. Santhanam, A. Rubio, and P. M. Ajayan, (2001), "Fast Electron Transfer Kinetics on Multiwalled Carbon Nanotube Microbundle Electrodes," *Nano Lett.*, **1**, 87–91.

[5] L. Zhu, J. Zhai, R. Yang, C. Tian, and L. Guo, (2007), "Electrocatalytic oxidation of NADH with Meldola's blue functionalized carbon nanotubes electrodes."

[6] M. Boujtita, J. P. Hart, and R. Pittson, (2000), "Development of a disposable ethanol biosensor based on a chemically modified screen-printed electrode coated with alcohol oxidase for the analysis of beer.," *Biosens. Bioelectron.*, **15**, 257–63.

[7] A. C. Pereira, M. R. Aguiar, A. Kisner, D. V. Macedo, and L. T. Kubota, (2007), "Amperometric biosensor for lactate based on lactate dehydrogenase and Meldola Blue coimmobilized on multi-wall carbon-nanotube," *Sensors Actuators B Chem.*, **124**, 269–276.

[8] S. D. Sprules, J. P. Hart, S. A. Wring, and R. Pittson, (1994), "Development of a disposable amperometric sensor for reduced nicotinamide adenine dinucleotide based on a chemically modified screen-printed carbon electrode," *Analyst*, **119**, 253.

[9] L. Qian and X. Yang, (2006), "Composite film of carbon nanotubes and chitosan for preparation of amperometric hydrogen peroxide biosensor.," *Talanta*, **68**, 721–7.

[10] H. J. Malmiri, M. Ali, G. Jahanian, and A. Berenjian, (2012), "Potential Applications of Chitosan Nanoparticles As Novel Support in Enzyme Immobilization," *Am. J. Biochem. Biotechnol.*, **8**, 203–219.

[11] O. V. Kharissova, B. I. Kharisov, and E. G. de Casas Ortiz, (2013), "Dispersion of carbon nanotubes in water and non-aqueous solvents," *RSC Adv.*, **3**, 24812.

[12] M. Zhang, C. Mullens, and W. Gorski, (2007), "Coimmobilization of Dehydrogenases and Their Cofactors in Electrochemical Biosensors," *Anal. Chem.*, **79**, 2446–2450.

[13] B.-Y. Wu, S.-H. Hou, F. Yin, J. Li, Z.-X. Zhao, J.-D. Huang, and Q. Chen, (2007), "Amperometric glucose biosensor based on layer-by-layer assembly of multilayer films composed of chitosan, gold nanoparticles and glucose oxidase modified Pt electrode.," *Biosens. Bioelectron.*, **22**, 838–44.

[14] H. Zhao and H. Ju, (2006), "Multilayer membranes for glucose biosensing via layer-by-layer assembly of multiwall carbon nanotubes and glucose oxidase.," *Anal. Biochem.*, **350**, 138–44.

[15] X. Zhou, F. Xi, Y. Zhang, and X. Lin, (2011), "Reagentless biosensor based on layer-by-layer assembly of functional multiwall carbon nanotubes and enzyme-mediator biocomposite," *J. Zhejiang Univ. Sci. B*, **12**, 468–476.

[16] K. Ariga, J. P. Hill, and Q. Ji, (2007), "Layer-by-layer assembly as a versatile bottom-up nanofabrication technique for exploratory research and realistic application.," *Phys. Chem. Chem. Phys.*, **9**, 2319–40.

[17] E. J. Cho, J.-W. Lee, M. Rajdendran, and A. D. Ellington, *Optical Biosensors: Today and Tomorrow*. Elsevier, (2011).

[18] R. C. Alkire, D. M. Kolb, and J. Lipkowski, Eds., *Advances in Electrochemical Science and Engineering*. Weinheim, Germany: Wiley-VCH Verlag GmbH & Co. KGaA, (2011).

[19] Y.-T. Shieh, H.-M. Wu, Y.-K. Twu, and Y.-C. Chung, (2009), "An investigation on dispersion of carbon nanotubes in chitosan aqueous solutions," *Colloid Polym. Sci.*, **288**, 377–385.

[20] M. Piano, S. Serban, N. Biddle, R. Pittson, G. A. Drago, and J. P. Hart, (2010), "A flow injection system, comprising a biosensor based on a screen-printed carbon electrode containing Meldola's Blue-Reinecke salt coated with glucose dehydrogenase, for the measurement of glucose.," *Anal. Biochem.*, **396**, 269–74.

[21] N. Z. Md Muslim, M. Ahmad, L. Y. Heng, and B. Saad, (2012), "Optical biosensor test strip for the screening and direct determination of l-glutamate in food samples," *Sensors Actuators B Chem.*, **161**, 493–497.

[22] V. N. Krishna, D. Karthika, D. M. Surya, M. Rubini, M. Vishalini, and Y. Pradeepa, (2010), "Analysis of Monosodium l-Glutamate in Food Products by High-Performance Thin Layer Chromatography.," *J. Young Pharm.*, **2**, 297–300.

[23] Z. C. Ye and H. Sontheimer, (1998), "Astrocytes protect neurons from neurotoxic injury by serum glutamate.," *Glia*, **22**, 237–48.

[24] F. Mizutani, Y. Sato, Y. Hirata, and S. Yabuki, (1998), "High-throughput flow-injection analysis of glucose and glutamate in food and biological samples by using enzyme/polyion complex-bilayer membrane-based electrodes as the detectors," *Biosens. Bioelectron.*, **13**, 809–815.

[25] N. Pasco, C. Jeffries, Q. Davies, A. J. Downard, A. D. Roddick-Lanzilotta, and L. Gorton, (1999), "Characterisation of a thermophilic L-glutamate dehydrogenase biosensor for amperometric determination of L-glutamate by flow injection analysis," *Biosens. Bioelectron.*, **14**, 171–178.

[26] R. J. Cosford and W. G. Kuhr, (1996), "Capillary biosensor for glutamate.," *Anal. Chem.*, **68**, 2164–2169.

[27] W. Laiwattanapaisal and J. Yakovleva, (2009), "On-chip microfluidic systems for determination of L-glutamate based on enzymatic recycling of substrate," *Biomicrofluidics*, **3**, 14104.

[28] O. M. Schuvailo, S. Gáspár, A. P. Soldatkin, and E. Csöregi, (2007), "Ultramicrobiosensor for the Selective Detection of Glutamate," *Electroanalysis*, **19**, 71–78.

[29] B.-C. Ye, Q.-S. Li, Y.-R. Li, X.-B. Li, and J.-T. Yu, (1995), "l-Glutamate biosensor using a novel l-glutamate oxidase and its application to flow injection analysis system," *J. Biotechnol.*, **42**, 45–52.

[30] T. Tsukatani and K. Matsumoto, (2005), "Sequential fluorometric quantification of γ-aminobutyrate and l-glutamate using a single line flow-injection system with immobilized-enzyme reactors," *Anal. Chim. Acta*, **546**, 154–160.

[31] S. L. Alvarez-Crespo, M. J. Lobo-Castañón, A. J. Miranda-Ordieres, and P. Tuñón-Blanco, (1997), "Amperometric glutamate biosensor based on poly(o-phenylenediamine) film electrogenerated onto modified carbon paste electrodes," *Biosens. Bioelectron.*, **12**, 739–747.

[32] R. Monošík, M. Streďanský, and E. Šturdík, (2013), "A Biosensor Utilizing l-Glutamate Dehydrogenase and Diaphorase Immobilized on Nanocomposite Electrode for Determination of l-Glutamate in Food Samples," *Food Anal. Methods*, **6**, 521–527.

[33] R. Doaga, T. McCormac, and E. Dempsey, (2009), "Electrochemical Sensing of NADH and Glutamate Based on Meldola Blue in 1,2-Diaminobenzene and 3,4-Ethylenedioxythiophene Polymer Films," *Electroanalysis*, **21**, 2099–2108.

[34] J. J. Burmeister and G. A. Gerhardt, (2003), "Ceramic-based multisite microelectrode arrays for in vivo electrochemical recordings of glutamate and other neurochemicals," *TrAC Trends Anal. Chem.*, **22**, 498–502.

[35] O. Frey, T. Holtzman, R. M. McNamara, D. E. H. Theobald, P. D. van der Wal, N. F. de Rooij, J. W. Dalley, and M. Koudelka-Hep, (2010), "Enzyme-based

choline and L-glutamate biosensor electrodes on silicon microprobe arrays.," *Biosens. Bioelectron.*, **26**, 477–84.

[36] E. S. McLamore, S. Mohanty, J. Shi, J. Claussen, S. S. Jedlicka, J. L. Rickus, and D. M. Porterfield, (2010), "A self-referencing glutamate biosensor for measuring real time neuronal glutamate flux.," *J. Neurosci. Methods*, **189**, 14–22.

[37] W. H. Oldenziel, G. Dijkstra, T. I. F. H. Cremers, and B. H. C. Westerink, (2006), "In vivo monitoring of extracellular glutamate in the brain with a microsensor.," *Brain Res.*, **1118**, 34–42.

[38] S. Qin, M. van der Zeyden, W. H. Oldenziel, T. I. F. H. Cremers, and B. H. C. Westerink, (2008), "Microsensors for in vivo Measurement of Glutamate in Brain Tissue," *Sensors*, **8**, 6860–6884.

[39] K. M. Wassum, V. M. Tolosa, J. Wang, E. Walker, H. G. Monbouquette, and N. T. Maidment, (2008), "Silicon Wafer-Based Platinum Microelectrode Array Biosensor for Near Real-Time Measurement of Glutamate in Vivo," *Sensors*, **8**, 5023–5036.

[40] Y. Hu, K. M. Mitchell, F. N. Albahadily, E. K. Michaelis, and G. S. Wilson, (1994), "Direct measurement of glutamate release in the brain using a dual enzyme-based electrochemical sensor," *Brain Res.*, **659**, 117–125.

[41] F. Tian, A. V Gourine, R. T. R. Huckstepp, and N. Dale, (2009), "A microelectrode biosensor for real time monitoring of L-glutamate release.," *Anal. Chim. Acta*, **645**, 86–91.

CHAPTER SIX

Conclusions and Future Studies

6. Conclusions

6.1. Fabrication of a Non-Reagentless Glutamate Biosensor

As described in Chapter 3, the non-reagentless glutamate biosensor based on MB-SPCE was successfully fabricated by drop coating the biopolymer CHIT, followed by GLDH, onto the surface of the working electrode. The utilisation of the electrocatalyst MB transducer, present within the ink, greatly reduced the potential required to electrocatalytically oxidize the NADH, in comparison to a plain carbon screen printed electrode. As a result, a low applied potential of only +100mV (vs. Ag/AgCl) resulted in the maximum response; this potential was ascertained using hydrodynamic voltammetry in the presence of NADH and was subsequently used for all amperometric studies. The low applied potential and the presence of CHIT on the WE, reduced the likelihood of interferences directly oxidising at the electrode surface resulting in unwanted current responses. The use of dummy biosensors fabricated using BSA measured any response generated by interfering compounds present in OXO cubes and serum such as ascorbic acid.

The biopolymer CHIT was used to successfully immobilize GLDH onto the surface of the transducer, without denaturing the enzyme and successfully retaining the enzyme within the biosensor matrix without leeching into free solution. This ensured that during amperometric studies, steady state currents were achieved.

The operating conditions such as the temperature and pH were optimised. The optimal conditions were 35ºC and pH 7 respectively. These conditions also ensured that a minimal amount of sample preparation was required to analyse both serum and food.

The amperometric biosensor was successfully applied to the determination of endogenous concentrations of glutamate present in both OXO cube and serum solutions. Sample preparations consisted of simply diluting the serum in phosphate buffer, whilst the OXO cube was dissolved in 50mLs of phosphate buffer and further diluted. Subsequent recovery

studies yielded high recoveries with low coefficients of variation, indicating that the biosensor fabrication technique was rapid, convenient and resulted in highly reproducible and simple to fabricate.

In relation to the objectives stated in Chapter 1, Section 1.8, we have successfully completed the following objectives in this section;

- Development of a glutamate biosensor utilising glutamate dehydrogenase, NAD^+ based on Meldola's Blue screen printed carbon electrodes.
- Immobilisation of the enzyme glutamate dehydrogenase to the surface of the working electrode the MB-SPCE to produce glutamate biosensors.
- Optimisation of the biosensor working conditions and the determination of the glutamate content of food and clinical samples utilising standard addition.

The limitation of the biosensor is the requirement of the cofactor to be present in free solution, however, immobilization of the cofactor was a novel aspect of later studies and is demonstrated within Chapters 4 and 5. In comparison to previously reported glutamate biosensors, the LOD compares favourably to other glutamate dehydrogenase biosensors and possesses a superior response time of 2s.

6.2. Fabrication of a Reagentless Microband Glutamate Biosensor

The biosensor described in Chapter 3 was further developed in order to fully integrate the cofactor NAD^+ onto the surface of the electrode in order to produce a reagentless device. The main advantage of a reagentless device is that this simplifies the fabrication process and utilisation of the device as all components of are immobilized on the surface. Reagentless devices are also of commercial interest. In the real time analysis of cells, in response to toxic effect, this is vital as additional cofactors added into free solution may disrupt the cells or reduce sterility.

The fabrication process was relatively simple and similar to that described in Chapter 3. The enzyme and co-factor were immobilised onto the surface of the MB-SPCE by drop-coating a mixture of GLDH-NAD^+-CHIT. Once dried the working electrode was covered with insulating tape and cut through laterally in order to define the microband edge. It is likely that the presence of the insulating tape and the absence of stirring the solution ensured that the biosensor components were retained on the surface of the electrode. The biosensor demonstrated a longer linear range and increased sensitivity in cell media compared with a phosphate buffer. This is likely due to enzyme promoters present in the cell media solution that may be enhancing the enzyme activity.

The biosensor was first successfully applied to toxicity testing using an end-point assay; whereby standard addition was used to quantify glutamate in cell media which had been in the presence of HepG2 cells exposed to various concentrations of paracetamol. Secondly, it was successfully applied to real time studies, whereby the glutamate released from cells was monitored over 8 hours. The results for both methods suggested that with increasing concentrations of paracetamol, increased concentrations of glutamate were released by cells, suggesting greater levels of toxicity.

In relation to the objectives stated in Chapter 1, Section 1.8, we have successfully completed the following objectives in this section;

- Further development of the biosensor to immobilize the cofactor NAD^+ onto the surface of the screen-printed carbon electrode.
- The miniaturisation of the biosensor in order to develop micro-band biosensors for the determination of glutamate released by HepG2 cells in response to toxic challenge.
- Development of an electrode holder to simultaneously immerse the biosensor within the cell media solution for the interrogation of the cells, whilst reducing evaporation and allowing for gas exchange between the cell media and atmosphere.

6.3. Fabrication of a Reagentless Macro Glutamate Biosensor utilising Carbon Nanotubes

In order to fabricate a conventional (macro) sized reagentless biosensors, the enzyme and cofactor must be fully immobilized to the surface of the biosensor, without leeching into free solution. This was achieved by utilising a mixture of multi-walled carbon nanotubes and chitosan, drop coated in a layer-by-layer procedure. The presence of additional water-based Meldola's Blue throughout the reaction layer resulted in an increase in sensitivity, which coupled with the MWCNT's, is considered to increase the electron shuttling rate from the outer layers of the biosensor, to the working electrode.

Although the layer-by-layer procedure is a little more complex, than that described earlier, the resulting biosensor produces steady state currents, over prolonged analysis times, indicating that all bio-components are strongly retained on the transducer surface. Consequently, this novel approach could be adapted to the fabrication of biosensors for the measurement of many different analytes.

The shelf life time of the proposed biosensor was at least 2 weeks without any change in sensitivity. This could be improved by utilising commercially available enzyme stabilisers.

In relation to the objectives stated in Chapter 1, Section 1.8, we have successfully completed the following objectives in this section;

- Development of a conventional sized reagentless glutamate biosensor.
- Optimisation of the biosensor components and working conditions, in order to apply the reagentless biosensor to the determination of glutamate in complex samples.

6.4. Overall conclusions

Enzyme-based biosensors for the determination of glutamate have been developed utilising three different fabrication techniques and for two different electrode dimensions. Non-reagentless and reagentless devices have also been developed. It has been shown that the biosensors in an amperometric assay, can be applied to the determination of glutamate in serum and food samples. Recovery studies were also carried out it was demonstrated that with high recovery values and low coefficients of variation could be obtained.

A biosensor was successfully applied to toxicity testing by incorporating the device into wells containing live HepG2 cells for continuous measurements. The same biosensor could also be used for toxicity testing using an end-point assay.

6.5. Future Studies

In order to increase the operating time for continuous monitoring of the glutamate released by cells, several modifications to the fabrication method could be investigated. The sterility of the biosensors and the culture medium containing cells could be improved. The biosensor could be sterilised by gamma radiation, without significantly affecting the enzyme, cofactor and the electrode material. Autoclaving is also possible but could result in the denaturing of the enzyme, cofactor and possibly damage the electrode material. The electrode holder, in addition to being cleaned by ethanol, could also be exposed to gamma radiation. By sterilising these components, this would increase the duration over which the real time studies can take place in the absence of bacterial or fungal infection. The microband biosensor could be further developed and integrated into a biosensor array for multiple analyte monitoring in real time. Multiple human cells lines could also be utilised in a multi-well format order to replicate *in vivo* responses *in vitro*. Additional applications include environmental toxicity monitoring and food safety.

Appendices

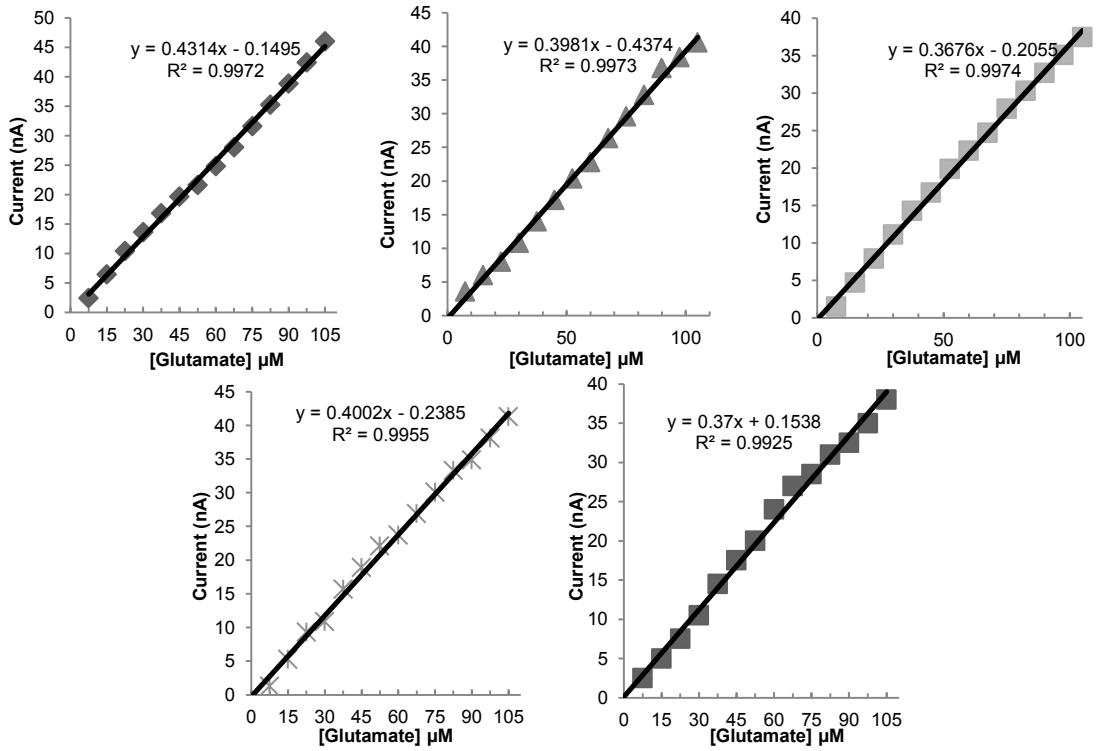

Appendix Figure 1) Five typical standard addition calibration plots obtained with five individual MWCNT-CHIT-GLDH-NAD$^+$-MB-SPCE.

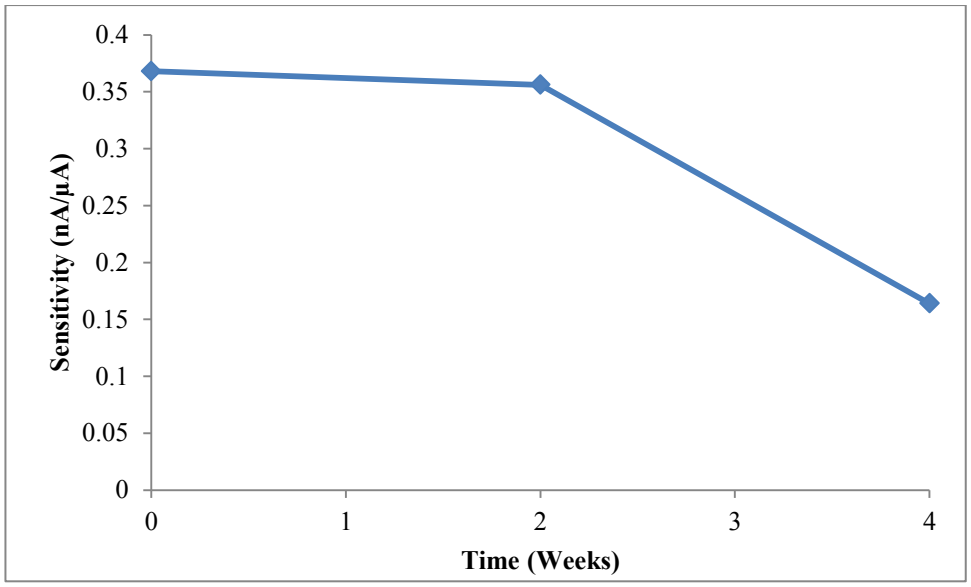

Appendix Figure 2) MWCNT-CHIT-GLDH-NAD+-MB-SPCE biosensor stability study.

t-Test: Two-Sample Assuming Equal Variances		
	Variable 1	*Variable 2*
Mean	52.07	93.30279
Variance	51.1923	295.1111
Observations	3	3
Pooled Variance	173.1517	
Hypothesized Mean Difference	0	
df	4	
t Stat	-3.83773	
P(T<=t) one-tail	0.009248	
t Critical one-tail	2.131847	
P(T<=t) two-tail	0.018495	
t Critical two-tail	2.776445	

Appendix Table 1) t-Test to determine the significance between the standard addition results for post 24hr 1mM and 5mM paracetamol doses.